Multi-vector Energy Systems Analysis for Heavy-duty Transportation Deep Decarbonization Using H_2 and Synthetic Fuels

by

Youssef H. Shaker

BASc Applied Science in Engineering Science – Energy Systems Engineering, University of Toronto, 2017

Submitted to the Institute for Data, Systems, and Society and the
Electrical Engineering and Computer Science Department
in partial fulfillment of the requirements for the degrees of

MASTER OF SCIENCE IN TECHNOLOGY AND POLICY

and

MASTER OF SCIENCE IN ELECTRICAL AND COMPUTER ENGINEERING

at the

MASSACHUSETTS INSTITUTE OF TECHNOLOGY

February 2024

Authored by: Youssef H. Shaker
Institute for Data, Systems, and Society
Electrical Engineering and Computer Science
January 18, 2024

Certified by: Dharik Mallapragada
Principal Research Scientist, MIT Energy Initiative, Thesis Supervisor

Certified by: Audun Botterud
Principal Research Scientist
Laboratory for Information and Decision Systems, Thesis Supervisor

Certified by: Priya Donti
Assistant Professor of Electrical Engineering and Computer Science, Thesis Reader

Accepted by: Frank R. Field III
Senior Research Engineer, Sociotechnical Systems Research Center
Interim Director, Technology and Policy Program

Accepted by: Leslie A. Kolodziejski
Professor of Electrical Engineering and Computer Science
Chair, Department Committee on Graduate Students

Multi-vector Energy Systems Analysis for Heavy-duty Transportation Deep Decarbonization Using H_2 and Synthetic Fuels

by

Youssef H. Shaker

Submitted to the Institute for Data, Systems, and Society and the
Electrical Engineering and Computer Science Department
on January 18, 2024 in partial fulfillment of the requirements for the degrees of

MASTER OF SCIENCE IN TECHNOLOGY AND POLICY

and

MASTER OF SCIENCE IN ELECTRICAL AND COMPUTER ENGINEERING

ABSTRACT

Policies focused on deep decarbonization of regional economies tend to emphasize electricity sector decarbonization in conjunction with electrification of end-uses and increasingly, on the use of hydrogen (H_2) produced via electricity for displacing fossil fuels in difficult-to-electrify sectors. One such use case is heavy-duty transport, which represents a substantial and growing share of global transport sector emissions given the increasing electrification of the light duty vehicle fleet. Here, we assess the bulk energy system impact of decarbonizing the heavy-duty vehicle (HDV) segment via use of either H_2 or drop-in synthetic liquid fuels produced from H_2 along with CO_2. Our analysis relies on soft-linking two modeling approaches: a) a bottom-up model of transportation energy demand that produces a variety of final energy demand scenarios for the same service demand and b) a multi-sectoral capacity expansion model, DOLPHYN, that co-optimizes power, H_2 and CO_2 supply chains subject to a variety of technological and policy constraints to meet the exogeneous final energy demand slate. Through a case study of Western European countries under deep decarbonization constraints for the year 2040, we quantify the energy system implications of varying levels of H_2 and synthetic fuels adoption in HDVs, under scenarios with and without CO_2 sequestration capacity availability. We find that substitution of liquid fossil fuels in the HDV segment is essential to meet the imposed deep decarbonization constraint across the modeled power, H_2, and transport sectors, particularly in the absence of CO_2 storage. Additionally, we find that utilizing H_2 HDVs reduces bulk system costs of deep decarbonization, while reducing fossil liquids demand, but could increase natural gas consumption in cases. While H_2 HDV adoption reduces the need for direct air capture (DAC), synthetic fuel adoption results in a greater need for DAC and also leads to system cost increases compared to scenarios without their adoption. The study highlights the trade-offs associated with different transportation decarbonization pathways, and underlines the importance of multi-sectoral consideration in decarbonization studies.

Thesis supervisor: Dharik Mallapragada
Title: Principal Research Scientist, MIT Energy Initiative

Thesis supervisor: Audun Botterud
Title: Principal Research Scientist
Laboratory for Information and Decision Systems

Thesis Reader: Priya Donti
Title: Assistant Professor of Electrical Engineering and Computer Science

Acknowledgments

I would to like to thank my supervisors Dharik Mallapragada and Audun Botterud for their invaluable feedback throughout my two and a half years at MIT. Their feedback has allowed me to expand my skillset and sharpen my research abilities. I would also like to thank Dr. Priya Donti in participating the review of this thesis.

I would also like to thank other researchers within MITEI such as Ruaridh Macdonald, Guiyan Zang, and Guannan He. Your guidance has been invaluable and key in keeping me on track. I could not have completed this research without the contributions of my fellow student researchers, Anna Cybulsky and Jun Wen Law.

I would like to thank our TPP cohort for always being there and keeping the last few years light and enjoyable. Special thanks goes out to MTIEI desk-mates, Serena Patel and Les Armstrong, the Econometrics support and therapy group Nirmal Bhatt and Deepika Raman.

I would like to thank my friends whom I could not have done this without, starting with Mouness Akour who helped me move and settle in mid-pandemic, and my imporptu roommate and nemesis Sharif Nami. Added thanks goes to the two Seifs, the two Youssefs, the two Amrs, the two Galals, Poloito, Shaikh, and Siraj.

I would like to thank my family for being the bedrock on which any achievement I make stands. Baba, Mama, Gulru, and Nony, I love you all so much. Among many things, I could have not gotten through the loss of Uzair without you.

My Lord, enable me to be grateful for Your favor which You have bestowed upon me and upon my parents and to do righteousness of which You approve. And admit me by Your mercy into the ranks of Your righteous servants.

In memory of Uzair Zafar, who left us too early. May he be granted the complete mercy of the All-Merciful, the company of the Beloved, and the highest rank.

Biographical Sketch

Youssef Shaker is an S.M. Candidate in the MIT Technology and Policy program and Electrical and Computer Engineering program, focusing on energy transition issues and transportation decarbonization. Prior to MIT, Youssef spent 4 years at ICF Consulting as part of the Demand-Side Management Analytics team, working on a range of projects for U.S., international utilities, and government entities. These projects explored topics such as ToU tariff design, demand-side management potential studies, energy efficiency program planning, and electrification potential studies. Moreover, Youssef has worked at Tesla, operating and managing a virtual power plant asset. Youssef also worked at Ontario's Independent Electricity Systems Operator as a Market Analyst, where he wrote reports on the state of the Ontario wholesale electricity market. Youssef recieved his Bachelors degree from the University fo Toronto with Honours, studying Energy Systems Engineering.

Contents

List of Figures

List of Tables

Chapter 1

Introduction

Modeled pathways for energy system decarbonization are generally based on a two-pronged strategy of: a) decarbonizing the power sector by expanding variable renewable energy (VRE) supply, and b) increasing use of electricity to displace fossil fuel use in final energy. To date, only the first part of this two-pronged strategy has yielded meaningful progress in major-emitting regions like the European Union and U.S. – for example, power sector greenhouse gas (GHG) emissions in the European Union (EU) for 2021 were 40% lower than 2005, as VRE generation increased from 16% to 38% over the same period [1], [2]. In contrast, GHG emissions from the EU transportation sector have remained largely unchanged over this period; electricity consumption as a share of total transportation energy consumption is less than 1% in 2021 [1], [2].

The electrification of light duty vehicles (LDVs) is seemingly well underway, as indicated by the share of plug-in hybrid (PHEVs) and battery electric vehicles (EVs) as a percentage of new car sales (PHEV and EV car sales in the EU have increased from 2% to 22 % of all new car sales between 2018 and 2022) [3]. However, the electrification of heavy-duty vehicles (HDV), which accounted for around 28% of the transportation sector's CO_2 emissions in EU in 2021, is uncertain due to several factors including concerns with payload reduction impacts, and refueling time associated with state-of-art battery and charging technologies and grid impacts [1], [4]–[7].

In addition to electrification, other decarbonization strategies being contemplated for HDVs include: a) direct use of hydrogen (H_2) produced from low-carbon sources, b) use of so-called synthetic liquid fuels (SFs) produced using electricity, H_2 and CO_2, and c) continued use of petroleum-based liquid fuels that are offset by atmospheric CO_2 capture using negative emissions technologies like direct air capture (DAC). Each of these pathways interact with the electric grid in different ways and thus will impact its decarbonization as well. For instance, production of SFs, also called e-fuels, will require substantial quantities of low-carbon H_2, which relies on the development of H_2 supply chain and possibly electricity supply chain [8]. Similarly, the CO_2 feedstock for SF production will necessitate deployment of CO_2 capture and possibly, transport infrastructure that could also be utilized to facilitate CO_2 sequestration where available. Besides technological coupling, decarbonization efforts across sectors are also coupled through policy instruments like emissions trading schemes (e.g. EU ETS) that allow for emissions reduction strategies across sectors to directly compete with each other. Here, we systematically explore the multi-sector impacts of the above-mentioned

strategies for HDV decarbonization, which as noted in the literature review, remains one of the lesser studied topics in the area of transportation decarbonization.

In this thesis, we use a multi-model approach, consisting of a bottom-up transportation energy demand model and a multi-vector energy system model, to study the role for H_2 and SF for heavy-duty vehicle (HDV) decarbonization and its bulk energy system impact (Figure 3.1). For the demand-side analysis, we develop a model to evaluate alternative energy demand scenarios for HDVs that accounts for factors like vehicle energy efficiency by vehicle sub-type, and market share of each vehicle type. We then use these resulting scenarios as inputs to the supply-side multi-vector energy infrastructure planning model, Decision Optimization for Low Carbon Power and Hydrogen Nexus (DOLPHYN), to investigate the impact of wide-scale heavy-duty transportation decarbonization on the bulk energy infrastructure [9]. As part of this work, we expand DOLPHYN to include a representation of the CO_2 infrastructure, including storage, transportation and utilization (in the form of SF production), as well as consideration of competition between conventional fossil fuels and liquid fuels. In this way, we are able to capture the interactions between the H_2, CO_2, and liquid fuels supply chains and their impact on the power sector which includes: a) changes in electricity consumption, b) inducing competition for constrained resources like VRE capacity for renewable electricity generation and CO_2 storage sites and c) affecting the available emissions budget for power and H_2 production as part of multi-sectoral decarbonization efforts. The goal of our analysis is to understand the drivers for H_2 and SFs adoption as part of cost-optimized deeply decarbonized power, H_2 and transportation sectors.

Our analysis focuses on a case study of Western Europe in 2040 under deep decarbonization scenarios, where policy deliberations have recently focused on a multi-sectoral decarbonization effort (e.g. via EU ETS), reducing reliance on fossil fuels, and deployment of H_2 and SFs for transportation decarbonization. There is also considerable uncertainty on the potential role for CO_2 storage in deep decarbonization scenarios for this region, with considerable public opposition to projects, as well as political and legislative barriers [10].

Specifically, we attempt to address the following questions for the case study of Western Europe decarbonization by 2040:

1. How does adoption of H_2 for heavy-duty transportation impact power and H_2 infrastructure and fossil fuel demand needs under-cost optimized decarbonization scenarios?

2. How does adoption of SFs for heavy-duty transportation impact power and H_2 infrastructure needs under-cost optimized decarbonization scenarios?

3. How do factors such as the availability of CO_2 sequestration sites and CO_2 emissions limits affect technology deployment?

This thesis is structured as follows: Chapter 2 covers some of the relevant policy discussion around transportation decarbonization in the European context, as well as literature on transportation decarbonization particularly in the context of macro-energy systems modelling. Chapter 3 outlines the methods used to answer key questions around heavy-duty transportation decarbonization, covering the demand-side model formulation, in addition to the SF supply chain formulation in DOLPHYN. Additionally, we detail the case-study used, key demand-side input assumptions, technology assumptions, and a summary of the

scenarios analyzed. Chapter 4 describes modeling results, in three sections: the first explores the impact of using H_2 for transportation decarbonization, the second explores the impact of using SFs for transportation decarbonization along with H_2, and the third explores some key sensitivity results. Chapter 5 delves into some key policy implications of this work on power and transportation decarbonization, with some discussion of the limitations of this work.

Chapter 2

Background and Literature Review

2.1 Policy Landscape

The European Union (EU) and other European countries have set aggressive decarbonization targets, with the aim of reaching carbon neutrality by the year 2050 [11]. As mentioned in the previous section, while many sectors have decarbonized in previous years, the transportation sector has not with emissions remaining relatively stable [1]. More specifically, the road transportation sector produces around one fifth of all emissions in the EU [12]. The heavy-duty vehicles (HDV) sector, is responsible for a quarter of all road transportation emission, and over 6% of total EU emissions [12]. To continue to make strides towards increasingly ambitious climate targets, policies that ensure the decarbonization of the transportation sector, and the heavy-duty transportation sector must be pursued. Broadly, transportation decarbonization strategies can fall into multiple different categories, these are: 1) increased efficiency 2) reduction in demand 3) modal shifts 4) fuel/vehicle technology shifts [13]. This project focuses on the last category of transportation decarbonization.

With regards to current policy, the EU has acknowledged the importance of transportation decarbonization under the EU Green New Deal [11]. The current regulation governing HDV emissions, the Regulation on CO_2 Emissions Standards for HDVs (Regulation EU 2019/1242), aims to reduce the emissions of new HDV vehicles by 30% by the year 2030 [12]. The regulation also provides some incentives for the development of low-emission ICE vehicles and zero-emission HDVs. There is also some technology agnostic incentivization of zero-emissions HDVs. In summary, the main focus of current policy proposals is the continued use of ICEs, albeit more efficient ICEs.

Further, the EU Commission has recently proposed an updated version of the Regulation on CO_2 Emissions Standards for HDVs [12]. The new proposal increases the stringency of emissions requirements by reducing the average emissions of new HDVs in 2040 by 90% compared to 2019-2020 levels [12]. The proposal further incentivizes the development of ZEV and LEV HDVs, and the development of charging and refueling infrastructure [12]. The proposed updated regulations also acknowledge the need for a modal shift in the use of HDVs with the introduction zero emission vehicles (ZEVs) under such updated regulations, as well as the utilization of low-carbon fuels [12].

As such, details around technology and fuel shifts in the HDV sector and their impacts

are still debated on the technological level and on the policy level. Specifically, the choices around technologies and fuels used to power decarbonziation is uncertain. For instance, vehicle manufacturers have committed to electrical heavy-duty vehicle concepts, despite some concerns around payload efficiency of high payload long-distance freight [14], [15]. While electrification has been the preferred method for other road transportation sectors, there is some question as to how electric batteries will fare in the heavy-duty transportation sector due to payload loss and refueling times [4]–[6]. Recently, alternative fuels infrastructure regulation, with specific provisions to support H_2 heavy-duty vehicles refueling, was agreed upon [16]. However, a robust implementation of a widespread H_2 transportation vehicles and networks is yet to be seen. We have also seen some discussions around the inclusion of SFs, also known as e-fuels, as a possible option for transportation decarbonization [17]. The utilization of SFs also raises some questions due to the process' emissions and energetics. Other options also include the continued use of liquid hydrocarbons, while offsetting emissions using direct air capture (DAC) technology. Regardless of the technological pathway chosen, each of these pathways has its advantages and disadvantages including cost, land-use, need for CO_2 sequestration, and continued use of hydrocarbons.

2.2 Literature Review

Previous literature on transportation decarbonization can be categorized into a few broad themes: 1) the techno-economics and efficiency of EVs, H_2 vehicles, and SFs [18], [19] 2) fleet evolution and the impact of policy interventions [20] 3) scenario-based characterization of the energy demand and emissions associated with transportation decarbonization under various technology scenarios [13] 4) investigating the impacts of transportation decarbonization on wider energy systems [21], [22].

Some studies have investigated the use of SFs and H_2 in transportation [18], [23], [24]. The unit efficiency and costs of the use of SFs have also been estimated in literature, where the grid interactions are generally treated in a static manner, i.e. a fixed emissions intensity and cost of grid electricity per scenario [18], [25]. These studies have quantified the costs, energy use, and emissions impact of such decarbonization without necessarily exploring what the adoption of SFs or H_2 would mean the entirety of the power, H_2, or CO_2 infrastructure in a given region.

Studies investigating the impacts of transportation decarbonization on wider energy systems are often focused on light duty vehicles (LDV) [20], [22], [26], [27]. Additionally, because electrification of LDVs appears to be imminent, many of these studies focus on the impacts on the power sector, while studies that consider the impacts on adjacent H_2 and CO_2 infrastructure are limited [22], [27], [28]. Given the interactions between the infrastructure for these vectors noted earlier, particularly in the case of SFs and H_2, it is important to consider relevant supply chains concurrently. For instance, some literature considers power, transportation, water, heating, and industry to assess biofuels in the transportation sectors [29].

Further, studies that focus on the wider energy system impacts of transportation decarbonization incorporate transportation demand using three methods. The first approach assumes a set amount of transportation energy demand, and then investigates the necessary

supply infrastructure to meet this demand [26]. The second approach relies on specifying transportation service demand (e.g. vehicle km or tonne-km), and then endogeneously optimizing for both energy and drivetrain choice to meet this demand [21]. The third uses a multi-model approach, which determines transportation demand exogenously using a transportation demand model, and uses said models' results as an input in a macro-energy systems model [27]. The latter approach, also considered in this study, allows for accounting for non-economic drivers impacting drivetrain adoption to meet transportation demand and evaluating the impact of such choices on the energy infrastructure investment and operations.

As noted in the introduction, in this study, we use a multi-model approach, consisting of a bottom-up transportation energy demand model and multi-vector energy system model, to study the role for H_2 and SFs for HDV decarbonization and its bulk energy system impact. With the literature and scope of this study in mind, the following are the novel elements of this study: 1) the multi-model approach allows for a holistic assessment of the multi-sectoral impacts on demand-side 2) we are able to more fully consider the impacts of HDV transportation decarbonization, a less explored topic in the macro-energy systems model literature 3) we study H_2 HDVs and SFs, both novel technologies with significant multi-sectoral implications.

Chapter 3

Methods and data

3.1 Overview

This section describes the methods used to answer the questions identified in Chapter 1 as well as the various data inputs used for the analysis. Section 3.2 describes the demand-side model setup and formulation, while Section 3.3 the supply-side formulation. Section 3.4 describes the case study set-up. We then move on to the model inputs: Section 3.5 details the demand-side inputs, while section 3.6 details the supply-side model inputs. Finally, we provide an overview of the scenarios used to answer our research questions of interest in Section 3.7.

For this study, we developed a multi-model approach, consisting of a bottom-up transportation energy demand model, and a multi-vector energy system model (DOLPHYN), to study the role for H_2 and SFs for heavy-duty vehicle (HDV) decarbonization and its bulk energy system impact (Figure 3.1). The results of the demand-side model are then input in the supply-side model.

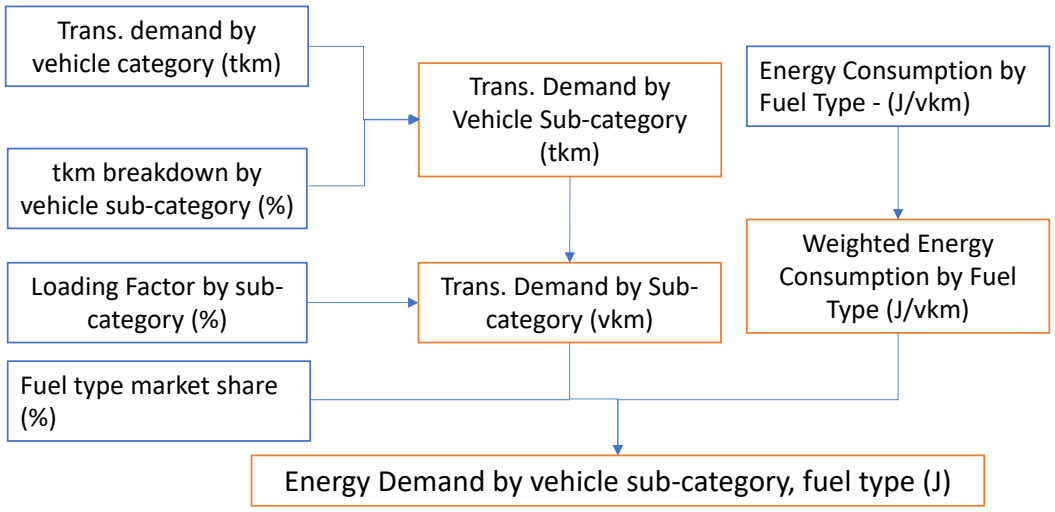

(a) Demand-side Model

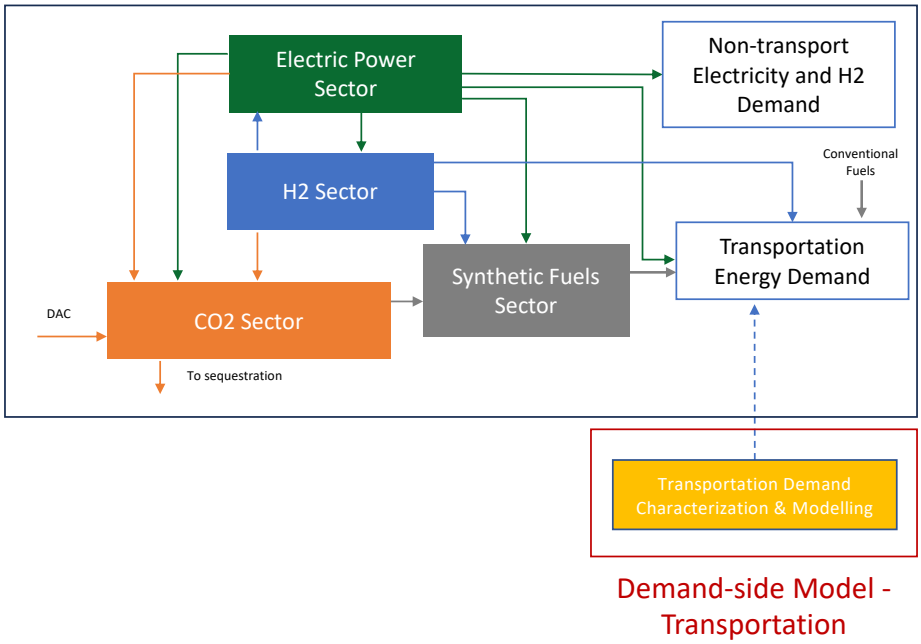

(b) Supply-side Model

Figure 3.1: Overview of supply and demand-side modelling details used for this study. a) Transportation demand model overview. Blue boxes are data inputs, while orange boxes are calculated values. b) Overview of DOLPHYN capacity expansion model and the link with the demand estimation model. The color of arrows highlight various vectors – green: electricity, blue: H_2, orange: CO_2, grey: fuels.

The demand-side model, summarized in Figure 3.1 (a), enables us to construct alternative fuel demand scenarios for the LDV and HDV transportation sector that are consistent in terms of delivering the same end-use service demand (e.g. passenger-km (pkm) for LDVs or tonne-km (tkm) for HDVs). Through the demand-side model, we are able to modify the marketshare for different vehicle types, and by extension their energy consumption. While the demand model allows for the creation of scenarios on the basis of vehicle efficiency, modal shifts, and demand reduction, we focus on shifts in vehicle/fuel types for this study.

The supply-side model, summarized in Figure 3.1 (b), is based on the DOLPHYN capacity expansion model (CEM), which evaluates the cost-optimal investments in electricity, H_2, carbon-capture utilization and sequestration (CCUS), and SF infrastructure, while adhering to a range of technology-specific and system-specific operational constraints, as well as imposed policy constraints [9], [30]. For this study, we expanded the DOLPHYN model in the following ways: 1) we added investment and operation of infrastructure for CO_2 sequestration, transmission and utilization (to produce SF), along with their energy and CO_2 interactions with the power and H_2 supply chains, and 2) modeled the ability to meet exogeneous liquid fuel demand, through a combination of fossil-derived fuels and SF production. The resulting modeling framework allows us to, for example, identify the location and scale of fossil fuel power generation with CO_2 capture in the electricity sector given inputs on the location and cost of CO_2 sequestration. Similarly, the liquid fuels supply chain allows for the production of SFs, which induces demand for H_2 and CO_2 that need to be balanced in the model.

3.2 Demand-side Model Description

This section details the mathematical formulation of demand-side model for generating alternative transportation demand scenarios. In Section 3.5, we detail the demand-side inputs used for this study. As shown in Figure 3.1, transportation demand, vehicle sub-category breakdowns, vehicle loading factors, vehicle market share, and vehicle energy consumption are combined together to create a demand profile. This model outputs the final energy consumption by fuel type (gasoline, diesel, electricity, H_2) for each timestep and country. To do so, we disaggregate transportation service demand (tonne-km (tkm) or passenger-km (pkm)) into the following categories: 1) light-duty passenger vehicles 2) buses and coaches 3) 2-wheelers, and 4) heavy-duty and light commercial vehicles. We further dissaggreate into vehicle types as shown in table 3.1. We also disaggregate demand by road type (urban, rural, highway). We then transform this service demand into vehicle km (vkm) demand using loading factors for freight vehicles and occupancy factors for passenger vehicles. We assign service demand to a specific vehicle drivetrain type (e.g. PHEV, H_2, Diesel ICE, etc.) Using energy consumption factors for a specific fuel per vkm, we arrive at a final energy consumption by fuel (e.g. diesel, gasoline, electricity, H_2). We further subdivide into timesteps. Table 3.2 shows the definitions of indices and sets used in the demand-side model. Table 3.3 contains key input parameters used in this model.

Vehicle Category	Vehicle Type
HDV & LCV	HDV Light + Short Distance
	HDV Light + Long Distance
	HDV Medium + Short Distance
	HDV Medium + Long Distance
	HDV Heavy + Short Distance
	HDV Heavy + Long Distance
	HDV Super-Heavy + Short Distance
	HDV Super-Heavy + Long Distance
	HDV Ultra-Heavy + Short Distance
	HDV Ultra-Heavy + Long Distance
	LCV
Passenger Car	Small
	Medium
	Large
Buses and coaches	Buses
	Coaches
Two-wheelers	Two-wheelers

Table 3.1: Service demand vehicle category and the vehicle types disaggregation categories

Indices and Sets	Definition
$r \in R$	r denotes a road type belonging to the set of road types R. Road types modeled are urban, suburban, and rural.
$v \in V$	v denotes a specific vehicle type in a set of all vehicle types V (e.g. small passenger vehicle, medium passenger vehicle, etc.).
$J \subset V$	J denotes a vehicle category (e.g., passenger cars, buses and coaches, heavy-duty, and light commercial vehicles) made up of vehicles $v \in V$. Vehicle types and categories modelled is show in Table 3.1
$V_{\text{pass}} \subset V$	V_{pass} is a subset of passenger vehicles made up from vehicles $v \in V$. Vehicle types and modelled is show in Table 3.1
$V_{\text{cargo}} \subset V$	V_{cargo} is a subset of cargo vehicles made up from vehicles $v \in V$.
$d \in D$	where d is a drivetrain type in a set of all drivetrain types (e.g. EV, PHEV H_2, Diesel ICE, etc).
$f \in F$	where f is a fuel type in a set of all fuel or drivetrain types (e.g. electricity, H_2, Biofuel, Diesel, Gasoline, etc).
$c \in C$	where c is a country in all countries in Western Europe.
$y \in Y$	where y is a year in possible analysis years (e.g. 2040, 2050)

Table 3.2: Demand model indices and sets

Input Parameter	Definition
$p_{\text{v,c,y}}$	Passenger km demand for a given vehicle type and country in a given analysis year.
$t_{\text{v,c,y}}$	Tonne km demand for a given vehicle type and country in a given analysis year.
$o_{\text{v,c}}$	Vehicle occupancy ratio vkm/pkm. Only defined for $v \in \text{V}_{pass}$.
$l_{\text{v,c}}$	Loading ratio vkm/tkm. Only defined for $v \in \text{V}_{cargo}$.
$s_{\text{v,c,r}}$	Road type share for a given vehicle type in a given country.
$m_{\text{v,d,y}}$	Market share for a given vehicle type for a given drivetrain type in a given year.
$k_{\text{r,v,d,f,y}}$	Energy demand per vehicle km for a vehicle v on road type r, for drivetrain d, for fuel f in year y.
$e_{\text{v,d,f,y}}$	Efficiency multiplier for a given vehicle type, for a given fuel type, in a given year.
$\tau_{\text{t,v,f}}$	Load shape factor (percent consumption in a given hour).

Table 3.3: Definitions of key demand model input parameters. the values of key parameters can be found in Section 3.5

The following equation combines key inputs to create the energy demand loadshape at time t for each of the fuel types in a given country. To do so, we first multiply vehicle service demand by a factor (occupancy ratio for passenger vehicles, and loading factor for freight vehicles) to calculate demand in vehicle distance (vkm). This is then multiplied by the road type share for a given vehicle type. We also subdivide the demand in vehicle distance by vehicle marketshare, which is the main lever used in this study. To convert this to energy consumption, we multiply by energy consumed per vkm for a given vehicle type, roadshare, fuel type, and year. We also have the option of multiplying by an efficiency factor, which could be used to assess the impact of efficiency measures. Finally, we multiply by a loadshape factor to calculate the energy consumption at a given timestep. The loadshape factor is the percentage of energy consumed in an hour out of total energy consumption. The first part of the equation calculates energy consumption for passenger vehicles, while the second calculates energy consumption for cargo vehicles.

$$\begin{aligned} E_{\mathrm{t,f,c,y}} = & \sum_{v \in V_{\mathrm{pass}}} \sum_{r \in R} \sum_{d \in D} p_{\mathrm{v,c,y}} \times o_{\mathrm{v,c}} \times s_{\mathrm{v,c,r}} \times m_{\mathrm{v,d,y}} \times k_{\mathrm{r,v,d,f,y}} \times e_{\mathrm{v,d,f,y}} \times \tau_{\mathrm{t,v,f}} \\ & + \sum_{v \in V_{\mathrm{cargo}}} \sum_{r \in R} \sum_{d \in D} t_{\mathrm{v,c,y}} \times l_{\mathrm{v,c}} \times s_{\mathrm{v,c,r}} \times m_{\mathrm{v,d,y}} \times k_{\mathrm{r,v,d,f,y}} \times e_{\mathrm{v,d,f,y}} \times \tau_{\mathrm{t,v,f}} \end{aligned} \tag{3.1}$$

The resultant loadshape is added to a given fuel type demand and is used as an input to the DOLPHYN model.

3.3 Supply-side Model Description

This section describes the modeling of the liquid fuels, including SFs within the supply-side model, DOLPHYN. DOLPHYN represents a multi-vector energy system in the form of a mixed-integer linear programming (MILP) optimization model. The full documentation of the DOLPHYN model can be found here [9]. Figure 3.2 shows a detailed diagram of DOLPHYN, including all the technologies modelled. While this work has resulted in contributions to the power, H_2, and CO_2 supply chains, the liquid fuel modelling represents a novel addition to DOLPHYN. Additionally, those works are documented elsewhere such as in [9], [30]–[32]. The CO_2 supply chain modelling, will be documented in detail in later work.

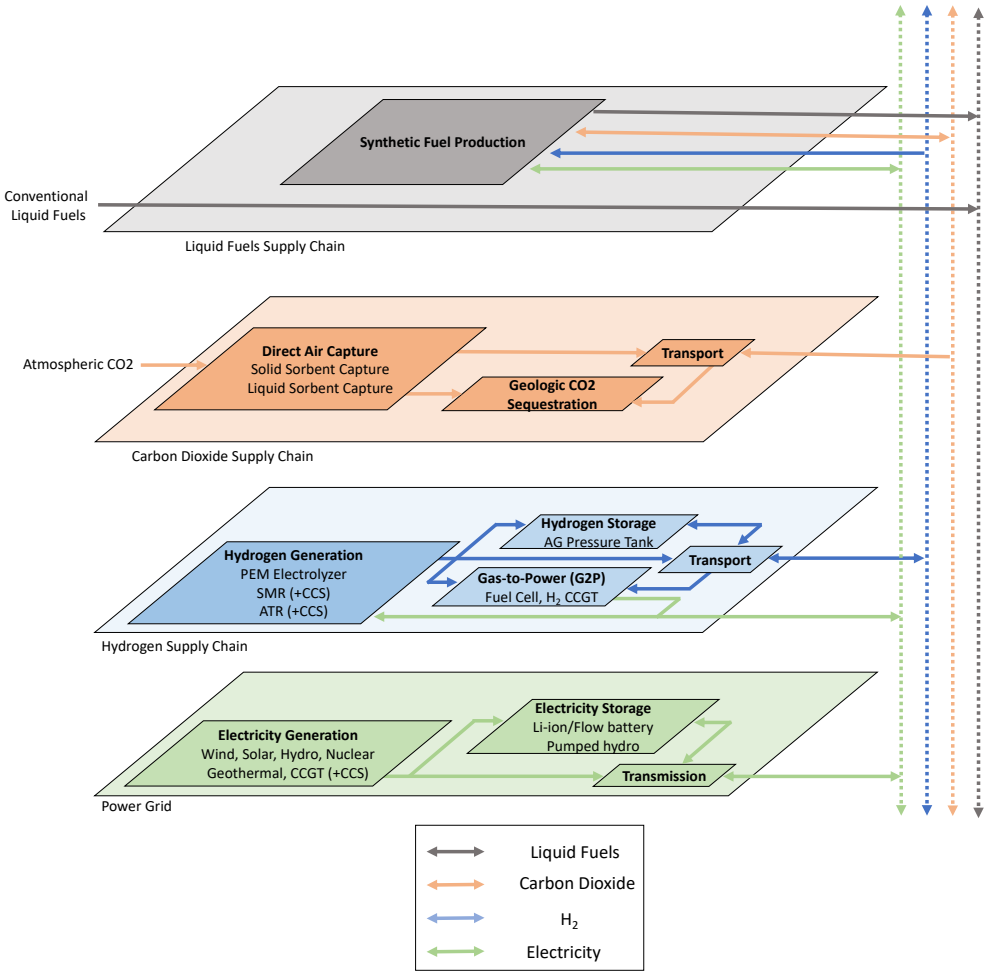

Figure 3.2: Overview of supply-side modelling details used for this study including all the technologies modelled. The color of arrows highlight various vectors – green: electricity, blue: H_2, orange: CO_2, grey: fuels. This diagram is adapted from a simillar diagram created by Jun Wen Law, Nicole Shi, and Dharik Mallapragada.

3.3.1 Liquid Fuel Model Formulation[1]

This section describes the formulation of the liquid fuels supply chain. To meet a specific demand of liquid fuels, the model has a choice to utilize conventional (fossil-based) or SFs. Synthetic fuel production arises from a set of resources F. Synthetic fuel plant performance is parameterized in terms of CO_2 input into the process. The model is set-up to account for up to 3 liquid fuel products: diesel, gasoline, and jetfuel. The user can also model an unlimited number of synthetic fuel process by-products. The by-product feature is designed to account for emissions and economic value of byproducts for which there is no exogeneous demand modeled. The emissions associated with these byproducts are accounted for the emissions balances, while the revenue from the sale of by-products are accounted for in the objective function. Any of the 3 modelled liquid fuels can also be modelled as by-products, in the case they are not explicitly modelled. In the case of this study, jet fuel demand is not modelled, and therefore jet fuel is considered a byproduct.

Liquid Fuel Model Notation

Notation	Description
$z \in \mathcal{Z}$	z denotes a zone, and $\mathcal{Z}$ is the set of zones in the network
$t \in \mathcal{T}$	t denotes a time step, and $\mathcal{T}$ is the set of time steps
$f \in \mathcal{F}$	Index and set of all synthetic fuels resources
$\mathcal{F}^z \in F$	Index and set of synthetic fuels resources in zone z
$k \in K$	k denotes a liquid fuel or by-products modelled in a set of all liquid fuels or by-products modelled K
$L \in K$	L denotes a subset containing liquid fuels modelled excluding by-products
$B \in K$	L denotes a subset containing by-products modelled excluding liquid fuels
$l \in \mathcal{L}$	Index and set of all liquid fuels modelled. Currently three liquid fuels are modelled (gasoline, diesel, and jetfuel).
$b \in \mathcal{B}$	Index and set of all synthetic fuels process byproducts

Table 3.4: Liquid Fuel Model Sets and Indices

Objective function

The total cost associated with the liquid fuel infrastructure includes four main elements as shown in equation 3.2 : 1) the capital cost of synthetic fuel production (see equation 3.3) 2) the operating cost of synthetic fuel production (see equation 3.4) 3) production credits for any byproducts that are not explicitly modelled (see equation 3.5), and 4) the cost of procuring liquid fossil fuels (see equation 3.6). These terms are added to the overall multi-sectoral model objective function, which includes cost associated with infrastructure for other vectors.

[1]This section is adapted from documentation of the liquid fuels module in DOLPHYN [9]. The modeling of liquid fuels was a result of a collaborative effort between Youssef Shaker and Jun Wen Law.

Notation	Description
$x^{\text{C,Syn}}_{f,t}$	CO_2 input into synthetic fuels resource f at time period t in tonnes of CO_2
$x^{\text{Syn}}_{f,l,t}$	Synthetic fuel l produced by resource f at time period t in MMBTU
$x^{\text{By,Syn}}_{f,b,t}$	Byproduct b produced by synthetic fuels resource f at time period in MMBTUt
$y^{\text{C,Syn}}_{f}$	Capacity of synthetic fuels resources in the liquid fuels supply chain in tonnes of CO_2/hr
$x^{\text{Conv}}_{z,t,l}$	Conventional fuel l purchased by zone z at time period t in MMBTU

Table 3.5: Liquid Fuel Model Decision Variables

Notation	Description
$D_{z,t,l}$	Demand for fuel l in zone z at time t
ζ_l	Percentage of fuel l that needs to be fulfilled using synthetic fuels
$\text{c}^{\text{Syn,INV}}_{f}$	Investment cost per tonne CO_2 input of synthetic fuels resource f
$\text{c}^{\text{Syn,FOM}}_{f}$	Fixed operation cost per tonne CO_2 input of synthetic fuels resource f
$\text{c}^{\text{Syn,VOM}}_{f}$	Variable operation cost per tonne of CO_2 input by synthetic fuels resource f
$\text{c}^{\text{Syn,FUEL}}_{f}$	Fuel cost per tonne of CO_2 input by synthetic fuels resource f
$\text{c}^{\text{By,Syn}}_{b}$	Selling price per mmbtu of byproduct by synthetic fuels resource (if any)
$\text{c}^{\text{Conv}}_{l}$	Purchase cost per mmbtu of conventional fuel
$\overline{y}^{\text{C,Syn}}_{f}$	If upper bound of capacity is defined, then we impose constraints on the maximum CO_2 input capacity of synthetic fuels resource
$\underline{y}^{\text{C,Syn}}_{f}$	If lower bound of capacity is defined, then we impose constraints on the minimum CO_2 input capacity of synthetic fuels resource
$\tau^{liquid}_{l,f}$	Amount of fuel l produced per tonne of CO_2 input at synfuel resource f
$\tau^{Byproduct}_{b,f}$	Amount of by-product b produced per tonne of CO_2 input at synfuel resource f
p^{power}_{f}	Power MWh per tonne of CO_2 in required for the plant f
$p^{hydrogen}_{f}$	H_2 tonnes per tonne of CO_2 in required for the plant f
μ^{emit}_{f}	Percentage of CO_2 emitted of the CO_2 in for a plant f
$\mu^{capture}_{f}$	Percentage of CO_2 captured of the CO_2 in for a plant f
λ_f	Emissions of plant fuel per tonne of CO_2 in for plant f
θ^{liquid}_{l}	Emissions per mmbtu for liquid fuel l
$\theta^{Byproduct}_{b}$	Emissions per mmbtu for by-product b
ω_t	Time-step weight for time-step t

Table 3.6: Liquid Fuels Model Parameters Description

$$min\ \mathrm{C}^{\mathrm{LF,Syn,c}} + \mathrm{C}^{\mathrm{LF,Syn,o}} - \mathrm{C}^{\mathrm{LF,Syn,r}} + \mathrm{C}^{\mathrm{Conv,o}} \tag{3.2}$$

The fixed costs associated with synthetic fuel production is defined such that:

$$\mathrm{C}^{\mathrm{LF,Syn,c}} = \sum_{f \in \mathcal{F}} y_f^{\mathrm{C,Syn}} (\times \mathrm{c}_f^{\mathrm{Syn,INV}} + \mathrm{c}_f^{\mathrm{Syn,FOM}}) \tag{3.3}$$

The variable costs associated with synthetic fuel production is defined such that:

$$\mathrm{C}^{\mathrm{LF,Syn,o}} = \sum_{f \in \mathcal{F}} \sum_{t \in \mathcal{T}} \omega_t \times \left(\mathrm{c}_f^{\mathrm{Syn,VOM}} + \mathrm{c}_f^{\mathrm{Syn,FUEL}} \right) \times x_{f,t}^{\mathrm{C,Syn}} \tag{3.4}$$

The credit associated with by-products is defined such that:

$$\mathrm{C}^{\mathrm{LF,Syn,r}} = \sum_{f \in \mathcal{F}} \sum_{b \in \mathcal{B}} \sum_{t \in \mathcal{T}} \omega_t \times x_{f,b,t}^{\mathrm{By,Syn}} \times \mathrm{c}_b^{\mathrm{By,Syn}} \tag{3.5}$$

The cost of conventional fuels is defined such that:

$$\mathrm{C}^{\mathrm{Conv,o}} = \sum_{z \in \mathcal{Z}} \sum_{l \in \mathcal{L}} \sum_{t \in \mathcal{T}} \omega_t \times \mathrm{c}_l^{\mathrm{Conv}} \times x_{z,t,l}^{\mathrm{Conv}} \tag{3.6}$$

Synthetic Fuel Production Constraints

The amount of SF produced at a given time-step is given by:

$$x_{f,l,t}^{\mathrm{Syn}} = x_{f,t}^{\mathrm{C,Syn}} \times \tau_{l,f}^{liquid} \quad \forall f \in F, t \in T, l \in L \tag{3.7}$$

The amount of byproducts produced at a given timestep is given by:

$$x_{f,b,t}^{\mathrm{Syn}} = x_{b,t}^{\mathrm{C,Syn}} \times \tau_{b,f}^{By} \quad \forall f \in F, t \in T, b \in B \tag{3.8}$$

For resources where upper bound $\overline{y_f^{\mathrm{C,Syn}}}$ and lower bound $\underline{y_f^{\mathrm{C,Syn}}}$ of capacity is defined, then we impose constraints on minimum and maximum SF resource input CO_2 capacity.

$$\underline{y_f^{\mathrm{C,Syn}}} \leq y_f^{\mathrm{C,Syn}} \leq \overline{y_f^{\mathrm{C,Syn}}} \quad \forall f \in \mathcal{F}$$

The required capacity is given by the following constraint such that the amount of CO_2 flowing into the plant does not exceed the plant's capacity:

$$x_{f,t}^{\mathrm{C,Syn}} \leq y_f^{\mathrm{C,Syn}} \quad \forall f \in \mathcal{F}, t \in \mathcal{T} \tag{3.9}$$

Liquid Fuels Balance Constraints

For each of the liquid fuels the following constraint is implemented to ensure that a sufficient combination synthetic fuel production and conventional liquid fuel procurement occurs to meet demand:

$$\sum_{z\in\mathcal{Z}}\sum_{t\in\mathcal{T}}\omega_t \times x^{\text{Conv}}_{z,t,l} + \sum_{f\in\mathcal{F}}\sum_{t\in\mathcal{T}}\omega_t \times x^{\text{C,Syn}}_{f,l,t} >= \sum_{z\in\mathcal{Z}}\sum_{t\in\mathcal{T}} D_{z,t,l} \quad \forall l \in L$$

(3.10)

Note that only one constraint is implemented across all zones and time-steps. This is to reflect the flexibility and interconnectedness of liquid fuel supply chain. The cost of transporting liquid fuels is already included in cost estimates, and is therefore not accounted for separately. Moreover, because this modeling approach presumes that the product distribution from synthetic fuel production cannot be changed without impacting the energy inputs or capital cost of the process, the amount of each fuel produced can potentially exceed the amount demanded. In this case, the fuel production is penalized from an emission perspective, without meeting any specific demand. Finally, because one constraint is implemented across all timesteps and zones, storage is not accounted for.

Additionally, to reflect possible synthetic fuel mandates, the following constraint is used to force the model to produce a specific amount of synfuels as a percentage of demand, if a specific fuel mandate is specified:

$$(\zeta_l - 1) \times \sum_{f\in\mathcal{F}}\sum_{t\in\mathcal{T}}\omega_t \times x^{\text{C,Syn}}_{f,l,t} + \zeta_l \times \sum_{z\in\mathcal{Z}}\sum_{t\in\mathcal{T}}\omega_t \times x^{\text{Conv}}_{z,t,l} = 0 \tag{3.11}$$

This is just a reorganization version of the following formula in a way that avoids nonlinearities:

$$\sum_{f\in\mathcal{F}}\sum_{t\in\mathcal{T}}\omega_t \times x^{\text{C,Syn}}_{f,l,t} / (\sum_{f\in\mathcal{F}}\sum_{t\in\mathcal{T}}\omega_t \times x^{\text{C,Syn}}_{f,l,t} + \sum_{z\in\mathcal{Z}}\sum_{t\in\mathcal{T}}\omega_t \times x^{\text{Conv}}_{z,t,l}) = \zeta_l \tag{3.12}$$

Note that only one synthetic fuel product percentage can be specified, otherwise, the model will become infeasible.

Synthetic Fuel Power Balance Term

The following expression reflects the power consumption associated with synthetic fuel production in a given zone that is added to the overall system power supply and demand balance at each time step and zone:

$$BalPowerLiquidFuel_{z,t} = \sum_{f\in F^z} \omega_t \times x^{\text{C,Syn}}_{f,t} \times p^{power}_f \quad \forall z \in Z, t \in T \tag{3.13}$$

This term is added to the overall power balance of the multi-sectoral model.

Synthetic Fuel H_2 Balance Term

The following expression reflects the H_2 consumption associated with synthetic fuel production in a given zone:

$$BalHydrogenLiquidFuel_{z,t} = \sum_{f \in F^z} \omega_t \times x_{f,t}^{\mathrm{C,Syn}} \times p_f^{hydrogen} \quad \forall z \in Z, t \in T \tag{3.14}$$

This term is added to the overall H_2 balance of the multi-sectoral model.

Liquid Fuel Emissions Balance Terms

The following expression shows the emissions associated with the liquid fuel production and consumption process. It is made up of 4 terms: 1) the component of CO_2 input into the plant that is released into the atmosphere during the fuel production process 2) emissions from the consumption of SF (all SFs produced are consumed even if there is no demand for them) 3) emissions from the consumption of byproducts of SFs production process, and 4) emissions from the consumption of conventional liquid fuels. This terms is added to the overall multi-sectoral CO_2 balance constraint.

$$\begin{aligned} BalEmissionsLiquidFuel_z = & \sum_{f \in F^z} \sum_{t \in \mathcal{T}} \omega_t \times x_{f,t}^{\mathrm{C,Syn}} \times \mu_f^{emit} \\ & + \sum_{f \in F^z} \sum_{t \in \mathcal{T}} \omega_t \times x_{f,t,l}^{\mathrm{Syn}} \times \theta_l^{liquid} \\ & + \sum_{f \in F^z} \sum_{t \in \mathcal{T}} \omega_t \times x_{b,t,l}^{\mathrm{Syn}} \times \theta_b^{Byproduct} \\ & + \sum_{t \in \mathcal{T}} \omega_t \times x_{l,z,t}^{\mathrm{Conv}} \times \theta_l^{liquid} \quad \forall z \in Z \end{aligned} \tag{3.15}$$

The following expression shows the emissions captured with the liquid fuel production and consumption process. It is made up of 2 terms: 1) the component of CO_2 input into the plant from all captured emissions, which is taken from the CO_2 captured in the system 2) emissions captured from the synthetic fuel plant. This term is added to the multi-sectoral CO_2 captured expression, which includes CO_2 captured from H_2 and power producing plants, as well as DAC.

$$\begin{aligned} BalEmissionsCapturedLiquidFuel_z = & - \sum_{f \in F^z} \sum_{t \in \mathcal{T}} \omega_t \times x_{f,t}^{\mathrm{C,Syn}} \\ & + \sum_{f \in F^z} \sum_{t \in \mathcal{T}} \omega_t \times x_{f,t}^{\mathrm{C,Syn}} \times \mu_f^{capture} \quad \forall z \in Z \end{aligned} \tag{3.16}$$

3.4 Case study: Western European decarbonization scenarios for 2040

The developed models are applied to the case study of Western Europe (Germany, France, the United Kingdom, Belgium, the Netherlands, Denmark, Sweden, and Norway) using a transportation energy demand model, and a 10-zone network representation for power, H_2, and CCUS supply chains. The network is shown in Figure 3.3. This region is central to European decarbonization efforts due to the availability of high quality onshore and offshore wind resources, domestic natural gas supply, and CO_2 sequestration potential. Countries in the region have also shown a significant commitment towards decarbonization and a willingness to invest in a H_2 supply chain (European Commission 2019). Starting with a brownfield power sector representation (i.e. existing power transfer capacity between zones and existing generation capacity), we explore the least-cost system outcomes for alternative technology, demand, and policy scenarios for 2040. Since we are focused on transportation energy demand and its energy system impacts, we fix the annual non-road transport electricity and H_2 demand for the region to be equal to the projections available from ENTSOE for their Distributed Energy Scenario at 2,081 TWh and 468 TWh, respectively [33]. The models sizes were around 6.5 million rows and 3.5 million columns with 24 million non-zero entries. Table 3.7 contains major case study assumptions.

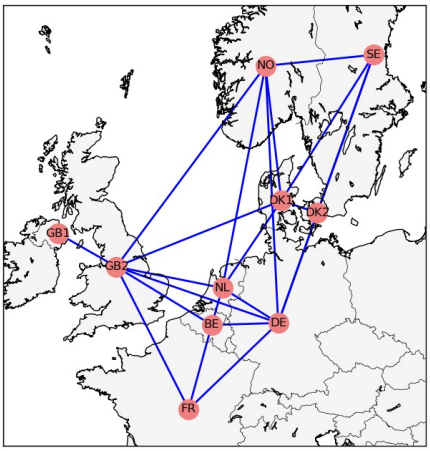

Figure 3.3: 10-zone model of the Western European region. The lines connecting the zones represent existing power transmission paths between the various zones. The transfer capacity across these transmission paths is a model decision variable.

3.5 Demand-side Model Inputs

This section will cover key demand-side model inputs. To begin with, vehicle category demand is constructed based on EU Reference scenarios for the year 2040 [35]. The scenarios provide the service demand in pkm and tkm for 4 vehicle categories. Demand for the UK

Table 3.7: Major case study assumptions. More details on demand-side input assumptions can be found in Section 3.5. Details on supply-side assumptions can be found in Section 3.6. Non-transportation demand is based on [34]. Transportation demand is an output of transportation demand model. Fuel price details can be found in Section A.5.

Parameter	Value
2040 Non-transportation Electric Demand	2,080.99 TWh
2040 Non-transportation H_2 Demand	468.39 TWh
2040 Non-HDV Transportation Energy Demand	381.66 TWh
2040 Non-HDV Transportation Electric Demand	303.15 TWh
Natural Gas Price	8.56 EUR/GJ
Fossil Gasoline Price	0.84 EUR/L
Fossil Diesel Price	0.93 EUR/L
Discount Rate	4.5%

and Norway is not directly available using the EU reference scenario; we therefore utilize demand from similar countries, Germany and Sweden, respectively, adjusted by population.

We then further disaggregate the demand for these vehicle categories into vehicle types as listed in table 3.1. This disaggregation is crucial as a vehicle tonnage and size affects its energy consumption. Vehicle demand is disaggregated on the basis of vehicle size for passenger vehicles and payload capacity for freight vehicles using TRACCS, a survey on transportation demand consumption [36].

To convert transportation service demand to distance demand, loading factors based on Eurostat are used. Payload factors from TRACCS energy demand inconsistent with historical data. Table 3.8 shows the loading factors used for each HDV & LCV vehicle category.

Table 3.8: Vehicle Payload by Category and Type

Vehicle Category	Vehicle Type	Vehicle Payload (Tonnes)
HDV & LCVs	LCV	0.40
	HDV - Light	1.36
	HDV - Medium	5.51
	HDV - Heavy	6.65
	HDV - Super Heavy	12.52
	HDV - Ultra Heavy	15.12

Additionally, the amount of vehicle distance travelled in each road type is based on [13], and is as shown in table 3.9.

The baseline market shares for each vehicle drive-train type are based on [13], and are modified throughout the scenarios as outlined in section 3.7. For plug-in hybrid electric vehicles, it is assumed that all urban distance utilizes electricity, and the rest of the distance

Table 3.9: Vehicle Road Type Share by Vehicle Category and Vehicle Type Based on [13]

Vehicle Category	Vehicle Type	Road Type Share		
		Rural	Urban	Highway
Buses and Coaches	Buses	0.6	0.3	0.1
	Coaches	0.12	0.59	0.29
Passenger Cars	All	0.3	0.45	0.25
Two-wheelers	All	0.3	0.45	0.25
HDV & LCVs	HDVs	0.12	0.25	0.63
	LCVs	0.42	0.3	0.28

utilizes liquid fuel (gasoline for passenger vehicles, and diesel for the rest). Table 3.10 shows the baseline market shares for each drivetrain type.

Table 3.10: Vehicle Baseline Market Share by Vehicle Category and Vehicle Type. The market share is divided by drivetrain type. Based on [13].

Vehicle Category	Vehicle Type	Market Share			
		Diesel	Electric	H_2	Hybrid Electric
Buses and Coaches	Buses		1		
	Coaches		0.4		0.6
Passenger Cars	Small		1		
	Medium		1		
	Large		0.5		0.5
Two-wheelers	Two-wheelers		1		
HDV & LCVs	LCV		0.6		0.4
	HDV - Light		0.6		0.4
	HDV - Medium	0.6			0.4
	HDV - Heavy	0.6			0.4
	HDV - Super Heavy	0.6			0.4
	HDV - Ultra Heavy	0.6			0.4

Finally, to convert vehicle distance demand into energy demand, we utilize energy consumption factors from the EU reference scenarios technology assumptions [37].

Non-electric demand for HDV and LCV energy is assumed to be flat, while electric demand assumed a loadshape based on the ENTSOE TYDNP study [34]. For this study, no efficiency multipliers are utilized.

3.6 Supply-side Model Inputs

This section will cover key supply-side model inputs. Further details can be found in Appendix A.

Table 3.11: Vehicle Energy Consumption by Vehicle Category and Vehicle Type (MJ/km). The energy consumption depends on the mode the vehicle is operating in. Based on [37].

Vehicle Category	Vehicle Type	Energy Consumption (MJ/vkm)			
		Diesel	Gasoline	Electric	H_2
Buses and Coaches	Buses			4.14	
	Coaches	9.99		4.14	
Passenger Cars	Small			0.50	
	Medium			0.54	
	Large SUV		2.70	0.65	
Two-wheelers	Two-wheelers			0.22	
HDV & LCVs	LCV	2.62		0.61	
	HDV - Light	4.98		2.02	
	HDV - Medium	7.18		2.66	4.32
	HDV - Heavy	10.07		4.68	6.72
	HDV - Super Heavy	13.87		5.94	9.12
	HDV - Ultra Heavy	13.87		5.94	9.12

The power system representation of this study is based on a brownfield representation of the European Grid, adapted from the representation used in the PYPSA-EUR model and data set [38]. PyPSA-EUR is a state-of-art capacity expansion model developed by researchers at TU Berlin, that also includes detailed data set for the European energy system. The existing available generation is based on data from the ENTSOE transparency platform [33]. No retirements are assumed. Costs and operational assumptions for power generation technologies are based on the NREL Annual Technology Baseline 2022 (using data for the year 2040, medium case) and Sepulveda et al. [39], [40]. The maximum available generation capacity and temporally resolved capacity factors associated with the VRE generation technologies is based on PYPSA-EUR data set. Additionally, we assume that existing power transfer capacities between regions can be expanded by up to 4 times. New power lines are assumed to have a maximum capacity of 5,000 MW. A greenfield representation of the H_2 and CO_2 systems are utilized for this study. THe candidate set of pipelines for CO_2 and H_2 pipelines is made up of all the possible combinations of zones (i.e. it is assumed that a pipeline could be built between any two modelled zones).

Since the focus of this is study is road transportation, the supply-side model considers supply-demand balance for two liquid fuels; diesel and gasoline. We assume that liquid fuel demand can be met in one of two ways. The first is using conventional hydrocarbons purchased at an exogeneously specified price (see Table 3.7) and the second is through SFs based on syngas production from CO_2 and H_2 followed by Fischer-Tropsch synthesis. Three SF plant configurations are modeled, summarized in Table 3.12: A) baseline SF plant based on Zang et al. and James et al. with 44% of the feed carbon recovered as liquid fuel, B) high CO_2 capture variant of the process described in Zang et al. where a portion of the vented CO_2 is captured for sequestration purposes and C) high fuel production variant of the process where a portion of the vented CO_2 is captured and recycled to syngas

generation unit to enhance liquid fuel production [25], [41], [42]. This option also results in increased use of H_2 for SF production as shown in Table 3.12. While technology cost and performance assumptions for option A are sourced from Zang et al. [25], those for option B are developed by combining the SF process configuration from Zang et al. with the CCS cost and performance assumptions from a natural gas power plant carbon capture study [25], [41]. The assumptions for option C is developed by assuming that the vented CO_2 is captured in a process similar to option B, but that the captured CO_2 is used as feed to the SF process instead of being stored. The model is allowed to choose between these 3 options as part of the optimization.

Additional co-product (i.e. jet fuel) from the SF production facility, for which we do not model an exogeneous demand, is credited for its market value in the objective function of the supply-side model and is included as an emissions source in the emissions constraint.

Table 3.12: Cost and performance assumptions for synthetic fuel production with different levels of CO_2 utilization. Process information for the right two plant scenarios is generated by approximately accounting for the cost and emissions for CO_2 capture from the flue gas produced by the baseline plant, using data for flue gas CO_2 capture for a natural gas combined cycle power plant [25], [41]. Some minor modifications for processes from original sources are made to ensure facility carbon balance is satisfied for the specified fuel carbon intensities. The carbon intensities of the diesel, gasoline, and jet fuel are 70, 67, and 68 kg of CO_2/GJ, respectively.

Syn Fuel Production Technology	Option A: Baseline Synfuel Plant	Option B: Synfuel Plant w/ Capture	Option C: Synfuel Plant w/ Capture and Recycling
CAPEX (MEur/MW of Fuel Out)	2.01	3.15	3.15
CO_2 Emissions (Tonnes of CO_2 / Tonne of CO_2 Feed)	0.56	0.06	0.11
H_2 Consumption (GJ of H_2 / Tonne of CO_2 Feed)	10.7	10.7	21.4
Electricity Consumption (GJ of Electricity / Tonne of CO_2 Feed)	0.13	0.39	0.76
Diesel Out (GJ / Tonne of CO_2 Feed)	1,879	1,879	3,687
Gasoline Out (GJ / Tonne of CO_2 Feed)	1,780	1,780	3,493
Jet Fuel Out (GJ / Tonne of CO_2 Feed)	3,204	3,204	6,288

We model DAC technologies based on solid-sorbent and solvent based schemes as per the cost and performance assumptions developed by NETL [43]. We model CO_2 geological sequestration sites and capacities as per the data available saline aquifers from the EU GeoCapacity project [43]. The model is allowed to invest in CO_2 pipelines to connect CO_2 sources and sinks.

Table 3.13 summarizes the list of technologies considered across various sectors in the supply-side modeling efforts.

Table 3.13: Summary of technologies considered in the supply-side analysis. **Bolded resources** have spatially-resolved capacity deployment limits. *Italicized resources* are not considered for expansion. CCGT w CCS, SMR w CCS, and ATR w CCS capture rates are 95.0%, 96.2%, and 94.5%, respectively. Detailed technology cost and performance assumptions are provided in Appendix A

Sector	Technologies considered
Power	**Utility-scale VRE**, CCGT w & w/o CCS, OCGT, Nuclear, Coal, Lignite, *Hydro*, *Pumped Hydro*, *Biomass*, Li-ion storage, **Transmission**
H_2	Steam Methane Reforming (SMR) w and w/o CCS, Autothermal Reforming (ATR) w CCS, Electrolyzer, Tank H_2 storage, CCGT-H_2, H_2 pipelines
CO_2	Direct air capture (DAC), CO_2 transport pipelines, and **CO_2 geological storage**
Liquid Fuels	Conventional Fuels, Synthetic Fuels

3.7 Scenarios evaluated

We evaluated alternative scenarios spanning different assumptions for compressed H_2 use for HDV transportation, minimum levels of SF utilization, and CO_2 sequestration availability, as shown in Figure 3.4. The evaluated CO_2 emissions constraint of 103 MTonne represents a high degree of deep decarbonization for power and transportation sectors. To contextualize the magnitude of the emission limit, 103 MTonnes, it corresponds to almost 90% reduction in electricity and heat production, and road transportation sector emissions relative to 2019 levels. Emission limits are enforced jointly across sectors, which allows for emissions trading across sectors.

To test the impact of CO_2 sequestration availability on model outcomes, we consider a baseline CO_2 sequestration potential scenario, which allows for up to 650 $MtCO_2$/year of sequestration distributed across the modelled region and an alternative scenario where no CO_2 sequestration is available. Widespread availability of CO_2 sequestration is likely to incentivize adoption of carbon capture technologies, while their limited availability could motivate greater reliance on renewable energy adoption and CO_2 utilization via SF.

To isolate the energy system impacts of H_2 and synthetic fuel use for HDVs, we evaluated the model across different H_2 and SF adoption. We create a baseline case (no H_2 HDV, no SFs HDV, bottom left in Figure 3.4) where all the HDV demand is met either through diesel either via internal combustion engine vehicles or PHEVs. For the purposes of this study, we assume that the percentage of plug-in hybrid EV-diesel vehicles and other EVs is static. The amount of H_2 HDVs is varied between none to medium to high, which is equivalent to 0%, 50%, and 100% of the demand satisfied by the diesel ICE vehicles in the baseline scenario.

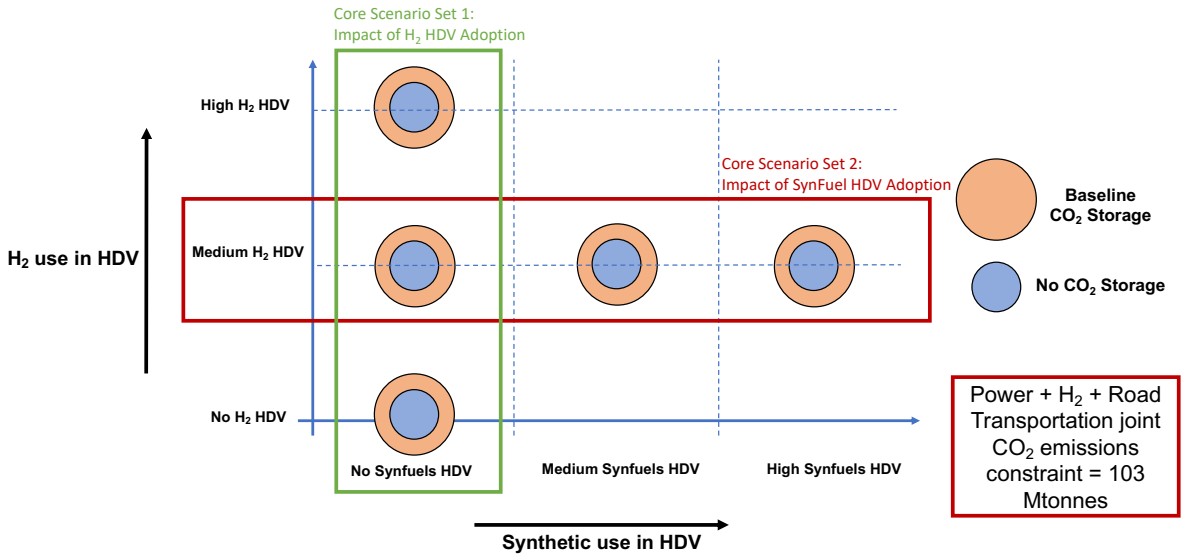

Figure 3.4: Summary study scenarios. Each bubble represents a scenario. The y-axis represents varying levels of H_2 HDV adoption (between 0 and 142 TWh of H_2 consumption), while the x-axis represents varying levels synthetic fuel adoption (between 0 and 128 TWh of Synthetic Diesel consumption). All scenarios are equivalent from an emissions capping perspective with a cap of 103 $MTCO_2$. HDV fleet represents all vehicle types with gross weight greater than 7.5 tonnes. Baseline CO_2 storage corresponds to maximum annual CO_2 storage injections equal to 650 $MtCO_2$/year. More details on the transportation demand scenarios can be found in 3.5 and 3.6. Synfuel = SF

Figure 3.5 shows the results of the demand-side model for the varying levels of H_2 HDV adoption. Similarly, the amount of SF use in HDVs is varied between none to medium to high, which is equivalent to 0%, 25%, and 50% of diesel demand in the baseline scenario. Figure 3.6 shows the energy consumption broken down by fuel type for the second set of core scenarios. This scenario set is motivated by recent policy discussions in the EU that utilize synthetic fuel production as part of a set of transportation sector decarbonization policies [44].

For these transportation energy demand scenarios, a few key points are to be noted: a) all scenarios assume a fixed amount of electricity use for LDV and some segments of HDV with a high degree of electrification (illustrated in Figure 3.5). This also implies that gasoline consumption for road transportation also remains constant across the scenarios, b) scenarios with increasing H_2 adoption leads to reduced end-use diesel consumption, c) HDV energy consumption represents a 36-42% of modeled road transportation energy consumption.

In addition to the core set of scenarios outlined above, we ran 4 additional sets of sensitivity scenarios summarized in table 3.14. The first is the based on core scenario set 1, but with a relaxed emissions constraint (258 $MtCO_2$ or roughly 25% reduction level compared to 2019 emissions from transport, power and heat production), as shown in Figure C.1. The second is based on core scenario set 1, but with sensitivities around natural gas price, +/- 30% of the baseline scenario natural gas price, as shown in Figure C.6. Natural gas price is

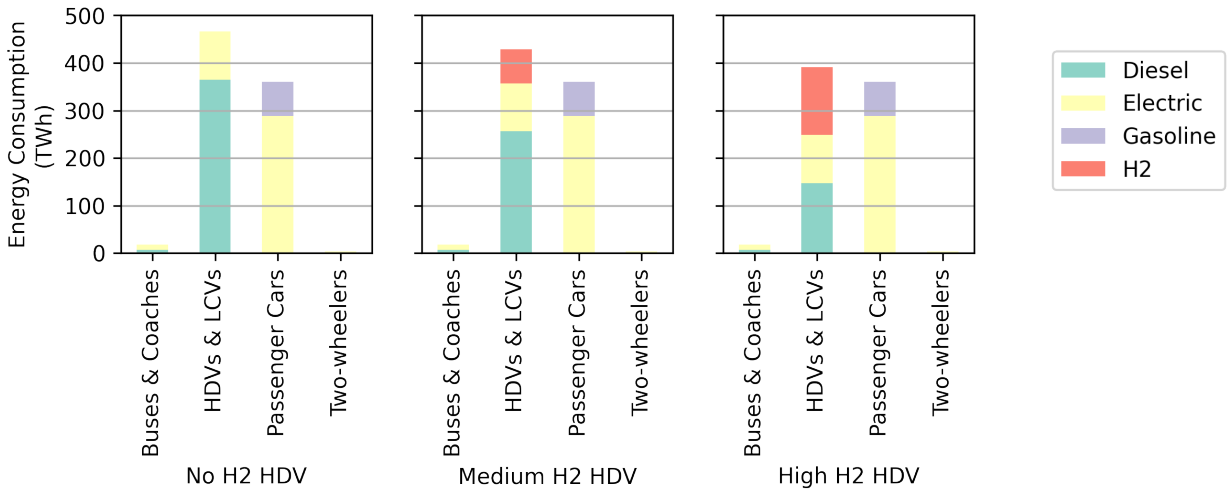

Figure 3.5: Transportation final energy consumption across different H_2 HDV adoption scenarios. HDV energy use included in the category Heavy-duty Vehicles and Light Commercial Vehicles (HDVs & LCVs), representing 71-76% of the category's energy consumption, and 36-42% of road transportation energy consumption.

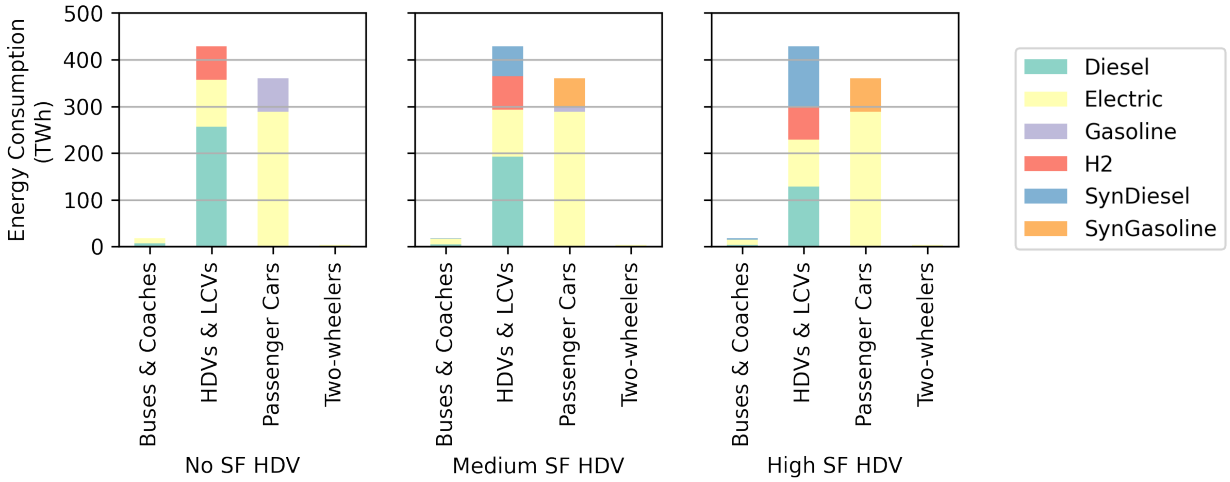

Figure 3.6: Transportation final energy consumption across different SF HDV adoption scenarios at medium H_2 HDV adoption. HDV energy use included in the category Heavy-duty Vehicles and Light Commercial Vehicles (HDVs & LCVs).

a key input as the relative price between natural gas and electricity determines the type of H_2 production, while the relative price between natural gas and liquid fuels determines the cost-effectiveness of H_2 and SF-based transportation decarbonization solutions.

The third sensitivity set focuses on the impact of lower levels of H_2 adoption in the transport sector. Here, we use the same assumptions as the core scenario set 2, but with a lower level of H_2 adoption C.14. Because the gross demand for diesel is higher in the absence of any H_2 adoption, the percentage of synthetic diesel out of diesel demand was adjusted to maintain the same gross amount of synthetic diesel demand across core scenario set 2 and

sensitivity set 3. The final set of sensitivities is the same as core scenario set 1, but with sensitivities around natural gas price, +/- 30% of the baseline scenario natural gas price, as shown in Figure C.19.

Table 3.14: Table summarizing sensitivity scenarios. Stringent emissions contraint refers to 258 $MtCO_2$ cap, while the relaxed emissions cap refers to the 103 $MTCO_2$ constraint. The baseline natural gas price is the price used in the core set of scenarios. The low and high natural gas prices are baseline -30% and +30%, respectively. More details on sensitivity cases and results can be found in Appendix 3.7

Scenario Set	H_2 HDV Adoption	SynFuel Adoption	Emissions Constraint	Natural Gas Price
Core Scenario Set 1	None, Medium, High	None	Stringent	Baseline
Core Scenario Set 2	Medium	None, Medium, High	Stringent	Baseline
Sensitivity Scenario Set 1	None, Medium, High	None	Relaxed	Baseline
Sensitivity Scenario Set 2	None, Medium, High	None	Stringent	Low, Baseline, High
Sensitivity Scenario Set 3	None	None, Medium, High	Stringent	Baseline
Sensitivity Scenario Set 4	Medium	None, Medium, High	Stringent	Low, Baseline, High

Chapter 4

Results

4.1 System impacts of H_2 adoption in HDVs

The power and H_2 generation impacts resulting from increasing H_2 adoption for HDVs under two CO_2 storage scenarios and without any SF utilization are highlighted in Figure 4.1 (see Figure 4.2 for capacity outcomes). In the absence of CO_2 storage, Figure 4.1 shows that the model produces an infeasible supply-side solution in the case of no H_2 use in HDVs. This infeasibility is a result of the emissions limit being lower than the CO_2 emissions associated with liquid fuel consumption in the transportation sector. Use of H_2 for HDVs, however, resolves the model infeasibility and leads to incremental H_2 supply via electrolytic hydrogen production that consumes 110.1 - 206.2 TWh of electricity or approximately 5.3 - 9.9% of non-H_2 sector electricity demand. Increasing the share of H_2 in HDVs from medium to high results in CO_2 emissions reduction in the transportation sector at the expense of increased power sector emissions through utilization of existing NG generation without CCS that displaces investments in wind and solar generation. For example, wind and solar generation share with high H_2 HDV is 75% compared to 77% in the medium H_2 HDV case. Moreover, this emissions trading across sectors results in a lower marginal abatement cost for the same emissions constraint (see Table S XX). In all cases, the maximum level of capacity deployment for VREs (including on-shore wind) is not reached for all regions.

The availability of CO_2 storage results in deployment of CCS technologies for power and H_2 generation as shown in Figure 4.1 which reduces the power sector impacts of H_2 adoption in HDV and also leads to a feasible solution without H_2 use. This is achieved via the deployment of DAC and CCS technologies in conjunction with CO_2 storage, as indicated in the CO_2 inflows in Figure 4.3. CO_2 storage availability also leads to deployment of CO_2 infrastructure, that is utilized by both DAC and CCS technologies in the power and H_2 sectors. Similar to the case without CO_2 storage, increasing H_2 use for HDVs leads to a greater role for gas-based power generation without CCS that comes at the expense of reduced liquid fuels in transport, gas generation with CCS and DAC deployment (Figure 4.3). At the same time, we see an increase in CCS-based H_2 production (greater carbon inflows in Figure 4.3) which highlights relative cost-effectiveness of deploying CCS in H_2 vs. power generation [45].

Despite achieving the same emissions target, scenarios with CO_2 storage result in: a)

greater overall CO_2 throughput as compared to scenarios without CO_2 storage, owing to greater total fossil fuel utilization (Figure 4.3 and 4.5) and b) lower marginal CO_2 abatement costs. The availability of CO_2 storage allows for greater NG consumption per unit of liquid fossil fuel displacement via H_2 across the medium to high H_2 use levels (Fig. 4.5 top panel). Despite these substitution effects, it is important to note that NG consumption in the scenarios are 61 - 65% lower than the 2019 levels. Additionally, the percentage of electricity produced by fossil fuel sources is 9.8 - 10.1% in our scenarios compared to 34% in 2015, despite a significant expansion of the power sector. It is worth noting that all CO_2 diagrams include all transportation emissions including non-HDV vehicle categories.

Comparing scenarios with and without CO_2 storage also reveals the complementary nature of VRE and electrolyzer deployment (Figure 4.1). This result, previously noted by other studies, is a result of the capability to operate electrolyzer in a flexible manner in conjunction with H_2 storage and H_2 pipelines, so as to maximize H_2 production during times and locations of low electricity prices, synonymous with abundant VRE electricity supply [45].

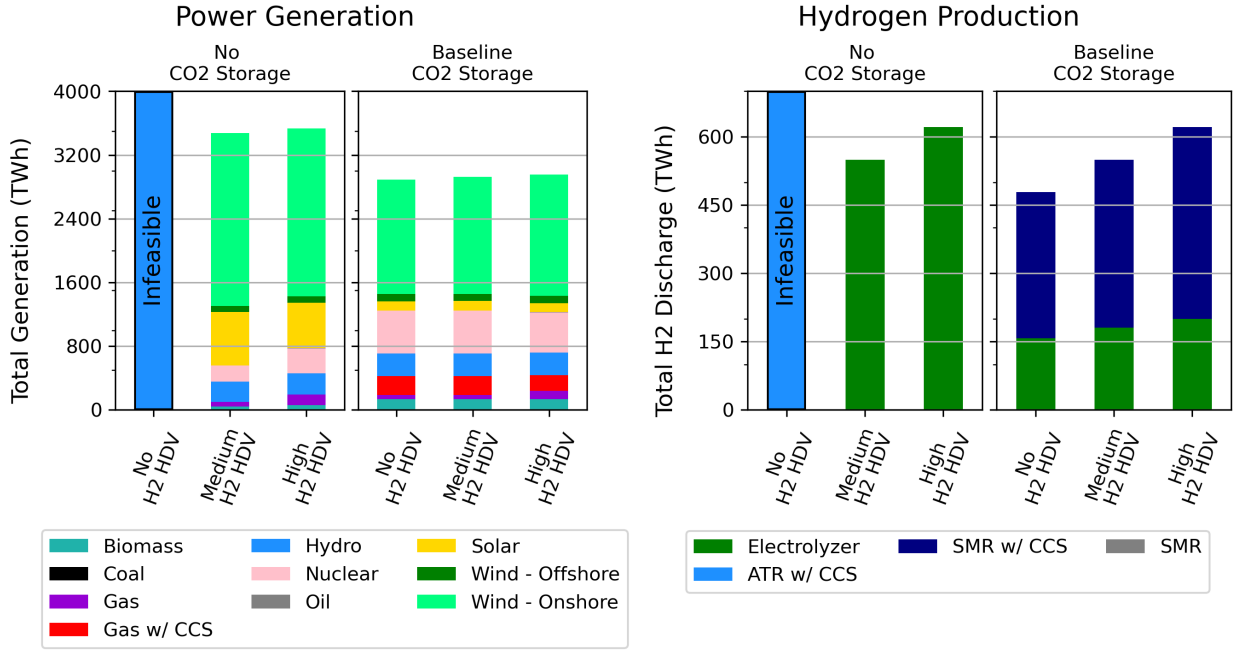

Figure 4.1: Power and H_2 generation for baseline and no CO_2 sequestration scenarios under no synthetic fuel adoption. The left set of charts shows power generation and the right set of charts shows H_2 generation. Within each panel, the amount of H_2 HDV adoption increases moving from left to right.

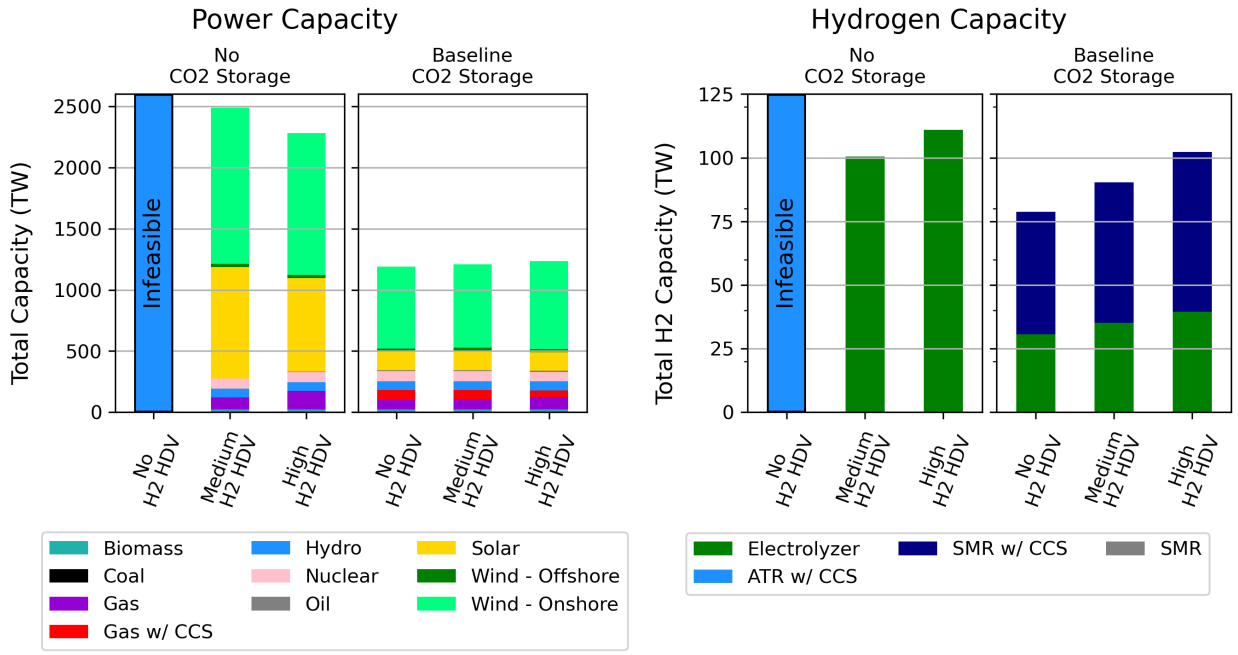

Figure 4.2: Power and H_2 capacity for baseline and no CO_2 sequestration scenarios under no synthetic fuel adoption. The left set of charts shows power generation and the right set of charts shows H_2 generation. Within each panel, the amount of H_2 HDV adoption increases moving from left to right.

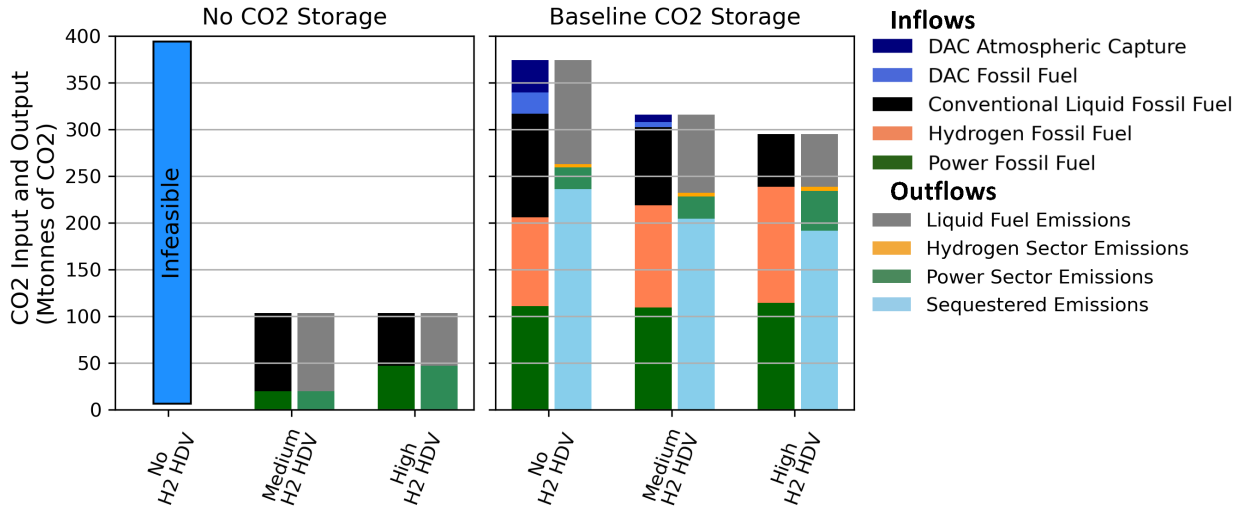

Figure 4.3: System CO_2 balance under varying levels of H_2 HDV adoption and no SF adoption. The subfigure on the left shows the CO_2 balance under no CO_2 sequestration availability, while the one on the right shows the CO_2 balance under baseline CO_2 storage availability. Within each subplot the H_2 HDV adoption level increases left to right. The leftward column represents CO_2 input into the system, while the rightward column represents CO_2 outputted by the system. This is a representation of Figure 5.1. All scenarios adhere to the same emissions constraint of 103 MTonnes. Emissions constraint can be calculated from the chart by subtracting sequestered emissions and DAC atmospheric capture from the emission outflows.

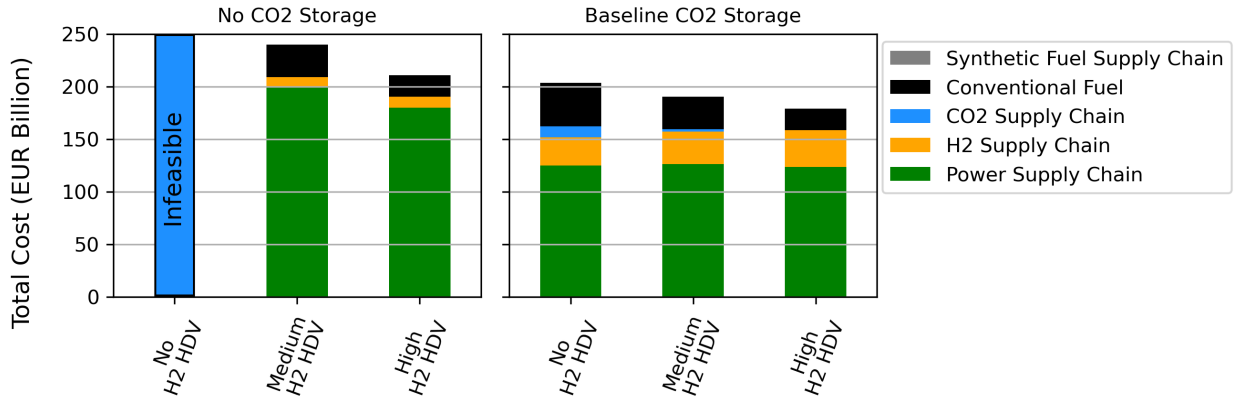

Figure 4.4: Annualized bulk-system costs under varying levels of H_2 HDV adoption and no SF adoption.The subfigure on the left shows the cost breakdown under no CO_2 sequestration availability, while the one on the right shows the cost breakdown under baseline CO_2 sequestration availability. Within each subplot the H_2 HDV adoption level increases left to right. The costs do not include vehicle replacement or H_2 distribution costs.

Irrespective of CO_2 storage availability, increasing H_2 use in the transportation sector reduces bulk energy system costs, with reductions of up to 6% observed when comparing the no H_2 HDV scenarios to the high H_2 HDV adoption scenarios. As seen in Figure 4.4,

the cost savings primarily stem from reduced liquid fuel consumption, but also lower power system costs due to reduced decarbonization of this sector and lower carbon supply chain costs due to the reduced reliance on DAC. These savings fully counteract the net increase in H_2 system costs associated with meeting the added H_2 demand. There are two important caveats to these findings. First, these results only represent bulk system costs and do not include the cost of distribution, refueling and vehicular infrastructure associated with H_2 use for HDV. H_2 use in HDV transportation would only be cost-effective, if the additional end-use infrastructure and equipment upgrades do not outweigh the bulk energy system cost savings estimated here. Second, because H_2 use displaces liquid fuels in lieu of increases in NG utilization in some scenarios, these results are sensitive to the relative price of NG and diesel,in the case with CO_2 storage available, which in this study was assumed to be 8.56 and 26.63 Eur/MMBtu, respectively (Table 3.7). In Figure C.12, we show how decreasing spread between NG and liquid fuel costs reduces the incentive for H_2 use in HDVs and vice versa (see section 4.3.2).

The results uncover trade-offs between the utilization of liquid fossil fuels and NG, as showin in Figure 4.5. In scenarios without CO_2 storage, the adoption of H_2 HDVs results in an increase of NG consumption. This occurs due to the reallocation of the emissions budget from the transportation to the power sector, allowing for expanded NG-based generation. The relationship is not as straight-forward in the scenarios with CO_2 storage: while the NG consumption increases due to the expansion of NG-based H_2 production, it decreases due to the contraction of DAC. The net change in NG consumption depends on the relative size of these two effects.

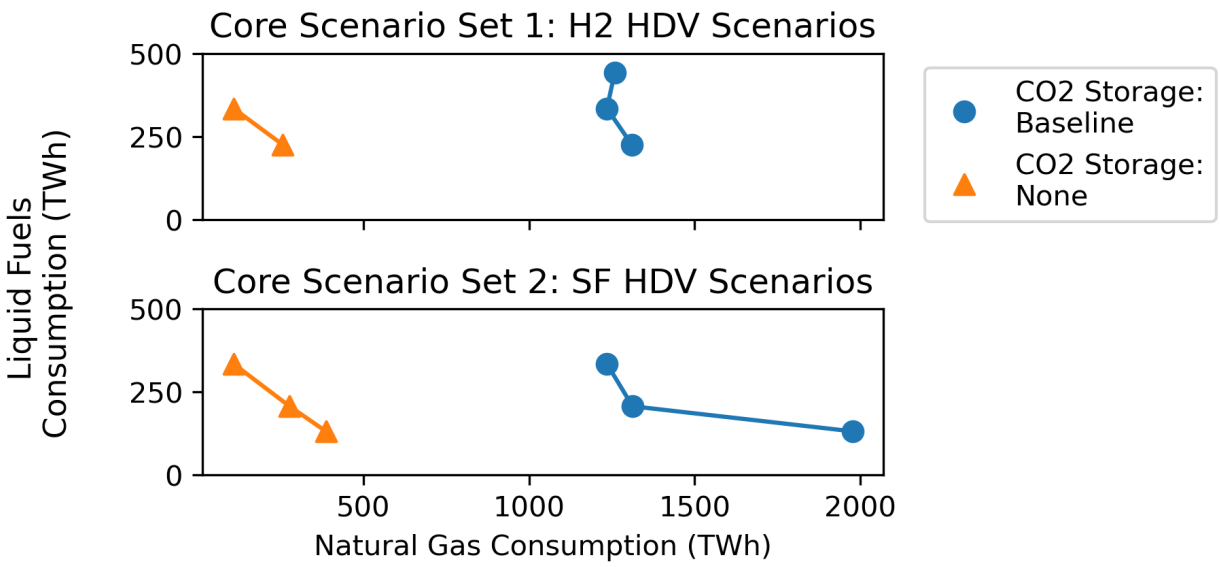

Figure 4.5: Trade-off between natural gas (NG) and liquid fossil fuel utilization. The subfigure on the top shows the relationship for the H_2 HDV scenarios(i.e. scenario set 1), while the one on the bottom shows the relationship for SF adoption scenarios (i.e. scenario set 2). Within each subplot the amount of natural gas consumption can be examined on the x-axis, while the amount of liquid fossil fuel consumption can be examined on the y-axis. The amount of H_2 and SF HDV adoption increases from top to bottom. The amount of liquid fossil fuel consumption includes diesel and gasoline, and excludes jet fuel as well as excess synthetic fuels.

4.2 System Impacts of Synthetic Fuel Adoption

The power and H_2 generation impacts resulting from SF production under various CO_2 storage scenarios and with medium H_2 HDV utilization are highlighted in Figure 4.6 (capacity results are shown in Figure 4.7). The production of SFs requires three inputs: H_2, CO_2 and small quantities of electricity inputs as shown in Table 3.12. The maximum CO_2 abatement potential of SFs is realized when the H_2 and electricity supply are sourced from low-carbon sources while the CO_2 is sourced from atmosphere. Consequently, we find that the hydrogen for initial levels of SF production is sourced primarily using electrolysis even when CO_2 sequestration is available (Figure 4.6). However, increasing electrolyzer deployment raises electricity demand and consequently, the average electricity price seen by the electrolyzer [46]. For further increases in SF production, it is more cost-effective to produce H_2 via NG SMR with CCS rather than electrolysis as shown in Figure 4.6. Overall, SF production is accompanied by an 142% increase in H_2 production vs. non-transport H_2 demand, as compared to 30% increase in the case of H2 use in HDVs (Figure 4.1), reflecting the lower energy efficiency of SF based decarbonization strategies (note these are not equivalent scenarios in terms of degree of decarbonization). By extension, and as a result of the expanded electrolyzer-based H_2 demand, a large incremental growth in power sector is also required for SF production, with a growth in power generation of 44% and 33% vs. non-transport power

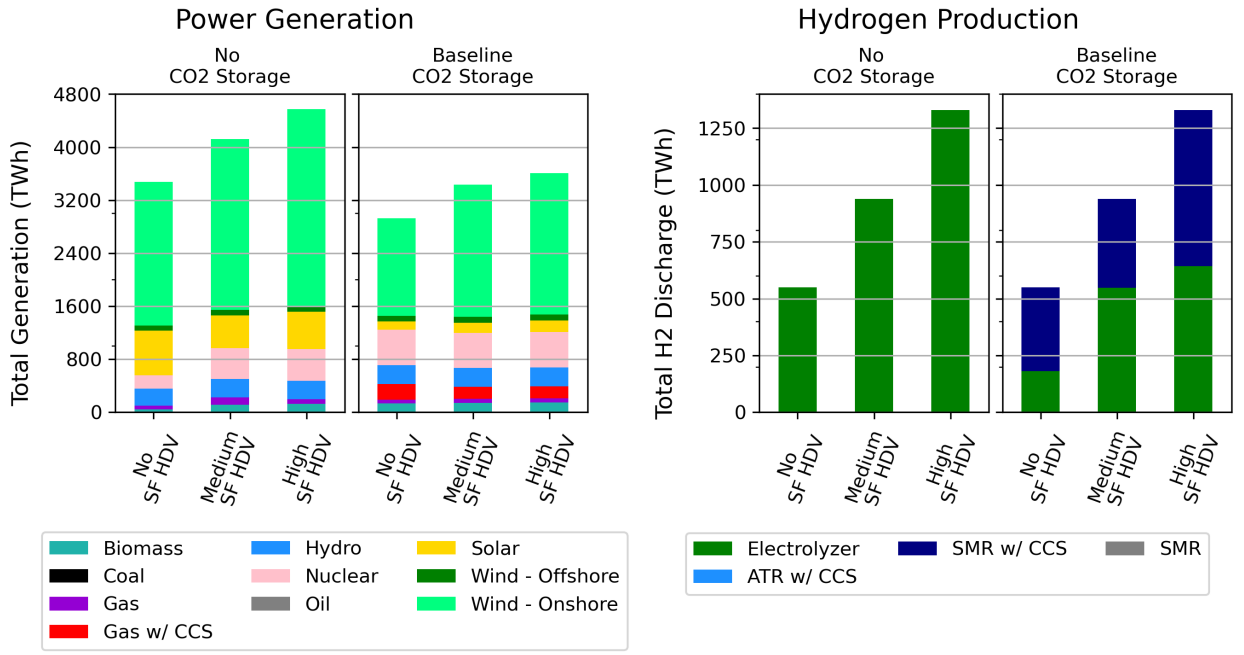

Figure 4.6: Power and hydrogen generation for baseline and no CO_2 sequestration scenarios under medium H_2 HDV adoption and varying scenarios of synthetic fuel adoption. The left set of charts shows power generation and the right set of charts shows H_2 generation. Within each panel, the amount of synthetic fuel adoption increases moving from left to right.

demand in the no CO_2 and baseline CO_2 storage cases, respectively. As shown in Figure 4.6, the growth in power sector generation resulting from SF adoption is dominated by VRE, primarily wind, reinforcing the synergies between electrolyzers and VREs noted earlier.

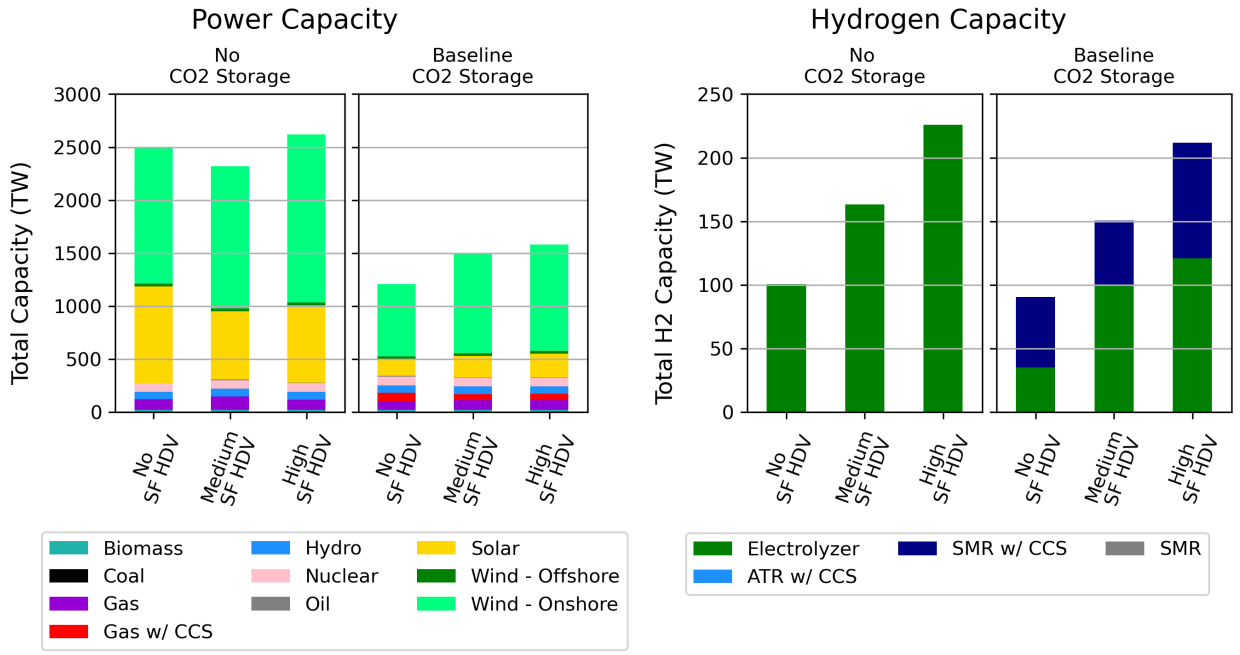

Figure 4.7: Power and H_2 capacity for baseline and no CO_2 sequestration scenarios under medium H_2 HDV adoption and varying scenarios of synthetic fuel adoption. The left set of charts shows power generation and the right set of charts shows H_2 generation. Within each panel, the amount of synthetic fuel adoption increases moving from left to right.

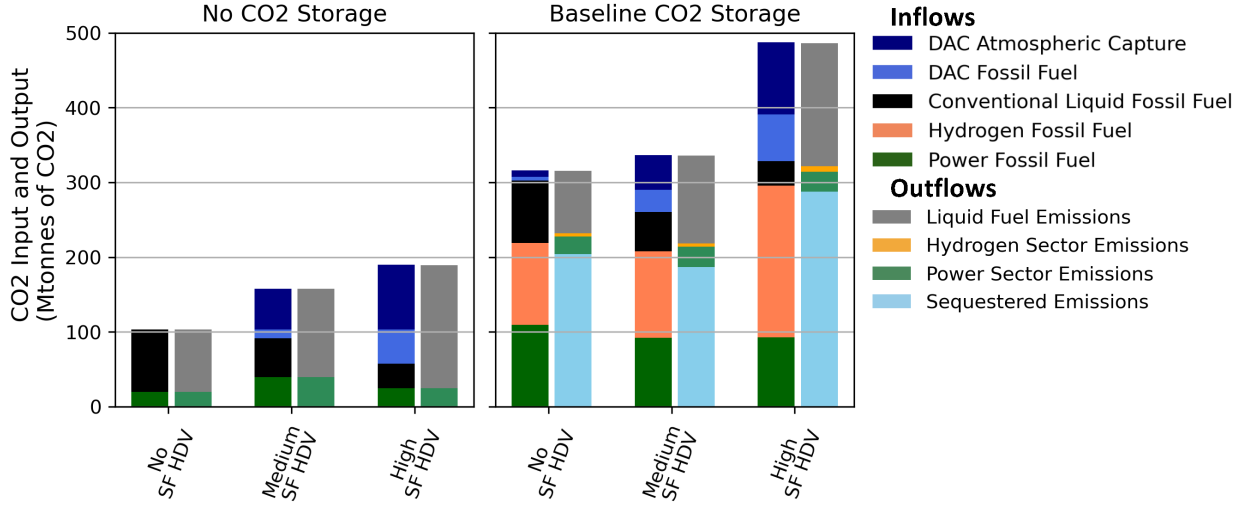

Figure 4.8: System CO_2 balance under varying levels of SF adoption and medium H_2 HDV adoption and varying scenarios of synthetic fuel adoption. The subfigure on the left shows the CO_2 balance under no CO_2 sequestration availability, while the one on the right shows the CO_2 balance under baseline CO_2 sequestration availability. Within each subplot the SF adoption level increases left to right. The leftward column represents CO_2 input into the system, while the rightward column represents CO_2 outputted by the system. This is a representation of Figure 5.1. Emissions constraint can be calculated from the chart by subtracting sequestered emissions and DAC atmospheric capture from the emission outflows.

In both CO_2 storage scenarios, increasing SF production also leads to additional DAC deployment, as highlighted in Figure 4.8, ensuring that the emissions constraint. This occurs despite the increasing share of liquid fuels used in HDV vs. no SF case (illustrated by the reduction of the size of the black stacks in Figure 4.8). Additionally, as the amount of SF adoption increases, an additional emissions penalty resulting is incurred from the production of jet fuels. Further, because excess gasoline is produced beyond system requirements in the high SF adoption case, there is a large increase in DAC deployment between the medium and high SF adoption cases. The excess gasoline results in an emissions penalty.

In the baseline CO_2 storage case, sequestration requirements are reduced in the medium SF case, but are subsequently increased to account for the expansion of NG based H_2 production with CCS. Among SF production processes considered, we see a consistent preference for the pathway with the lowest overall emissions as noted in Table 3.12, option B. In other words, pathways that maximize feed carbon conversion into one of two co-products, either SF or captured CO_2, are preferred over pathways with lower carbon conversion.

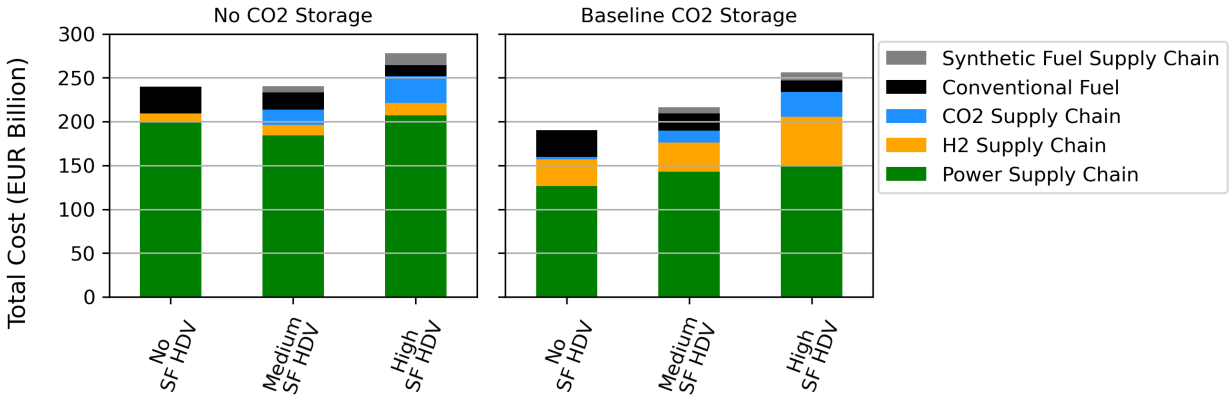

Figure 4.9: Annualized bulk-system costs under varying levels of SF adoption and medium H_2 HDV adoption and varying scenarios of synthetic fuel adoption. The subfigure on the left shows the cost breakdown under no CO_2 sequestration availability, while the one on the right shows the cost breakdown under baseline CO_2 sequestration availability. Within each subplot the SF adoption level increases left to right. The costs do not include vehicle replacement or H_2 distribution costs.

The cost impacts of the adoption of SFs are shown in Figure 4.9 where we see that cost savings from reduced purchases of liquid fossil fuel are more than offset by cost increases resulting from expanding energy infrastructure of other vectors (H_2, CO_2, electricity) to produce SFs. Thus, per our modeled assumptions, SFs would not be cost-optimal to deploy across any of the scenarios evaluated here (note that we modeled SF adoption as a minimum requirement per Eqn. 3.3.1). Interestingly, in both CO_2 storage cases, the adoption of SFs increases costs by differing magnitudes; in the no CO_2 storage scenario, system cost increase by 3% and 14% for the medium and high SF adoption cases, respectively. In the baseline case, the costs increase is more even; the costs only increase by 14% from the No SF case to the Medium SF case, and then 18% from the Medium SF to the High SF case. As such, the system cost increase resulting from SF deployment is lower when no CO_2 storage is available

due to the limited number of abatement options in the power generation and H_2 sectors, particularly in cases where no excess by-products exist.

In this set of scenarios, we also observe trade-offs between the utilization of liquid fossil fuels and NG, as showing in Figure 4.5. In all scenarios, we see an increase in the amount of NG consumed as a result of SF deployment. The increase results from the increased adoption of DAC, expansion of NG-based H_2 production, and SF production processes. This is particularly true in the high SF case, where there is a large expansion of DAC, in addition to an expansion of NG-based H_2 production.

4.3 Sensitivities of Emissions Constraints, Natural Gas Price, and Level of Fuel Substitution in HDV Sector

4.3.1 Sensitivity Scenario Set 1: Sensitivity to Stringency of Emissions Constraint

The first sensitivity scenario set is based on core scenario set 1, but at a relatively relaxed emissions cap (detailed results can be found in Section C.1). This sensitivity explores the importance and effectiveness, or lack thereof, of transportation decarbonization measures under relatively more relaxed emissions constraints. This sensitivity highlights how the viability of low-carbon fuels like H_2 (and by extension SFs) are impacted in the case of less stringent decarbonization targets for 2040.

Per Figure C.3, for scenarios with no CO_2 storage, the added H_2 demand is met through grey H_2, while in baseline CO_2 storage scenario, the added H_2 demand from H_2 HDVs is met using blue H_2. The substitution of fossil fuels in the transportation sector also reduces the need for fossil fuel substitution in the power sector (See Figure C.3), resulting in the expansion of fossil fuel power generation in the baseline scenario in the form of NG in the no sequestration case. In the baseline CO_2 sequestration case, we also see a substitution of less polluting fossil fuel power generation for more polluting fossil fuel generation (i.e. a substitution of NG with CCS to NG, and NG to coal), as seen in Figure C.3).

In contrast to the stringent emissions constraint case, we also see no deployment of DAC under relaxed CO_2 constraints (See Figure C.4). In addition, the bulk system cost savings are lower compared to the stringent emissions cap case (See Figure C.5): for the no CO_2 storage case, the cost reduction between medium and high H_2 HDV adoption is 4% compared to 12% in the stringent emissions cap case. For the baseline CO_2 storage case, the cost reduction between no H_2 HDV adoption and high H_2 HDV adoption is 8%, compared to 12% in the stringent emissions case. This highlights the increased importance of transportation decarbonization under stringent emissions constraints.

4.3.2 Sensitivity Scenario Set 2: Impact of Natural Gas Prices on H_2 HDV Adoption Scenarios

The second sensitivity scenario set is based on core scenario set 1, but with varying NG prices (See Section C.2 for detailed results). This sensitivity analysis is motivated by the recent volatility in NG supply following the Russian invasion of Ukraine in Feb 2022 [47]. While our base case NG prices are based on the assumption that supply for NG in European context is based on liquified natural gas (LNG), there is considerable uncertainty in the future evolution of the LNG market itself. For these reasons, our sensitivity focuses on testing how our model outcomes regarding H_2 and SF adoption change with changes in NG prices.

The impacts of NG prices under the no CO_2 scenario are almost negligible due to low levels of NG consumption. This is due to the lack of alternative methods of H_2 production,

since blue H_2 is not feasible without storage. The lack of CO_2 storage means that the emissions budget is met through the use of a limited amount of NG in the power sector (See Figure C.7). The impacts in baseline CO_2 storage case are more substantial. For instance, the amount of H_2 produced using electrolyzers increases from 101.75 TWh to 217.7 TWh in medium H_2 HDV case between the low NG price and the high NG price sensitivities (See Figure C.9). Additionally, a shift away from NG power generation towards VREs also occurs; in the medium H_2 HDV case for instance, the percentage of wind and solar generation increases from 52% in the low NG price case to 61% in the high NG price case. Additionally, the fossil-based generation shifts from gas w/ CCS towards gas (See Figure C.7). This combination of shifts in H_2 generation and power production, as well as a reduction in DAC deployment, results in a reduction of CO_2 sequestration requirements from 273 MTonnes of CO_2 to 163 MTonnes of CO_2 (See Figure C.11). The cost savings arising from the increased adoption of H_2 HDVs from none to high with baseline CO_2, decreases from 13% in the low NG price case to 11% in high NG price case (See Figure C.12). While the cost savings margin decreases with higher price of NG, the limited change suggest that the results are somewhat robust to the price of NG. Finally, the cost of NG has a large impact on the total amount of NG consumption as seen in Figure C.13; the amount of fuel consumption increases by around 75% for the baseline CO_2 storage case.

4.3.3 Sensitivity Scenario Set 3: Effect of H_2 adoption on the System Impacts of Synthetic Fuel Adoption

The third sensitivity scenario set is based on the the second core scenario set, but with no H_2 HDVs as opposed to a medium level of H_2 HDV adoption (See Section C.3 for detailed results). The motivation behind this scenario is to explore the robustness of the results to the base level of H_2 HDVs. As in core scenario set 1, without the adoption of transportation fuel substitution measures and with the lack of CO_2 storage availability, the supply-system is infeasible. However, we see that the adoption of SFs allow for sufficient system decarbonization to meet the necessary emission constraints (See Figure C.15). This highlights the key role SFs can play in highly decarbonized systems. In the no CO_2 storage case, the expansion of the power sector to meet electrolyzer demand in H_2 sector is notable, mostly occurring with the expansion of VREs. Additionally, we see that the existence of a utilization pathway allows for the deployment of DAC, even in the absence of CO_2 storage C.17. In the baseline CO_2 storage case, the H_2 demand is met with a mixture of blue and green H_2 (See Figure C.15).

If we compare this scenario set with core scenario set 1, we notice a few key trends. The first is that the cost of decarbonziation with SFs is higher than the cost of decarbonization with H_2. Secondly, is that we see a greater role for DAC when SFs are utilized. This role expands with greater transportation sector decarbonization. Finally, the role of NG is larger when decarbonization using SFs occurs.

4.3.4 Sensitivity Scenario Set 4: Impact of Natural Gas Prices on SF HDV Adoption Scenarios

The final sensitivity is based on the second core scenario set, but with varying NG prices (See Section C.4 for detailed results). The impact of the higher NG prices mirrors some of the findings in the second sensitivity scenario set discussed earlier. The impacts of NG prices on the power and H_2 supply mixes under the no CO_2 storage scenario are also almost negligible due to low levels of NG consumption. The lack of CO_2 storage means that the emissions budget is met through the use of a limited amount of NG in the power sector (See Figure C.20). Further, as in the second scenario sensitivity set, higher NG prices result in a larger share of H_2 production from electrolyzers. In particular, the amount of H_2 produced using electrolyzers increases from 266.3 TWh to 647.9 TWh in medium H_2 HDV case between the low NG price and the high NG price sensitivities (See Figure C.21). Additionally, the cost increases from the increased adoption of SynFuel from none to high, increases from 33% in the low NG price case to 34% in high NG price case under baseline CO_2 storage, and increases from 15% in the low NG price case to 17% in high NG price case under the no CO_2 storage(See Figure C.25). Finally, the amount of gas consumption decreases from 1617-2354 TWh in the low NG price case to 955-1167 TWh in the high NG price case.

Chapter 5

Discussion

5.1 Takeaways and Implications

Our analysis reveals the inter-dependence between different sectoral decarbonization strategies, resulting from system carbon balance shown in Fig. 5.1. These strategies include: 1) fossil fuel substitution in the transportation sector (e.g. use of H_2 or SFs) 2) fossil fuel emissions abatement via CO_2 sequestration, 3) fossil fuel substitution in power and H_2 production, and 4) atmospheric CO_2 removal. All these strategies change the inflows and outflows of CO_2 into the system as highlighted in Figure 4.3 and 4.8. We see how the emphasis on each decarbonization strategy changes depending on CO_2 storage availability and emissions constraints (see sensitivity results in appendix). For example, as H_2 use in HDVs increases, the reliance on fossil fuel substitution in the power and H_2 sector, carbon sequestration (when available) and atmospheric carbon removal decreases. In contrast, the adoption of SFs generally increases the reliance on atmospheric carbon removal and sequestration, when available, as well as the role for fossil fuel substitution in power and H_2 production mix. Below we discuss the policy implications of our findings, while considering the prevailing policy landscape in the European context that was the basis for our case study. A summary of key takeaways and findings can be found in Table 5.1.

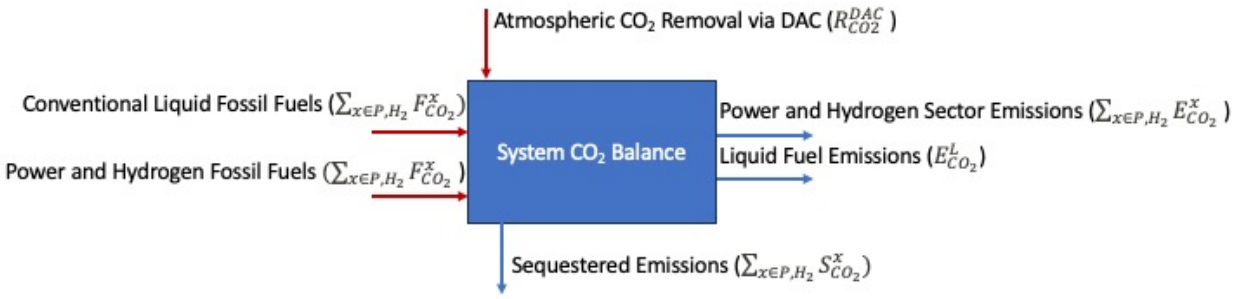

Figure 5.1: System emissions balance corresponding to equation 1. All terms are assumed to be positive in value.

In the absence of CO_2 storage, deep decarbonization of power, H_2 and transportation

sectors without liquid fossil fuel substitution (using H_2, SFs, or other methods not considered in this study) in the power sector may not be viable, as illustrated by the infeasible outcomes from the modeled scenarios mimicking these conditions. This finding reinforces the importance of demand-side measures to enable transportion decarbonization in order to reduce fossil fuel consumption, including HDV vehicle efficiency improvements, as well as regulations to phase out new ICE vehicle sales etc.. Such measures have been introduced by some of the countries in our case study (e.g. U.K), albeit to a limtied extent so far.

We find that the bulk system cost savings result from adopting H_2 directly in HDVs, as opposed to bulk system cost increases resulting from using H_2 to first produce SFs that are then used in HDVs. While the bulk system cost savings are one measure of relevance, several other factors need to be considered when comparing the two different fuel options. In the case of H_2, substantial investment in distribution, refueling, and vehicular infrastructure will be needed. This is not accounted in our analysis. For SFs, these costs are expected to be minimal since SFs can use the existing vehicular, distribution, and refueling infrastructure developed for fossil-based liquid fuels, thereby minimizing impact on vehicle owners and operators.

We find that SFs adoption tends to be most cost-effective in the absence of CO_2 sequestration capacity and when deployed at a limited scale. The widespread adoption of SFs (high SF adoption scenario representing 50% of HDV demand) results in much larger cost impacts irrespective of the CO_2 storage assumption. These cost increases stem from the significant investment in not only H_2 and by extension electricity supply chains but also CO_2 supply chains, in particular deployment and substantial scale up of emerging DAC technologies, as well as CO_2 transportation infrastructure. Additionally, the production of excess liquid fuel byproducts incurs an emissions penalty. Further, the system carbon balance (Figure 4.8) with SFs has many more components than the system without SFs adoption. At an individual producer level, ascertaining the low-carbon nature of SFs will require establishing regulations and possibly new tracking mechanisms that account for the induced grid emissions associated with each new load. Recent discussions in the U.S. and European context on ascertaining the carbon intensity of low-carbon H_2 are a harbinger to the challenges facing carbon intensity assessment for SFs producers, who also have to consider embodied emissions burdens of the CO_2 feedstock. These factors could create uncertainty around supply of SFs and incentivize certain vehicle owners, particularly fleet operators with fixed routes and high utilization (e.g. city buses, fleets operating across major freight corridors) to choose the more capital intensive yet energy efficient option of H_2-based HDVs to decarbonize their operations. Finally, the lack of flexibility in SF production should be noted in that the amount of each product of SF production is determined by the set-up of the process from a chemical engineering perspective. Modifying the outputs to meet demand can have implication on process efficiency, or may not be possible. In some of the scenarios explored in this study, the amount of synthetic gasoline produced exceeded the demand for gasoline, highlighting the drawbacks of the the SF production process.

This study also illustrates how the availability of CO_2 sequestration impacts energy system decarbonization. While spatially-resolved estimates of technical CO_2 storage capacity have been developed, other factors like social acceptance might constrain practically available CO_2 sequestration capacity. At the same time, limiting sequestration capacity results in increased reliance on electrolyzer-based H_2 production and consequently VRE generation

for power generation, highlighting societal tradeoffs implicit in the choice of decarbonization pathway. Another interesting trade-off revealed in our analysis is the increase in NG consumption in lieu of liquid fossil fuels displacement via H_2 or SFs adoption. This is particularly relevant for policy makers to consider given the precariousness of European NG supply after the Russian invasion of Ukraine. In our standard cases, our NG prices are synonymous with long-term projections for liquified natural gas prices. That assumption, combined with the deep decarbonization emissions constraint ensure that overall NG consumption levels for power and H_2 production are well below 2019 levels in our cases. At the same time, we find that substitution of fossil liquids with NG is part of many of the cost-optimized decarbonization scenarios studied here and potentially provides a roadmap for reducing fossil liquid fuel imports in the European context, at the cost of increasing NG imports and reliance.

The integrated energy system modeling framework used here allows for co-optimizing supply chains for electricity, H_2, CO_2 and liquid fuels and thus evaluate potential cross-sectoral impacts of multi-sector deep decarbonization. Through the case of power-H_2-transportation interactions in the European context, we highlight key enabling opportunities for cost-beneficial sector coupling across sectors. Importantly, as opposed to sectoral emissions goals or prescribed technology carveouts, such as policies part of the Inflation reduction Act in the U.S., a joint emissions reduction approach (e.g. carbon tax or cross-sectoral emissions cap), allows for leveraging a broader suite of technologies and their synergistic operational interactions (e.g. electrolyzer and VRE operation, deploying CCS where it is most cost-effective) [48]. In practice, the economic efficiency gains of joint emissions reduction efforts may be realized through carbon trading similar to the EU ETS, that includes multiple sectors.

5.2 Limitations and Further Work

Due to the complexities of multi-sectoral systems analysis, there are a few limitations associated with this study. The first is on the emissions and cost accounting for jet fuel emissions. Ideally, jet fuel supply chains and demand would be accounted for. However, because this study is only focused on road transportation, we exclude demand for jet fuel from the model. To account for synthetic jet fuel in terms of emissions and costs, we penalize jet fuel emissions, while crediting them as a by-product sold on the market. This does not fully account for the emissions benefits of utilizing jet fuels in the transportation sector. An alternative study that incorporate jet fuel demand could exhibit further benefits to the utilization of SFs. In a similar vein, in some scenarios (the high SF HDV scenarios) excess gasoline is produced beyond what is demanded in the passenger sector. In this case, the demand is penalized from an emissions perspective. In any case, while different approaches may be taken to account for costs and emissions from by-products, the potential inflexibility of SF production processes is notable. As exhibited in this study, this does not occur unless SFs are adopted on a very wide-scale.

Additionally, further work can be done integrating a fleet turnover model into this analysis, to account for costs and lifetimes of vehicle replacements. Given the longer lifetimes of HDVs, it is worth noting that some fleet operators may be locked into a specific vehicle technology. Current policies around HDVs in the EU are promoting more efficient ICE HDVs. The cost of turning over these vehicles prior to the end of their life could prove to raise the

Table 5.1: Summary of Advantages and Disadvantages of Transportation Decarbonization Strategies

	Advantages	**Disadvantages**
H_2 Heavy-duty Vehicles	• Reduces decarbonization burden on other sectors • Reduced bulk system costs • Reduces need for CO_2 Sequestration	• Relies on unproven technologies (SMR w/ CCS, Electrolyzers, H_2 vehicles) • Costs of distribution network, refueling infrastructure, and vehicle replacement could be high • Increases natural gas consumption in most cases
Synthetic Fuels	• Reduces decarbonization burden on other sectors • Utilizes existing liquid fuel vehicles and infrastructure • Beneficial in cases with no CO_2 storage	• Continued reliance on liquid fossil fuels • Increases DAC deployment • Increases system CO_2 throughput • Relies on unproven technologies (synthetic fuel production)

cost of adoption H_2 HDVs, and would increase the cost-effectiveness of SFs.

This study also does not account for distribution costs of HDVs beyond a high-level accounting for distribution and refueling costs. In reality, the distribution and refueling costs of H_2 and liquid fuels could be significant. Given that this is a macro-energy system study, we focus the bulk-system. More generally, due to the forward-looking nature of this study, many unproven technologies are assessed including DAC, CCS plants, large scale H_2 production, and SF production. Whether these technologies materialize and at what cost is still unknown.

Another consideration is to expand the available technology options for HDV decarbonization. In this study we only considered two decarbonization pathways for two types of vehicles, H_2 HDVs and SF. Both these solutions have not materialized at a large scale. Additionally, other options could also materialize such as EV HDVs, NG vehicles, or a further expansion of biofuels. EV HDVs, in particular, could hold more promise due to synergies with passenger vehicle electrification. It is worth noting that the level of electrification is

kept constant throughout this study. Further analysis should be completed to analyze the full tapestry of possible options.

Finally, in this study we assumed no generation retirements. This assumes that much of the generation units could have their lifetimes extended at no cost.

Chapter 6

Conclusions

In this context, our analysis leads to a few key policy-relevant observations. First, we find that H_2 use for HDVs reduces bulk system (power-H_2 and transportation) cost of deep decarbonization and decreases demand for fossil fuel liquid but could increase overall natural gas (NG) consumption compared to equivalent decarbonization scenarios without H_2 use for HDVs. Part of the cost saving stems from the substitution of more expensive conventional fossil liquid fuels (vs. natural gas on a per GJ of energy basis) for H_2 in end-use that also reduces need for atmospheric CO_2 removal via modeled DAC technologies. Ultimately their cost-effectiveness will depend on the cost of distribution and refueling infrastructure. As a result, policies that encourage the provision of H_2 distribution and refueling infrastructure should be encouraged. Second, limitations on CO_2 storage availability increase the bulk system cost savings (in absolute terms) of adopting H_2 use for HDVs. Third, the deployment of synthetic fuels results in substantial expansion of power and H_2 production capacity, with a preference for non-fossil fuel generation sources (electrolyzrs for H_2 production and VRE for power generation) to maximize carbon abatement benefits of synthetic fuel use. The second order impacts of SF adoption on other sectors should be considered when creating policies that encourage SF adoption. Fourth, while synthetic fuel adoption generally increases bulk system costs, the cost increases vs. no synthetic fuel adoption case are the lowest in case CO_2 storage availability is constrained and fossil fuels (natural gas and fossil liquids) are expensive. In the European context, where the above conditions appear to be true, synthetic fuels could be viewed as limited but viable decarbonization strategy, so long as the supporting power and H_2 infrastructure requirements can be satisfied. The role for H_2 for transport decarbonization reduces the upstream burden on the power and H_2 sectors but comes with the additional downstream challenges of deploying extensive distribution, refueling and vehicular infrastructure. Finally, our analysis highlights that the optimal-level of sectoral decarbonization is dependent on the technology pathways adopted and reinforces the use of multi-sector emissions reduction strategies similar to the European emissions trading system rather than sector specific decarbonization approaches being contemplated in other regions (e.g. U.S.). This study exhibits the importance of multi-sectoral analysis and planning, and by extension policymaking, showing that choices made in the transportation decarbonization space have far-reaching impacts in other sectors.

Appendix A

Supply-side (DOLPHYN) Inputs

A.1 Power Network, Cost, and Operational Assumptions

The power system used in this study is based on a brownfield representation of the European Grid created by PYPSA-EUR [38].We utilize the 37-node representation of the European continent (which reduced to 10 nodes when we exclude countries outside of the region of interests. All countries are represented as one node, apart from Denmark and the UK, which are each represented using two nodes.

Transmission costs and upgrades are based on PYPSA-EUR network representations [38]. In the model, both AC and DC transmission are treated as the same. We assume that existing power transmission capacities can be expanded by up to 4 times. Additionally, we assume that new lines can be built between certain regions up to a capacity of 5000 MW.

The existing available generation is based on data from the ENTSOE transparency platform [33]. We assume that this capacity will be available in the year 2040.

The following table shows the key cost and operational assumptions for generation and storage technologies:

Generation Technology	Power CAPEX (Eur/ kW)	Energy CAPEX (Eur/ kWh)	FOM (Eur/ MW/ yr)	VOM (Eur/ MWh)	Heat Rate (MMBTU / MWh)	Capture Rate	Round Trip Efficiency	Lifetime (Yrs)
Onshore Wind	851	-	32	0	-	-	-	30
Offshore Wind	3,751	-	69	0	-	-	-	30
Solar	680	-	13	0	-	-	-	30
Biomass	-	-	136	5.2	13.5	-	-	45
Nuclear	6,431	-	131	2.6	10.46	-	-	60
Hydro	-	-	56	0	-	-	-	100
OCGT	785	-	19	1.6	10.1	-	-	30
CCGT	937	-	25	4.6	6.5	-	-	30
CCGT w/ CCS	1,794	-	52	3.7	7.2	0.95	-	30
Coal	2,733	-	67	7.2	10.0	-	-	30
PHS	1,991	-	16	0.5	-	-	0.87	100
Battery	137	208	18	0	-	-	0.85	30

Table A.1: Power Technology Cost and Operational Assumptions

All costs assumptions are based on the NREL ATB [39]. All operational assumptions are based on Supelveda et al. [40].

The maximum available generation capacity and temporally resolved capacity factors associated with the variable renewable energy generation technologies is based on PYPSA-EUR [38]. We assume no possible expansion in biomass plants. Additionally, we assume that only nuclear existing (without a phase-out), planned, and under-construction units will be in-operation by 2040, in line with [34].

A.2 Hydrogen Cost and Operational Assumptions

We model hydrogen generation, transmission, storage, and G2P technologies. A greenfield representation of the hydrogen system is utilized for this study.

We modelled electrolyzers, SMR, SMR w/ CCS, and ATR w/ CCS technologies. We also model above ground hydrogen storage. Cost and operational assumptions for fossil fuel based plants (SMR, SMR w/ CCS, and ATR w/ CCS) are based on [49]. Cost and operational assumptions for electrolyzers are based on [50], assuming 2050 costs. Costs and operational assumptions for G2P is based on [39]. Storage technology cost assumptions are based on [51]. The following table shows key hydrogen generation technologies cost and operational assumptions:

H_2 Production Technology	CAPEX (Eur/ kTonne-H_2/ yr)	FOM (Eur/ kTonne-CO_2/ hr/yr)	VOM (Eur/ Tonne-CO_2)	Electricity Input (MWh/ Tonne-H_2)	Natural Gas Heat Rate (GJ/ Tonne H_2)	Capture Rate	Lifetime (Yrs)
SMR	15,715	539	0.08	0.65	184.4	-	25
SMR w/ CCS	38,232	1,183	0.22	2.04	196.1	0.96	25
ATR w/ CCS	30,218	917	0.33	4.00	184.3	0.95	25
Electrolyzers	18,954	37.30	-	45.00	45.0	-	20

Table A.2: Hydrogen Production Technology Cost Assumptions

G2P Technology	CAPEX (Eur/ MW)	FOM (Eur/ MW/yr)	VOM (Eur/ MWh)	Conversion Efficiency (MWh/ tonne-H_2)
CCGT G2P	816,095	24,570	1.57	21.65

Table A.3: G2P Technology Cost Assumptions

Storage Technology	CAPEX (Eur/kTonne-H_2/hr)	CAPEX (Eur/kTonne H_2)	FOM (Eur/kTonne H_2/yr)	Lifetime (Yrs)
Underground Storage	1,859	504	1.02	30

Table A.4: Hydrogen Storage Technology Costs Assumptions

A.3 CO_2 Sequestration Assumptions

A.3.1 DAC Cost and Operational Assumptions

We model liquid and solid sorbet direct-air capture (DAC) technologies. The following are the cost and operational assumptions associated with DAC technologies:

DAC Technology	CAPEX (Eur/ kTonne CO2/hr)	FOM (Eur/ kTonne CO2/hr)	VOM (Eur/ Tonne CO2)	Heat Rate (MMBTU/ Tonne CO2)	Capture Rate	Lifetime (Yrs)
Solvent DAC	12,606	342	57.8	12.2	0.99	30
Sorbent DAC	30,684	1,041	59.8	26.6	0.89	30

Table A.5: Direct Air Capture Technology Operation and Cost Assumptions. Costs based on Plant Size.

Additionally, we assume that a carbon dioxide pipeline network can be built without restrictions.

A.3.2 Geological Sequestration Assumptions

CO_2 geological sequestration capacities are based on the EU GeoCapacity project for all countries except Sweden [52]. Sweden geological storage is based on [53]. We utilize the conservative assumption. In addition, we assume that only geological storage in saline aquifers is viable. Additionally, since our model captures on year, we divide the available capacity by 100 to account for the long-term need for CO2 storage, as well as the utilization for CO2 capture for other purposes such as industrial sequestration. In addition to DAC, we assume that CO2 captured from the power and hydrogen sectors through PSC is combined with any CO2 captured from DAC. This captured CO_2 is either utilized using the synthetic fuel pathway or is stored.

Table A.6 shows the modelled available capacity for geological CO_2 storage:

Country	CO2 Storage (Mt/yr)
Belgium	199
Germany	14,900
Denmark	2,554
France	7,922
United Kingdom	7,100
Netherlands	340
Norway	26,031
Sweden	3,400

Table A.6: CO2 Geological Sequestration Availability by Country

A.4 Liquid Fuels Assumptions

A.4.1 Synthetic Fuels Cost and Operational Assumptions

Since the focus of this is study is road transportation, we focus on two liquid fuels; diesel and gasoline. We assume that liquid fuel demand can be met in one of two ways. The first is using conventional hydrocarbons and the second is through synthetic fuels.

Three synfuel plan configurations are modelled. The first is a synfuel plant is based on Zang et al. and James et al.. [25], [41]. Additionally, we model two modified plant configurations, the first captures a portion of the vented CO2, while the second captures and recycles the vented CO2.

The following parameters show the synthetic fuels cost and operational assumptions:

Syn Fuel Production Technology	Syn Fuel Plant	Syn Fuel Plant w/ Capture	Syn Fuel Plan w/ Recycling
CAPEX (Eur/kTonne CO2 In / hr)	3,634	5,682	11,153
FOM (Eur/kTonne CO2 In / hr)	193	244	480
VOM (Eur/Tonne CO2 In)	8.5	9.5	18.7
Lifetime (Yrs)	40	40	40
CO2 Utilized (%)	0.46	0.46	0.89
CO2 Captured (%)	0.00	0.50	0.00
CO2 Released (%)	0.56	0.06	0.11
H2 In (Tonnes/Tonne of CO2 In)	0.09	0.09	0.18
Electricity In (MWh/Tonne CO2 In)	0.036	0.107	0.211
Diesel Out (MMBTU/Tonne CO2 In)	1,781	1,781	3,495
Gasoline Out (MMBTU/Tonne CO2 In)	1,687	1,687	3,311
Jet Fuel Out (MMBTU/TonneCO2 In)	3,037	3,037	5,960

Table A.7: Syn Fuel Production Operation and Cost Assumptions

Since jet fuel is a by-product on the synthetic fuel process we are modelling, but the aviation sector is not included in our model, we assume a "credit" associated with the production of jet fuels.

A.5 Fuel costs

Fuel	Fuel Cost (Eur/MWh)
Nuclear	1.5
Biomass	7.0
Coal	6.2
Lignite	5.8
Natural Gas	30.8
Gasoline	69.3
Diesel	96.2
Jet fuel	44.8

Table A.8: Fuel Cost Assumptions

The source for the nuclear, coal, and lignite costs is the 2022 TYNDP study [34]. The price of natural gas is based on natural gas futures viewed in June 2022 for the Dutch TTF [54]. The natural gas prices reflected in the TYNDP are significantly lower than natural gas futures. Given the state of current state of European natural gas supply, we believe that relying on futures estimate is more reasonable. Additionally, ENTSOE-TYNDP does not list biomass prices. The price for biomass is based from PyPSA technology database [55].

The price for gasoline and diesel is based on German gasoline and diesel averaged for 2022 ex-tax, while jet fuel prices are based on the 2022 U.S. Gulf Coast Kerosene-Type Jet Fuel Spot price. [56]–[58]. These prices are then projected out to 2050 by scaling them in accordance to the ENTSOE TYNDP study crude oil projection [33].

A.6 Non-transportation demand

The baseline electricity and hydrogen demand is based on ENTSOE projected demand scenarios, excluding any road transportation demand [34]. We utilize the Distributed Energy scenario for the year 2040.

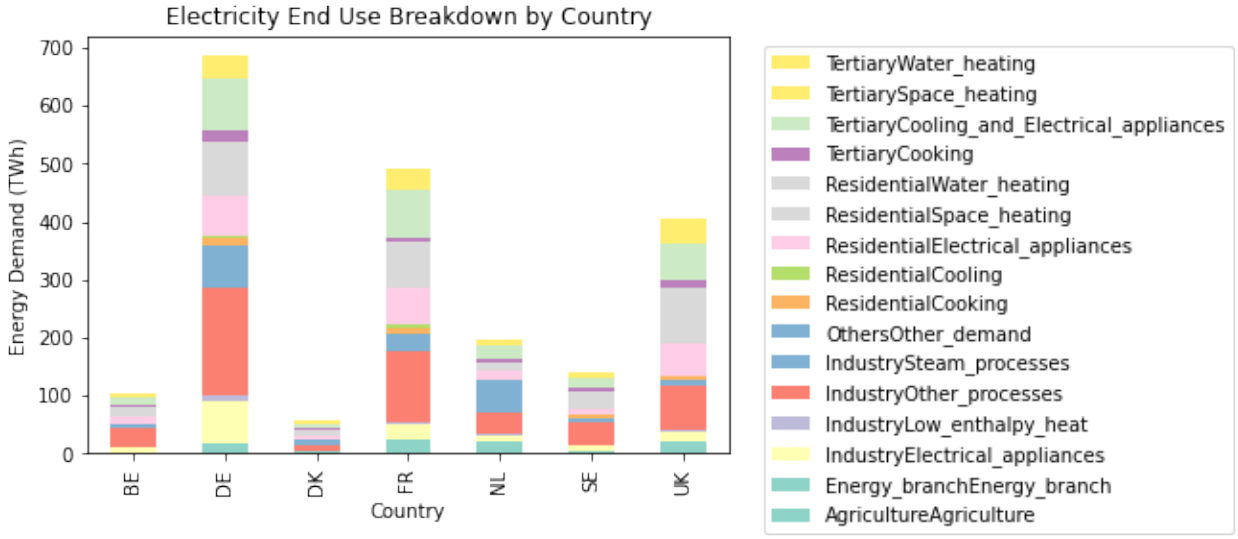

Figure A.1: Non-transportation electric demand broken down by country and end-use as reported by ENTSOE

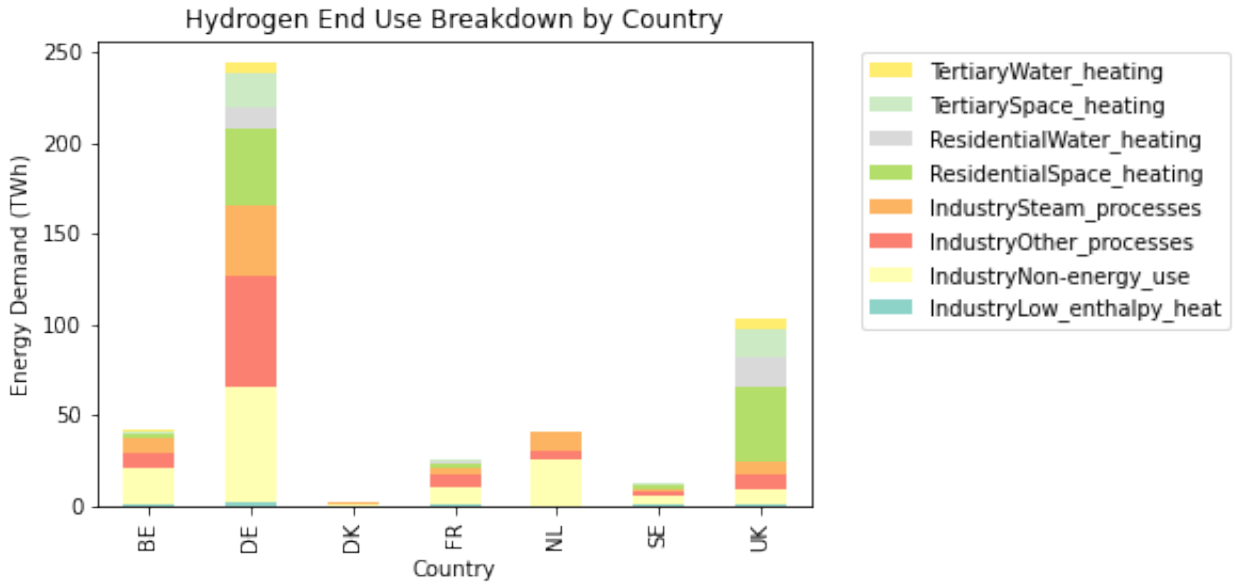

Figure A.2: Non-transportation H_2 demand broken down by country and end-use as reported by ENTSOE

A.7 Emissions Constraint

We establish a combined system cap on the power, hydrogen, and transportation sectors. This is reflective of a combined emission trading market. To establish a baseline, we add transportation and power sector emissions from the year 2015. We assume that by the year 2040, we will require a 90% reduction in power sector emissions and a 40% reduction in transportation emissions. It is worth noting that specific economy-wide emissions targets for the year 2040 have not been set for the EU, let alone sectoral emissions targets. As a result, we model a range of emissions sensitivities.

Appendix B

Practical Considerations: Run Tools and Requirements

The first step for model creation is to create a basic DOLPHYN model that does not contain transportation demand. Then, a transportation scenario is created using the transportation demand model. This scenario is overlayed on top of a non-transportation scenario demand, and outputs a new set of DOLPHYN inputs with the required transportation demand, as well as any other inputs that are modified for a given scenario. Multiple of these scenarios are created simultaneously to create one scenario set. These scenarios sets are then run on the MIT Supercloud. The results are then processed using a post-processing script to extract key insights. In this section we explain some of the key considerations that helped us process this large collection of scenarios. The transportation demand model, script used to generate scenario sets, and post-processing script can be found here [59].

In terms of DOLPHYN model considerations, we utilized a couple of techniques t improve model tractability/ These are: 1) time domain reduction, and 2) linearized-unit commitment. To improve the tractability of the model, we utilize a time domain reduction, which reduces the time domain into 100 representative days using a clustering algorithm. This clustering algorithm takes into account demand and VRE resource availability to select the most representative period. We cluster on the basis of non-transportation demand to avoid clustering separately for each model to avoid differing results. As noted in [60] "the time-domain reduction preserves chronological variability of energy demands and VRE resource availability, as well as the correlations among them, while reducing the model size to still be computationally tractable." We also utilize a linearized unit-commitment simplification for thermal and hydrogen production units.

Choosing the correct solver and solver parameters is key to run such optimization models successfully. The Gurobi solver (v9.5.1) was used to run these models on Julia (v1.7.3). Given the size of the model, and the amount of varying inputs, the solver often encountered numerical issues. To solve these issues, optimizer solver settings were tweaked and modified. Key optimizer settings were found to be: 1) numerical focus (increased numerical focus means solver uses greater precision as model is solved), 2) bar homogeneous (algorithm to detect infeasibility and unboundedness. Slower than default algorithm). Finally, to reduce solve time, the Crossover parameter was set to 0. The Crossover parameter transforms an interior solution into a basic solution for added accuracy. This was forgone to allow the

models to be solved, as crossover can often take a very large amount of time to terminate. It is worth mentioning that other solvers may have different optimal parameters, and that the best parameter settings will be different depending on the model make-up. Also, the numerical performance of the solver improved with successive updates to the solver, so it is important to utilize the latest available solver.

In total, we ran 48 separate DOLPHYN models for this study. Each model would take 2 hours on a standard personal computer 16 GB RAM 6-core machine. To decrease the runtime required, jobs were run in parallel on the MIT SuperCloud, a high performance computing (HPC) cluster [61] on 8 Intel Xeon Platinum 8260 nodes. Each node has 48 cores, and each core has 4 GB of RAM. We ran each of the jobs on a separate node. Even though it should be possible to run more than 1 job per node at a time, sometimes memory issues are encountered that prevent jobs from terminating properly.

After running the results, post-processing functions were used to create visualization of model results. These functions were very useful in providing an idea of the success of the model runs and key insights. The functions created are flexible enough to handle multiple different scenario set cases.

Appendix C

Sensitivity Scenarios

C.1 Sensitivity Set 1: Core Scenario Set 1 with Relaxed Emissions Constraint

The following diagram shows where this sensitivity lies on the scenario matrix.

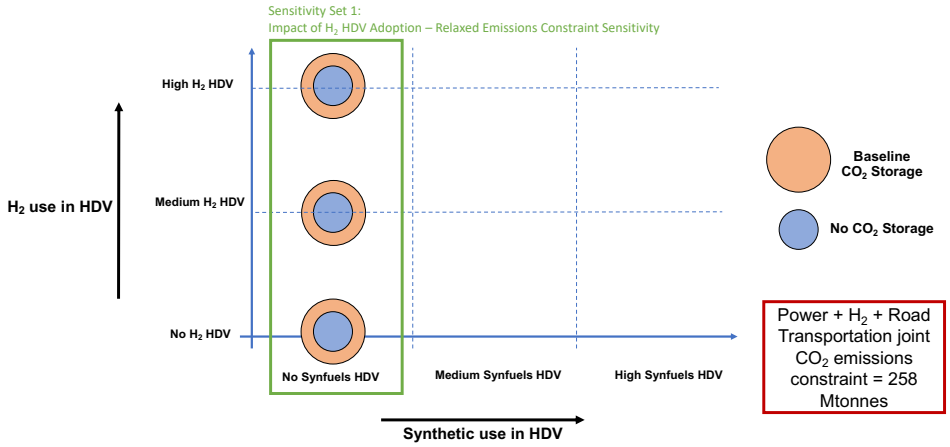

Figure C.1: Sensitivity set 1 scenario matrix. Each bubble represents a scenario. The y-axis represents varying levels of H_2 HDV adoption, while the x-axis represents varying levels synthetic fuel adoption. All scenarios are equivalent from an emissions capping perspective with a cap of 258 $MTCO_2$. HDV fleet represents all vehicle types with gross weight great than 7.5 tonnes.

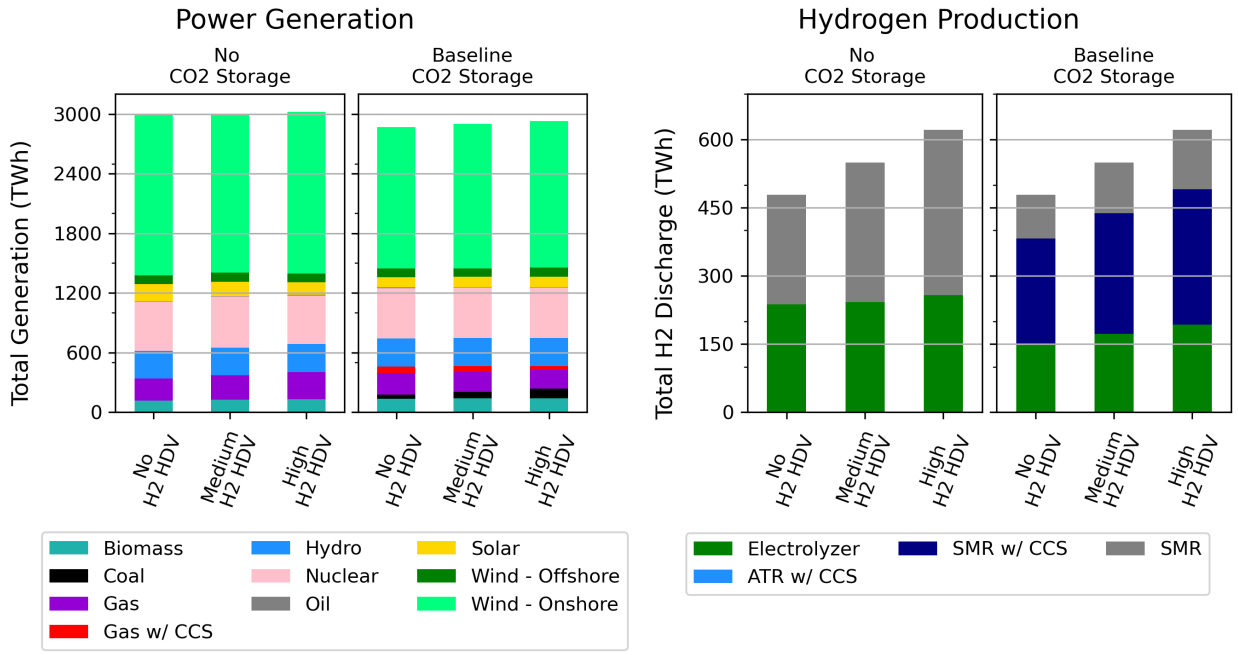

Figure C.2: Power and H_2 generation for baseline and no CO_2 sequestration scenarios under no synthetic fuel adoption. The left set of charts shows power generation and the right set of charts shows H_2 generation. Within each panel, the amount of H_2 HDV adoption increases moving from left to right. CO_2 constraint is relaxed compared to core scenario set 1.

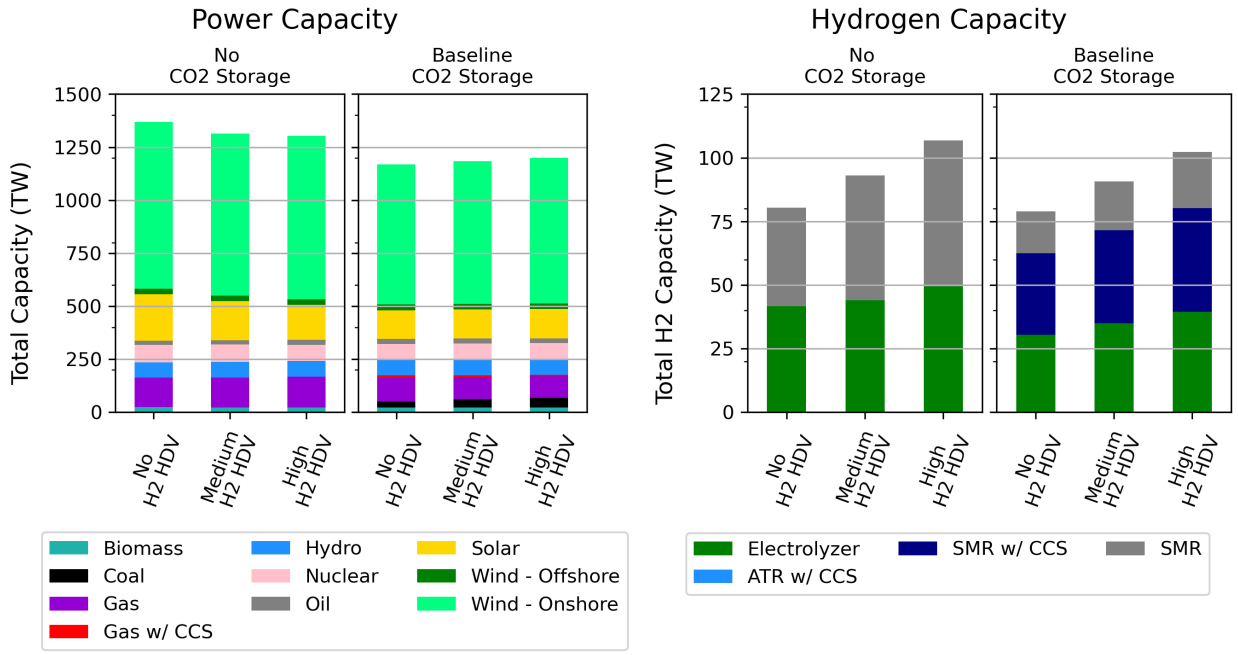

Figure C.3: Power and H_2 capacity for baseline and no CO_2 sequestration scenarios under no synthetic fuel adoption. The left set of charts shows power generation and the right set of charts shows H_2 generation. Within each panel, the amount of H_2 HDV adoption increases moving from left to right.CO_2 constraint is relaxed compared to core scenario set 1.

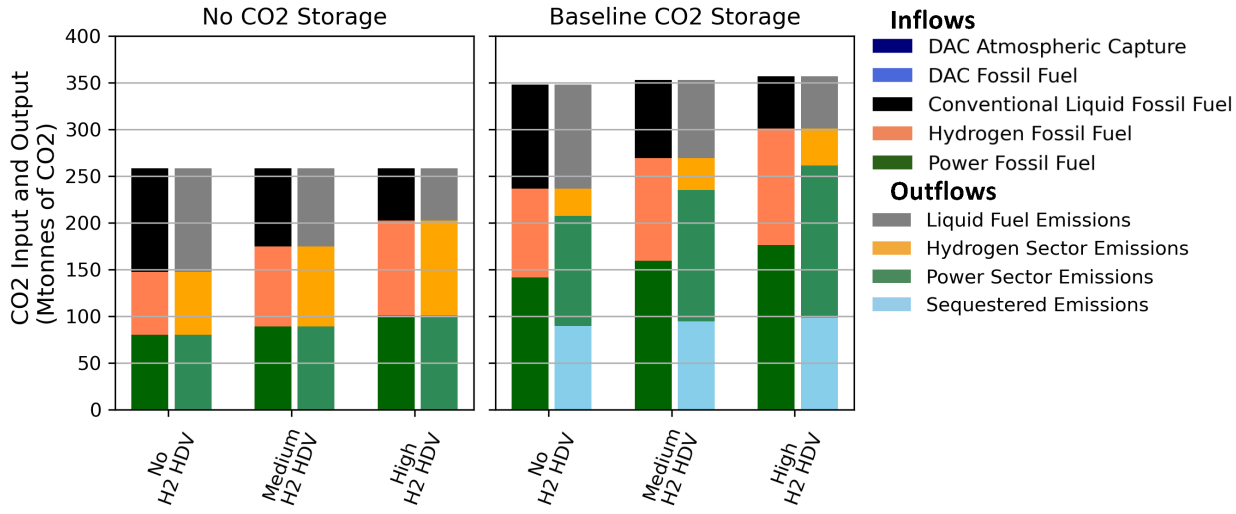

Figure C.4: System CO_2 balance under varying levels of H_2 HDV adoption and no SF adoption. The subfigure on the left shows the CO_2 balance under no CO_2 sequestration availability, while the one on the right shows the CO_2 balance under baseline CO_2 storage availability. Within each subplot the H_2 HDV adoption level increases left to right. The leftward column represents CO_2 input into the system, while the rightward column represents CO_2 outputted by the system. All scenarios adhere to the same emissions constraint of 258 MTonnes. CO_2 constraint is relaxed compared to core scenario set 1. Emissions constraint can be calculated from the chart by subtracting sequestered emissions and DAC atmospheric capture from the emission outflows.

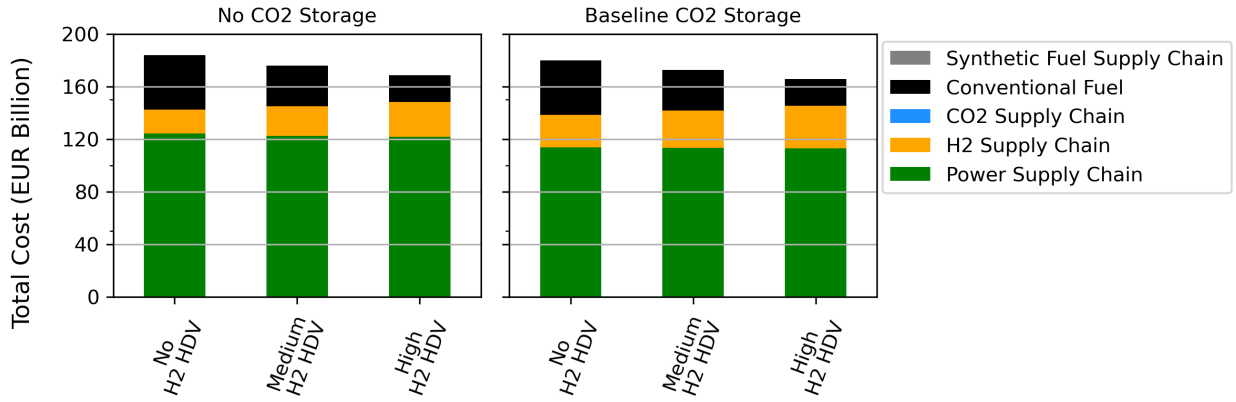

Figure C.5: Annualized bulk-system costs under varying levels of H_2 HDV adoption and no SF adoption.The subfigure on the left shows the cost breakdown under no CO_2 sequestration availability, while the one on the right shows the cost breakdown under baseline CO_2 sequestration availability. Within each subplot the H_2 HDV adoption level increases left to right. CO_2 constraint is relaxed compared to core scenario set 1. The costs do not include vehicle replacement or H_2 distribution costs.

C.2 Sensitivity Set 2: Core Scenario Set 1 Natural Gas Price Sensitivity

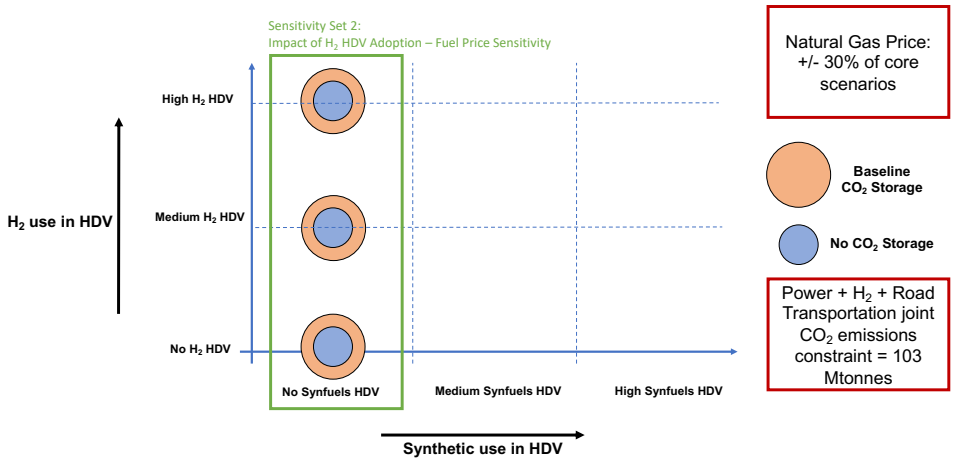

Figure C.6: Sensitivity set 2 scenario matrix. Each bubble represents a scenario. The y-axis represents varying levels of H_2 HDV adoption, while the x-axis represents varying levels synthetic fuel adoption. All scenarios are equivalent from an emissions capping perspective with a cap of 103 $MTCO_2$. HDV fleet represents all vehicle types with gross weight great than 7.5 tonnes. This scenario is based on core scenario set 1, but with +/-30% NG prices.

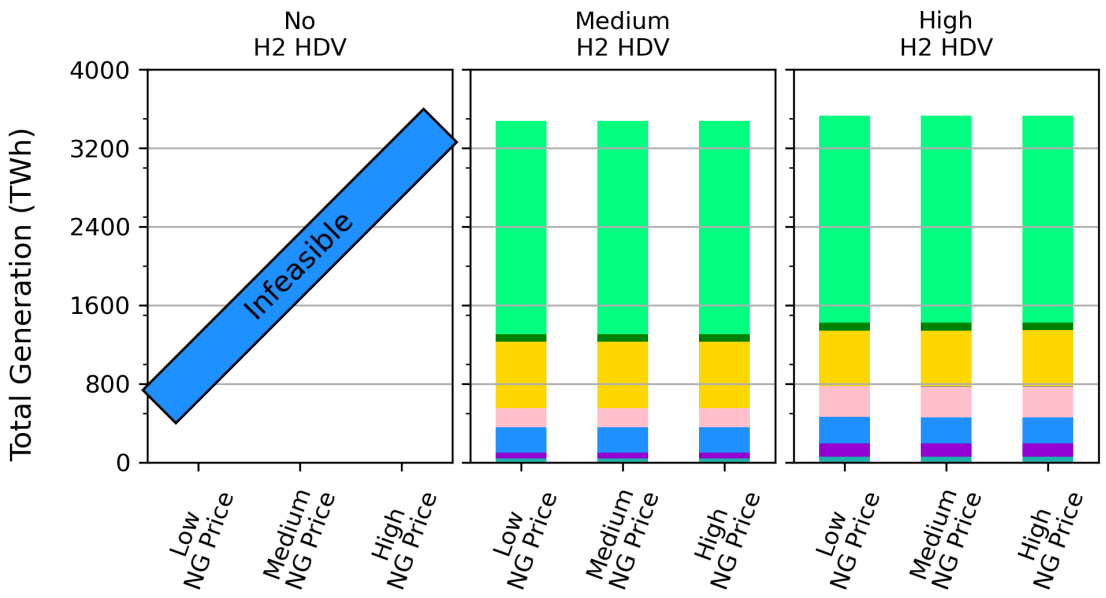

(a) No CO_2 Storage

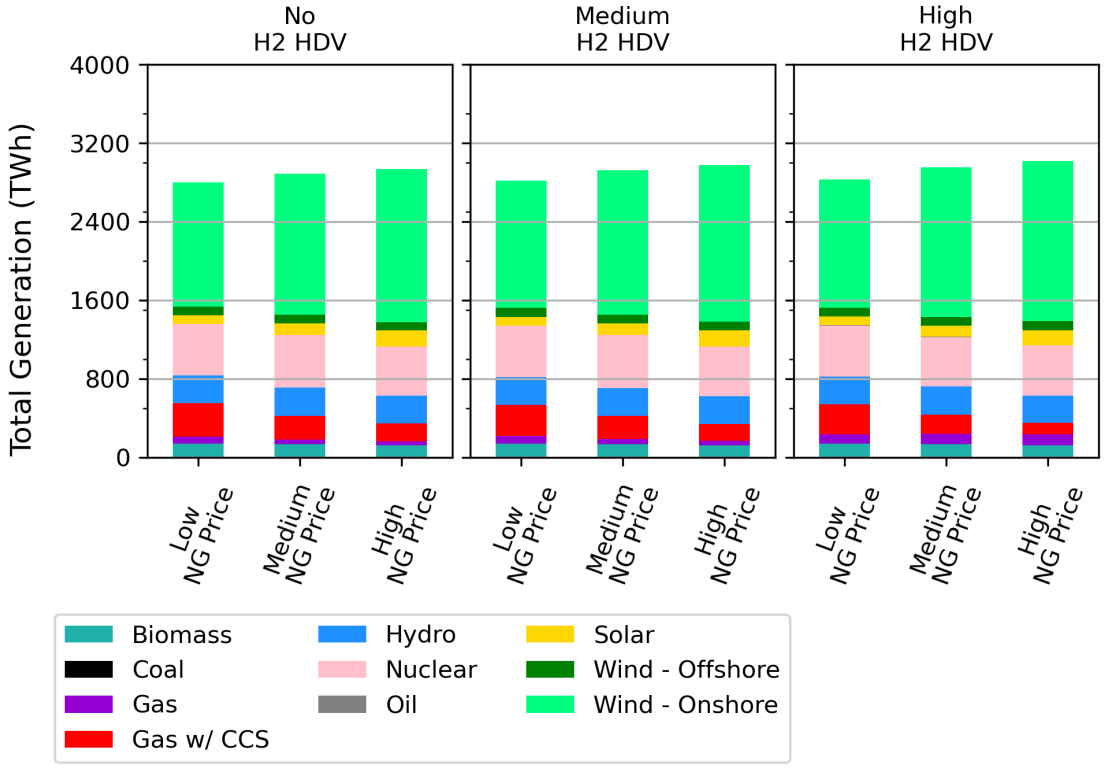

(b) Baseline CO_2 Storage

Figure C.7: Power generation for no (sub-figure a) and baseline (sub-figure b) CO_2 sequestration scenarios under no synthetic fuel adoption. The price of natural gas increases left to right. Within each panel, the amount of H_2 HDV adoption increases moving from left to right. The middle panels correspond to the core set of scenarios

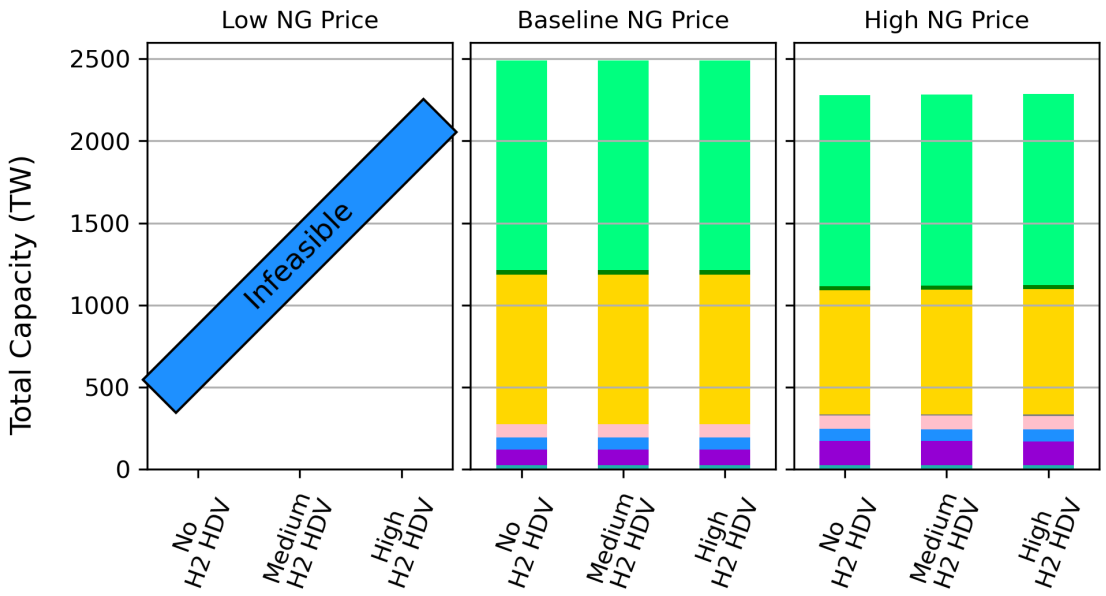

(a) No CO_2 Storage

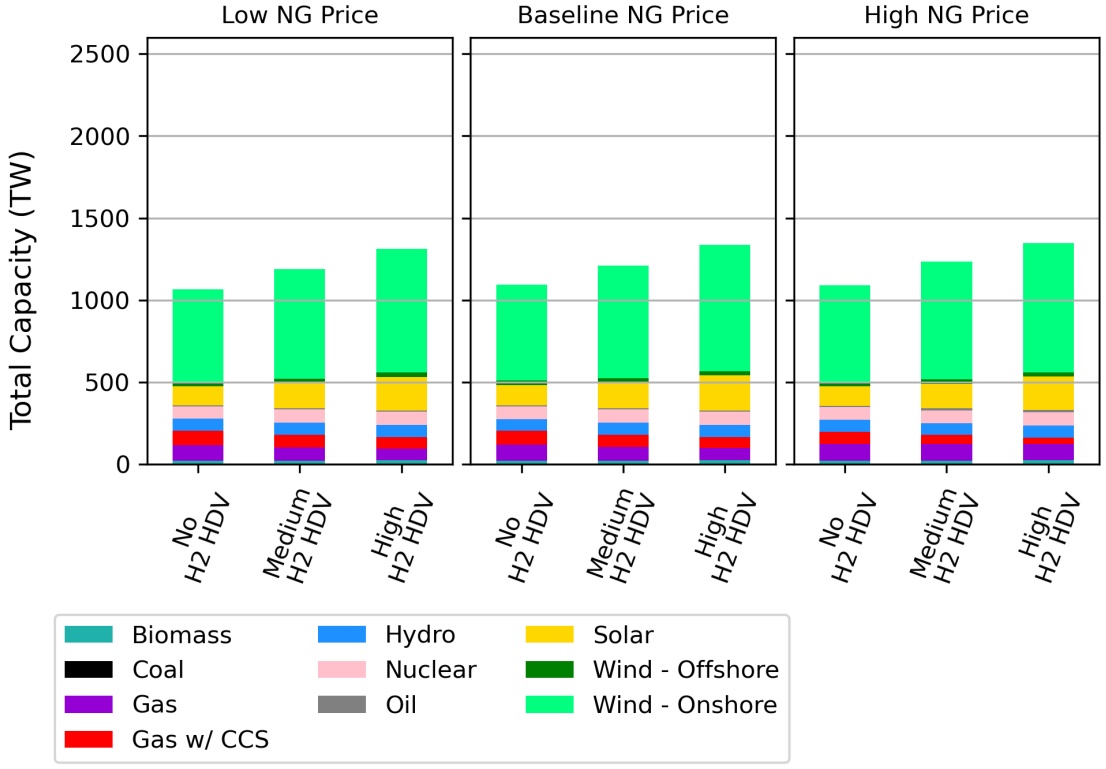

(b) Baseline CO_2 Storage

Figure C.8: Power capacity for no (sub-figure a) and baseline (sub-figure b) CO_2 sequestration scenarios under no synthetic fuel adoption. The price of natural gas increases left to right. Within each panel, the amount of H_2 HDV adoption increases moving from left to right. The middle panels correspond to the core set of scenarios

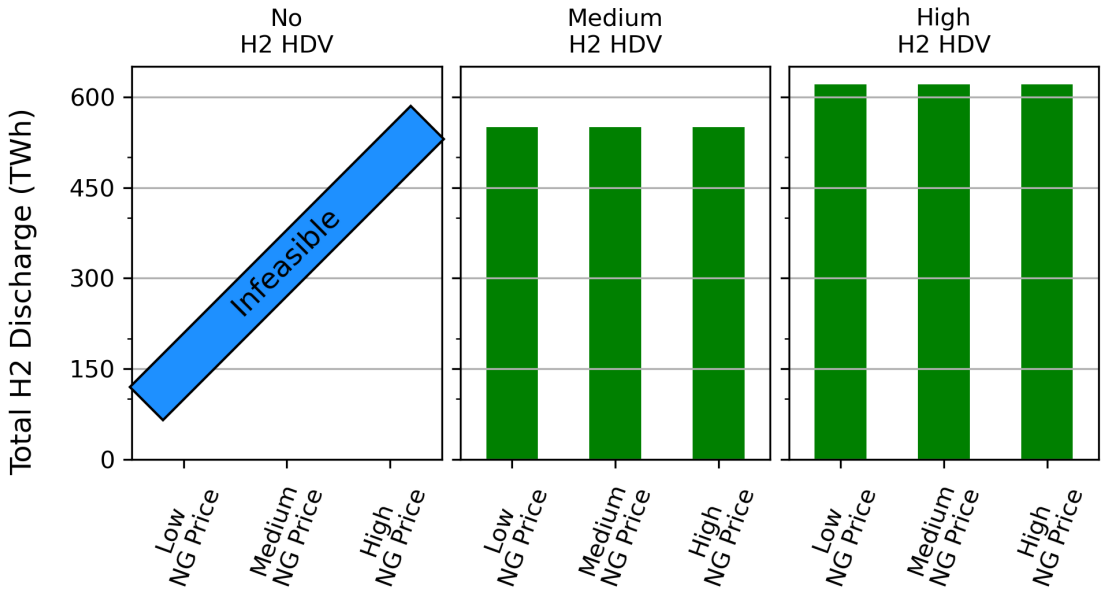

(a) No CO_2 Storage

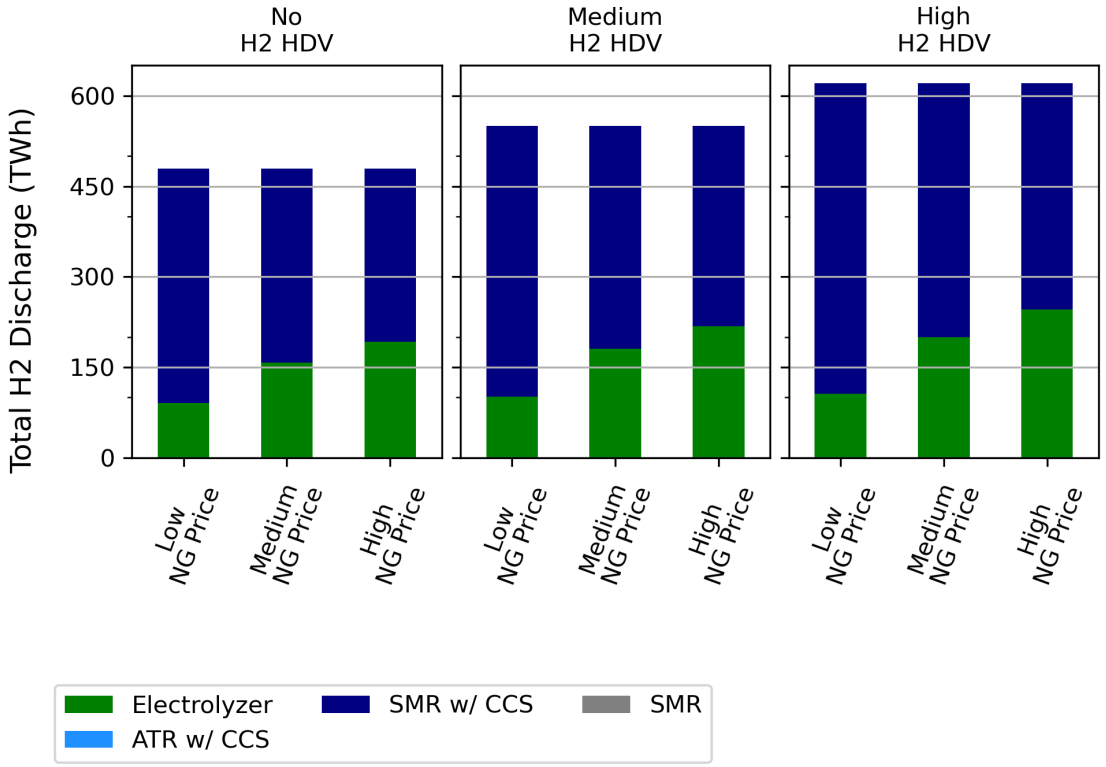

(b) Baseline CO_2 Storage

Figure C.9: H_2 generation for no (sub-figure a) and baseline (sub-figure b) CO_2 sequestration scenarios under no synthetic fuel adoption. The price of natural gas increases left to right. Within each panel, the amount of H_2 HDV adoption increases moving from left to right. The middle panels correspond to the core set of scenarios.

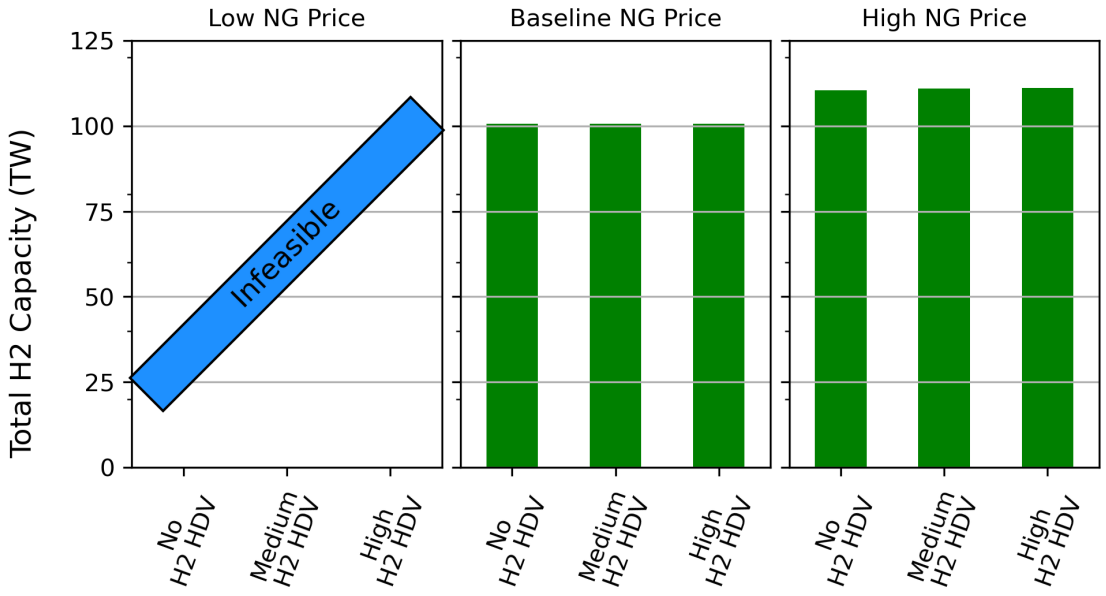

(a) No CO_2 Storage

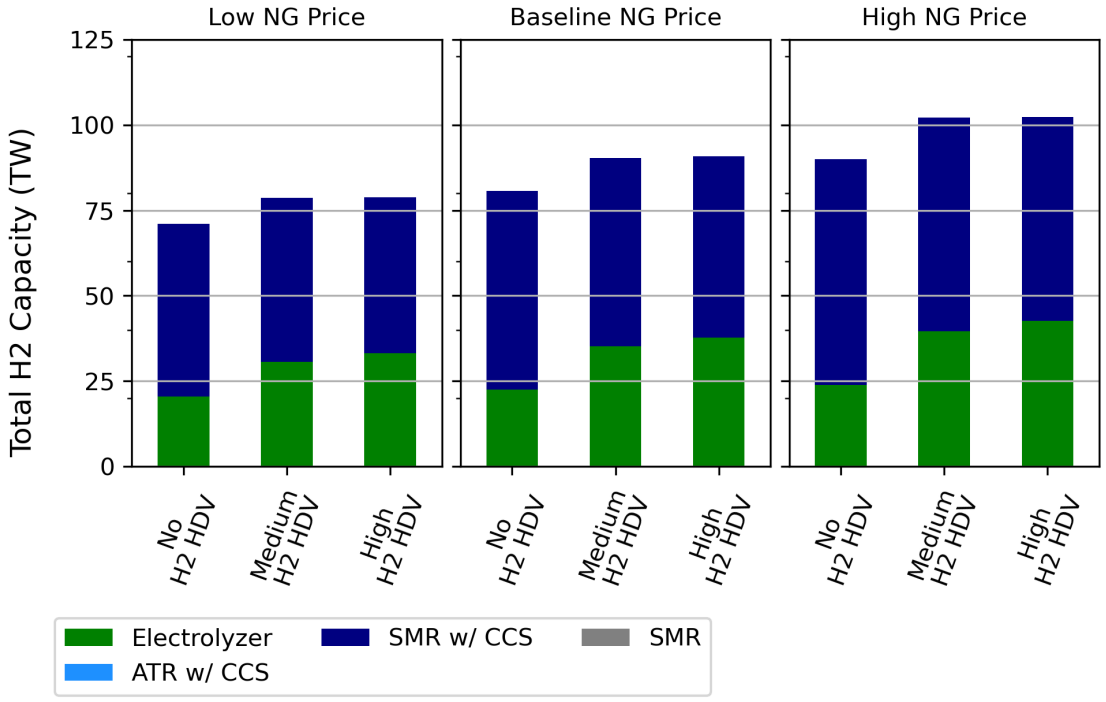

(b) Baseline CO_2 Storage

Figure C.10: H_2 capacity for no (sub-figure a) and baseline (sub-figure b) CO_2 sequestration scenarios under no synthetic fuel adoption. The price of natural gas increases left to right. Within each panel, the amount of H_2 HDV adoption increases moving from left to right. The middle panels correspond to the core set of scenarios

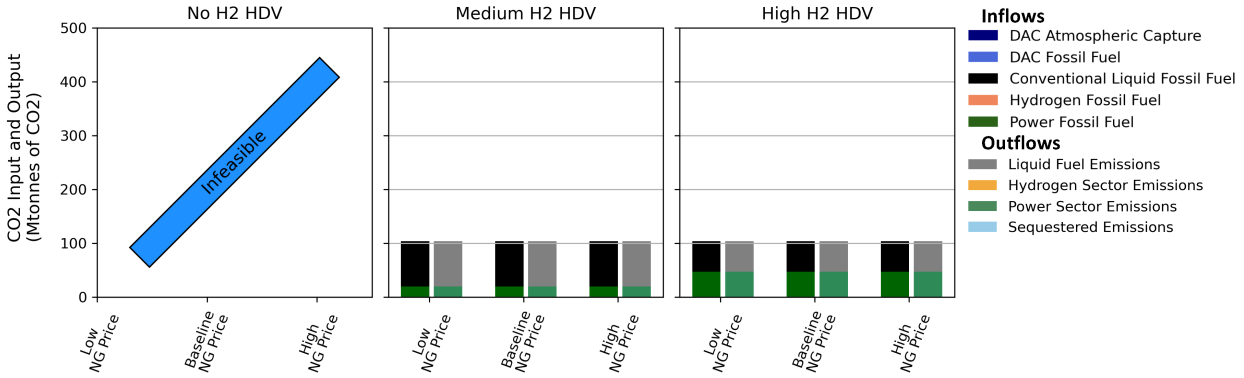

(a) No CO_2 Storage

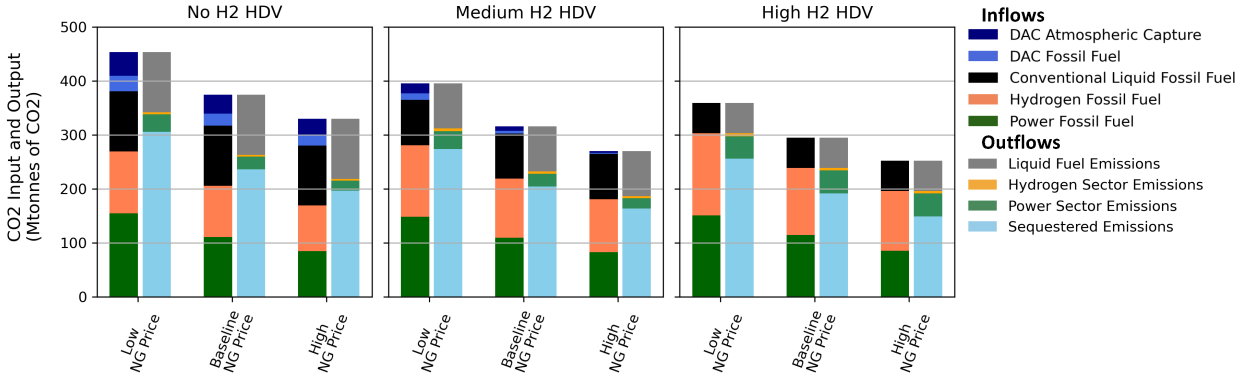

(b) Baseline CO_2 Storage

Figure C.11: System CO_2 balance under varying levels of H_2 HDV adoption and no SF adoption for no (sub-figure a) and baseline (sub-figure b) CO_2 sequestration scenarios. The price of natural gas increases left to right. Within each subplot the H_2 HDV adoption level increases left to right. The leftward column represents CO_2 input into the system, while the rightward column represents CO_2 outputted by the system. All scenarios adhere to the same emissions constraint of 103 MTonnes. The middle panels correspond to the core set of scenarios. Emissions constraint can be calculated from the chart by subtracting sequestered emissions and DAC atmospheric capture from the emission outflows. Emissions constraint can be calculated from the chart by subtracting sequestered emissions and DAC atmospheric capture from the emission outflows.

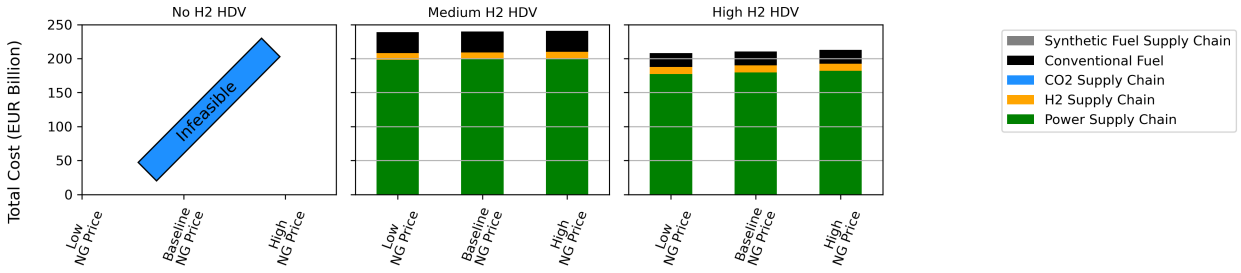

(a) No CO_2 Storage

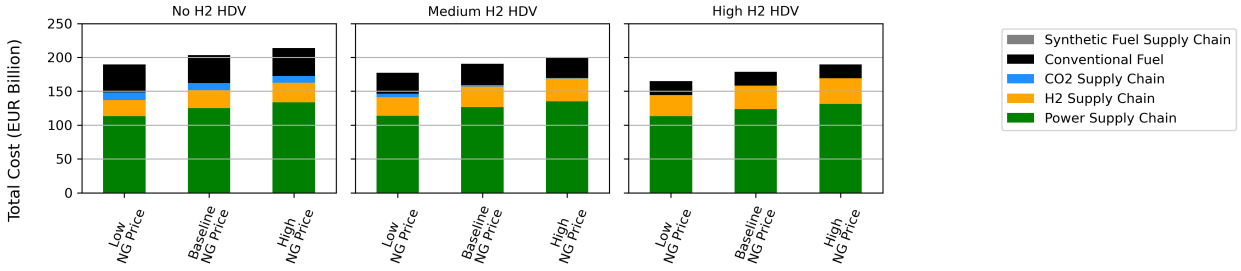

(b) Baseline CO_2 Storage

Figure C.12: Annualized bulk-system costs under varying levels of H_2 HDV adoption and no SF adoption for no (sub-figure a) and baseline (sub-figure b) CO_2 sequestration scenarios. The price of natural gas increases left to right. Within each subplot the H_2 HDV adoption level increases left to right. The middle panels correspond to the core set of scenarios. The costs do not include vehicle replacement or H_2 distribution costs.

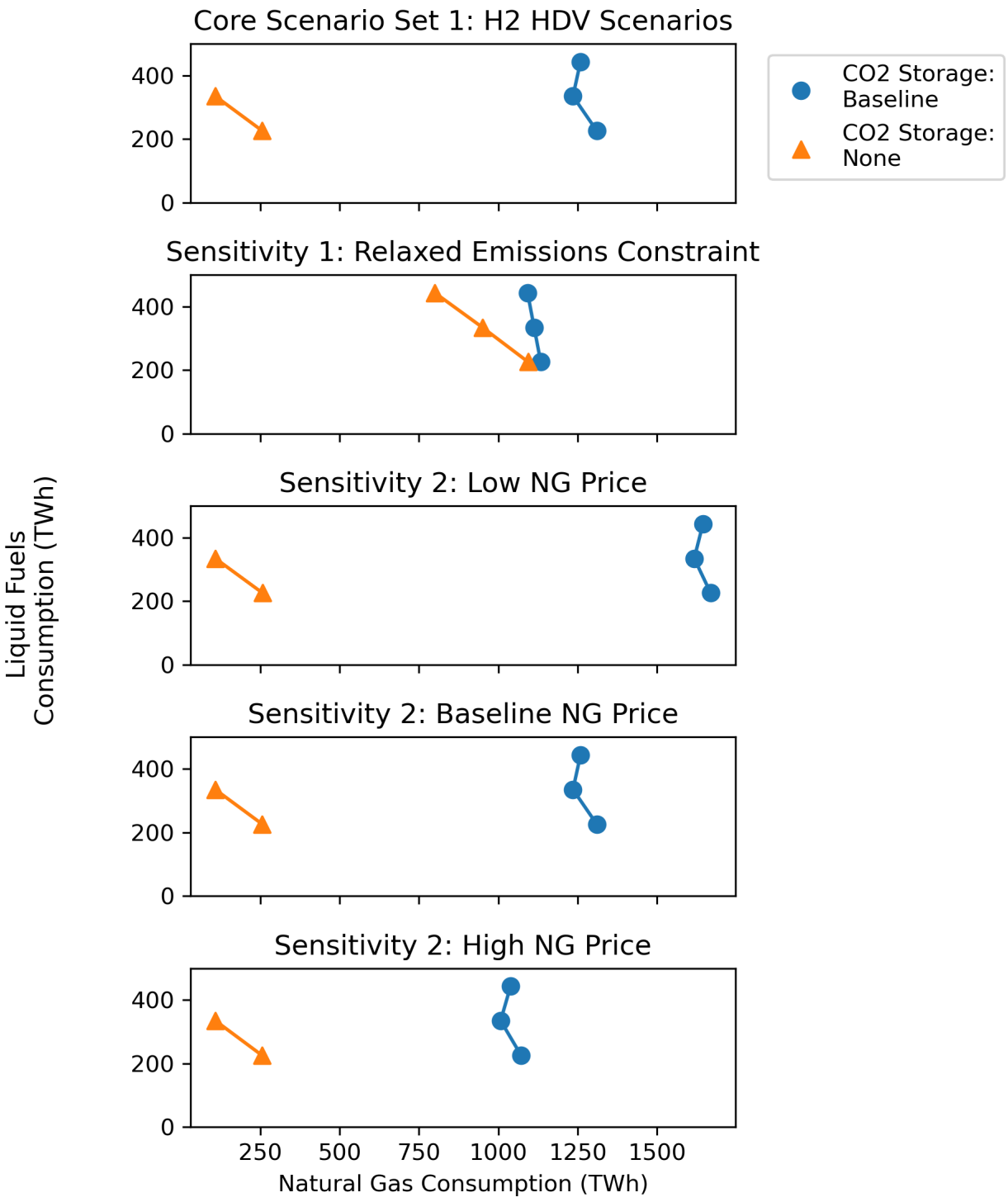

Figure C.13: Trade-off between natural gas (NG) and liquid fossil fuel utilization for scenarios where amount of H_2 HDVs is varied. The subfigure on the top shows the relationship for the H_2 HDV scenarios(i.e. scenario set 1), while the second plot shows the results for the relaxed emission sensitivity (i.e. sensitivity scenario set 1). The last 3 shows the results for the natural gas price sensitivities (i.e. sensitivity scenario set 2). Within each subplot the amount of natural gas consumption can be examined on the x-axis, while the amount of liquid fossil fuel consumption can be examined on the y-axis. The amount of H_2 and SF HDV adoption increases from top to bottom. The amount of liquid fossil fuel consumption includes diesel and gasoline, and excludes jet fuel as well as excess synthetic fuels.

C.3 Sensitivity Set 3: Core Scenario Set 2 with No H_2 HDV Deployment

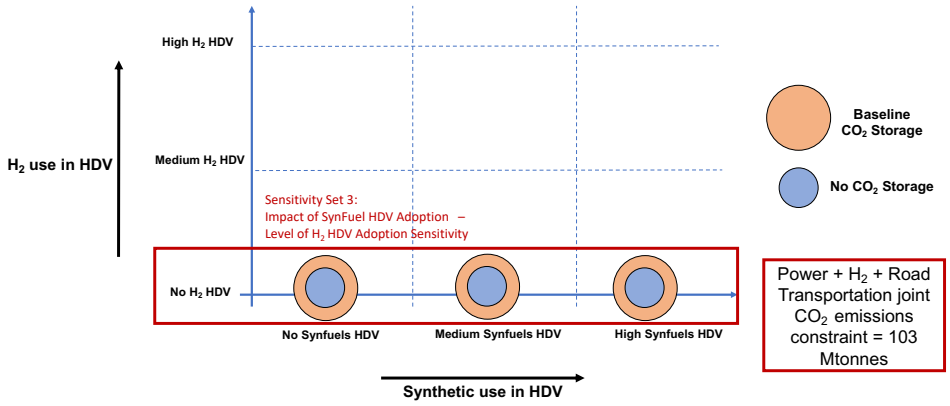

Figure C.14: Sensitivity set 3 scenario matrix. Each bubble represents a scenario. The y-axis represents varying levels of H_2 HDV adoption, while the x-axis represents varying levels synthetic fuel adoption. All scenarios are equivalent from an emissions capping perspective with a cap of 103 $MTCO_2$. HDV fleet represents all vehicle types with gross weight great than 7.5 tonnes. This scenario set is based on core scenario set 2, but with no H_2 HDVs adoption instead of medium H_2 HDV.

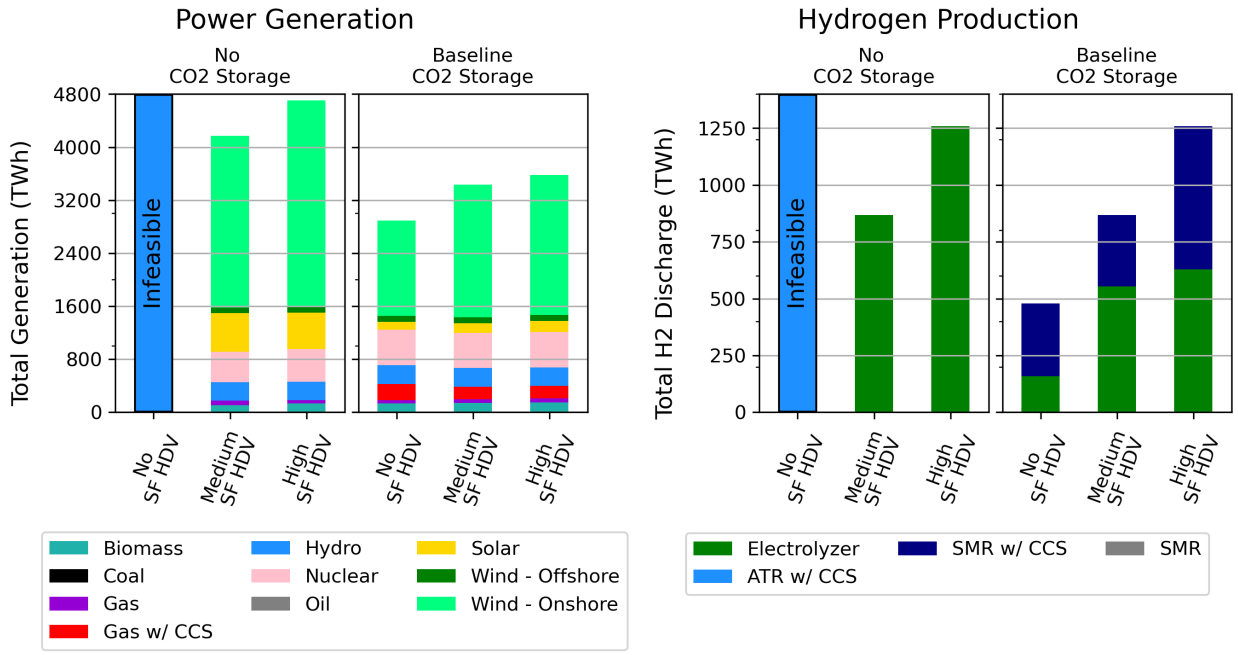

Figure C.15: Power and hydrogen generation for baseline and no CO_2 sequestration scenarios under no H_2 HDV adoption. The left set of charts shows power generation and the right set of charts shows H_2 generation. Within each panel, the amount of synthetic fuel adoption increases moving from left to right.

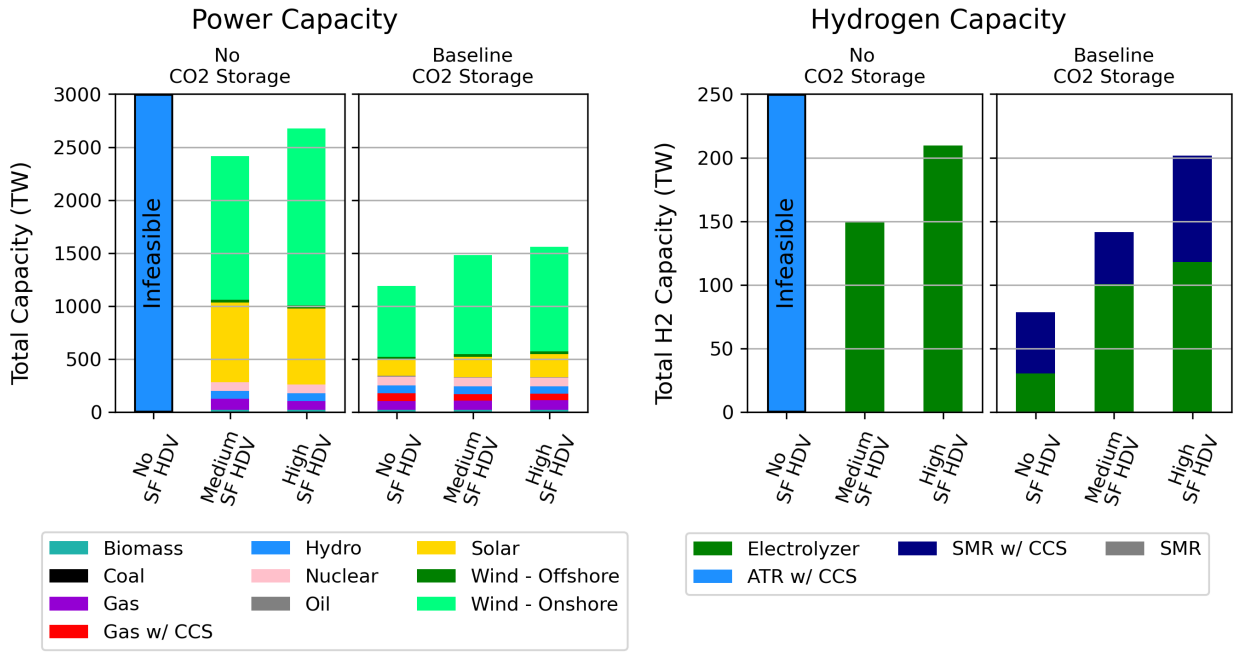

Figure C.16: Power and H_2 capacity for baseline and no CO_2 sequestration scenarios under no H_2 HDV adoption. The left set of charts shows power generation and the right set of charts shows H_2 generation. Within each panel, the amount of synthetic fuel adoption increases moving from left to right.

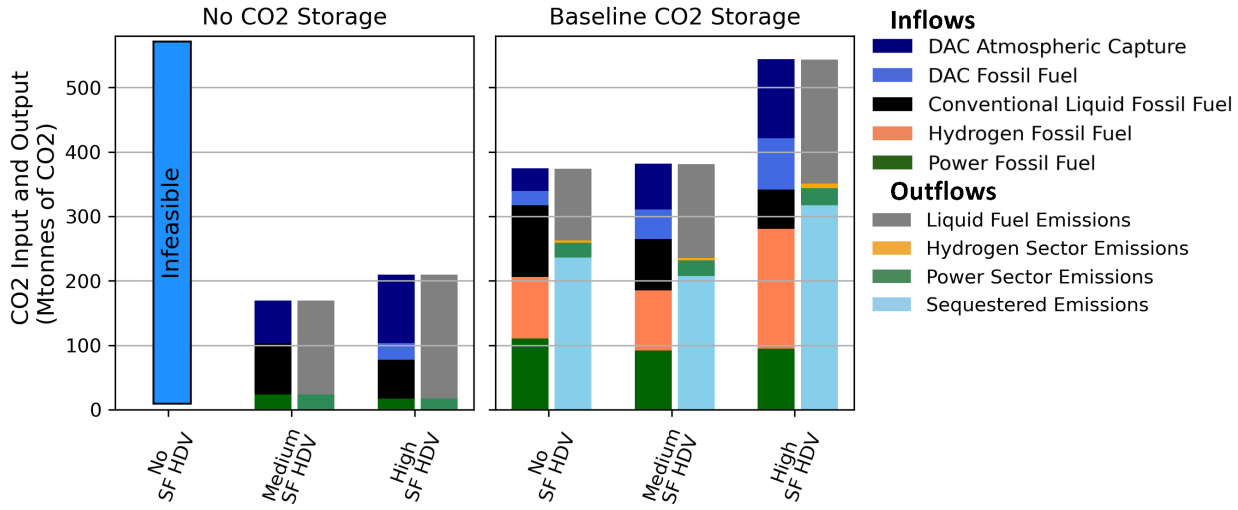

Figure C.17: System CO_2 balance under varying levels of SF adoption and no H_2 HDV adoption. The subfigure on the left shows the CO_2 balance under no CO_2 sequestration availability, while the one on the right shows the CO_2 balance under baseline CO_2 sequestration availability. Within each subplot the SF adoption level increases left to right. The leftward column represents CO_2 input into the system, while the rightward column represents CO_2 outputted by the system. Emissions constraint can be calculated from the chart by subtracting sequestered emissions and DAC atmospheric capture from the emission outflows. Emissions constraint can be calculated from the chart by subtracting sequestered emissions and DAC atmospheric capture from the emission outflows.

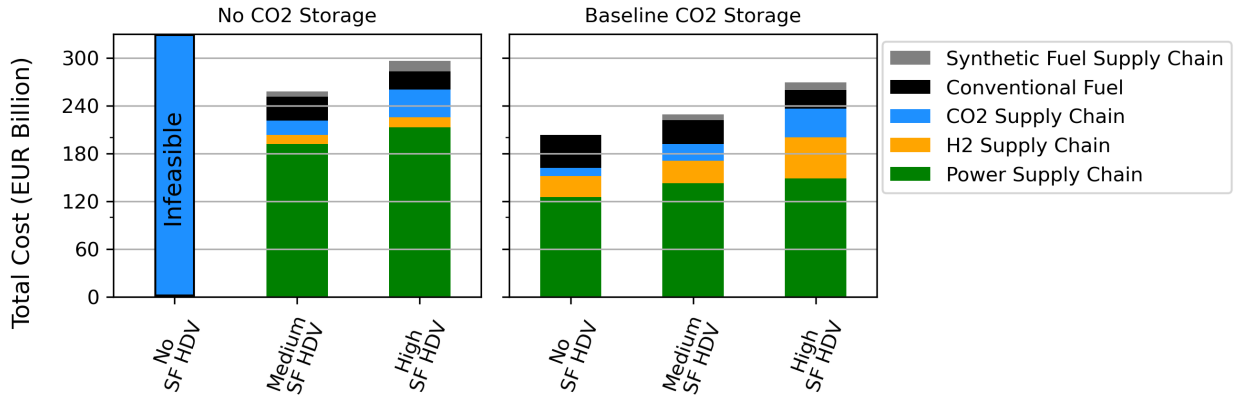

Figure C.18: Annualized bulk-system costs under varying levels of SF adoption and no H_2 HDV adoption.The subfigure on the left shows the cost breakdown under no CO_2 sequestration availability, while the one on the right shows the cost breakdown under baseline CO_2 sequestration availability. Within each subplot the H_2 HDV adoption level increases left to right. The costs do not include vehicle replacement or H_2 distribution costs.

C.4 Sensitivity Set 4: Core Scenario Set 2 with Natural Gas Price Sensitivity

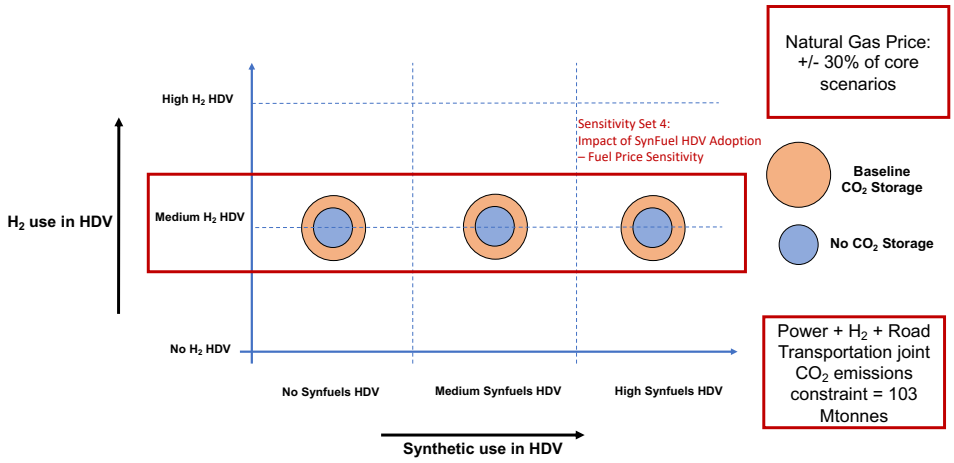

Figure C.19: Sensitivity set 4 scenario matrix. Each bubble represents a scenario. The y-axis represents varying levels of H_2 HDV adoption, while the x-axis represents varying levels synthetic fuel adoption. All scenarios are equivalent from an emissions capping perspective with a cap of 103 $MTCO_2$. HDV fleet represents all vehicle types with gross weight great than 7.5 tonnes. This scenario is based on core scenario set 2, but with +/-30% NG prices.

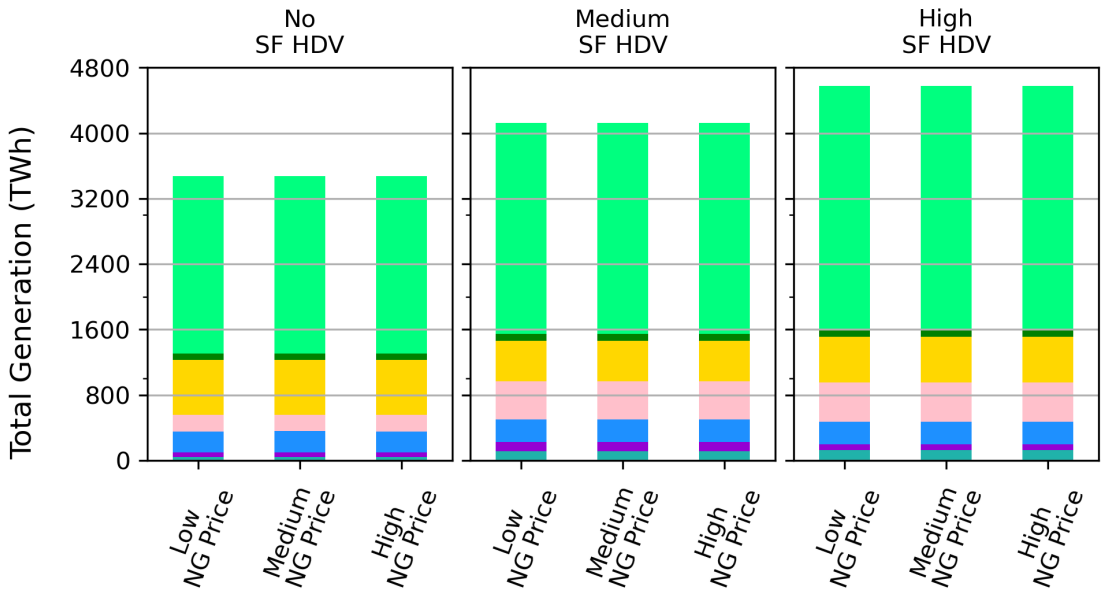

(a) No CO_2 Storage

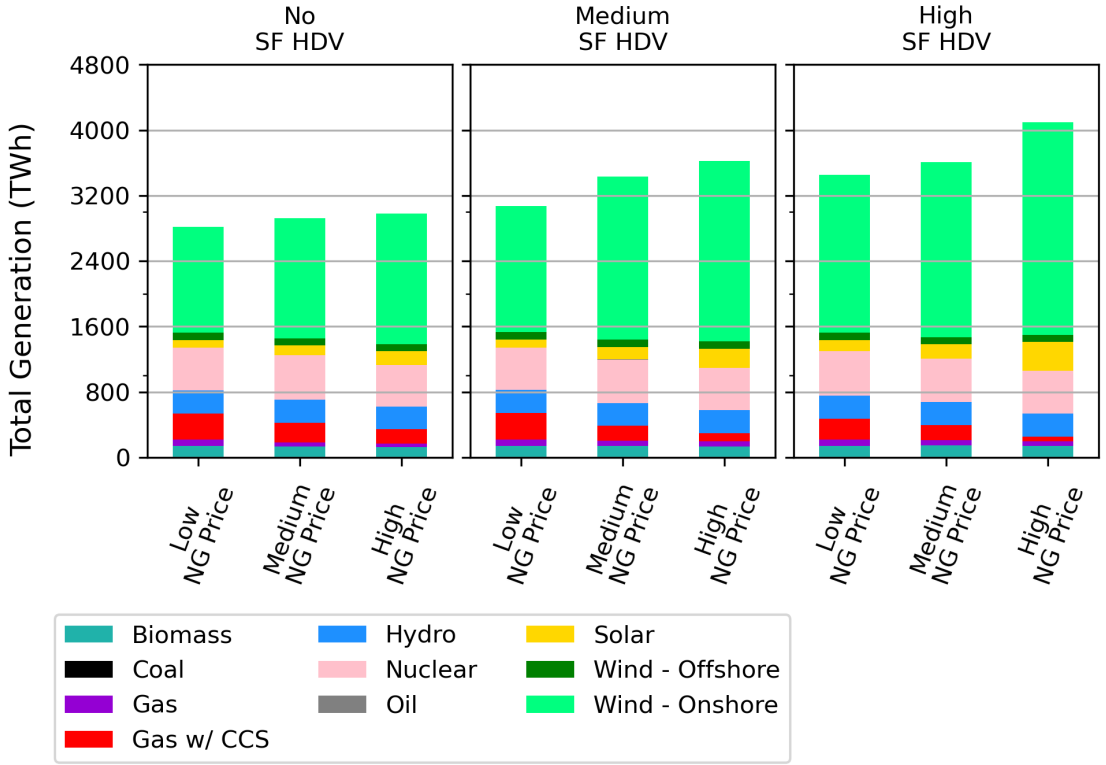

(b) Baseline CO_2 Storage

Figure C.20: Power generation for no (sub-figure a) and baseline (sub-figure b) CO_2 sequestration scenarios under no synthetic fuel adoption. The price of natural gas increases left to right. Within each panel, the amount of H_2 HDV adoption increases moving from left to right. The middle panels correspond to the core set of scenarios

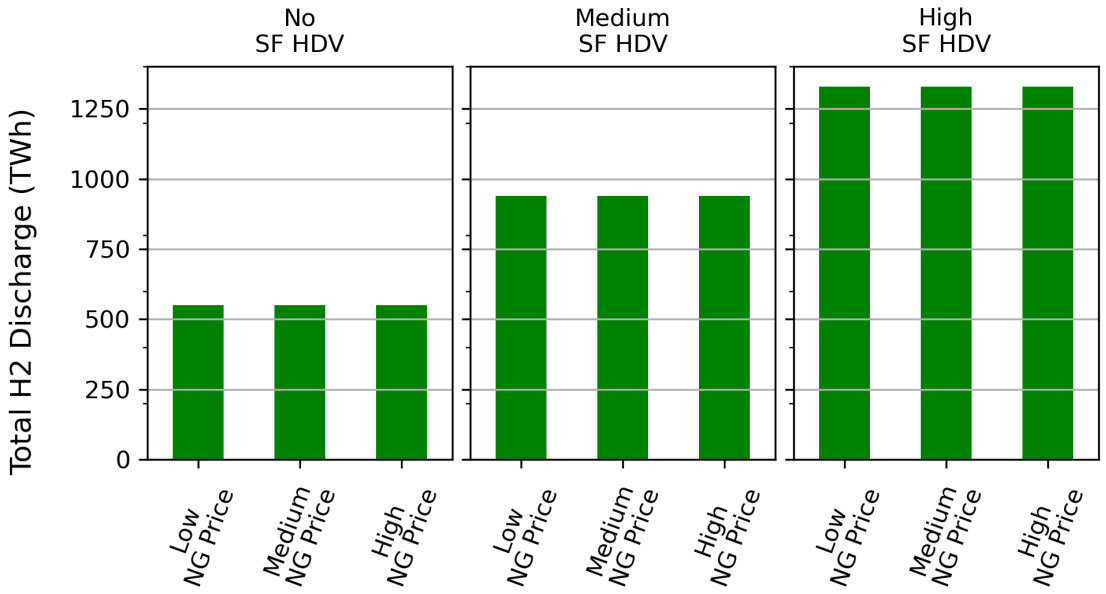

(a) No CO_2 Storage

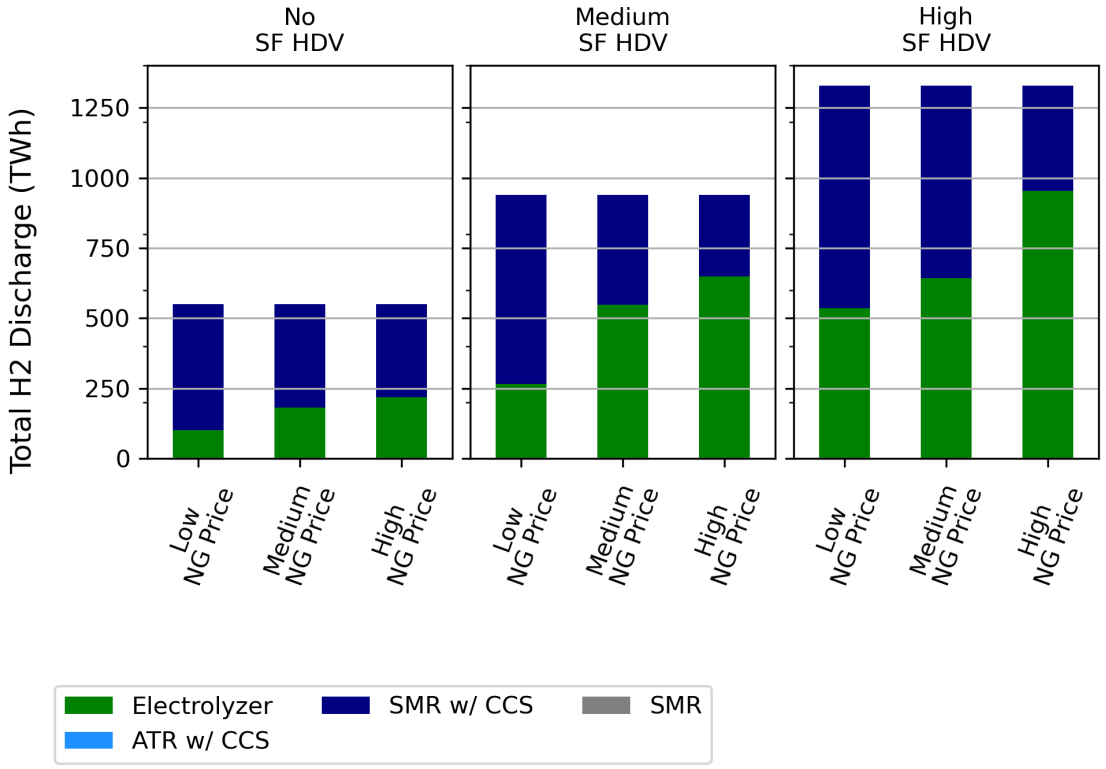

(b) Baseline CO_2 Storage

Figure C.21: H_2 generation for no (sub-figure a) and baseline (sub-figure b) CO_2 sequestration scenarios under no synthetic fuel adoption. The price of natural gas increases left to right. Within each panel, the amount of H_2 HDV adoption increases moving from left to right. The middle panels correspond to the core set of scenarios.

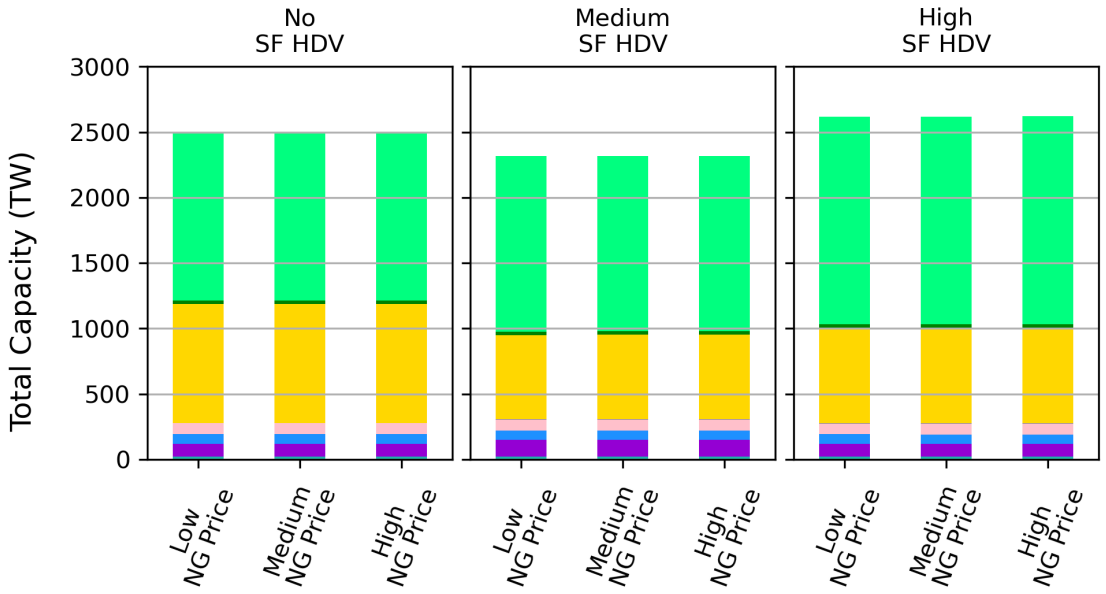

(a) No CO_2 Storage

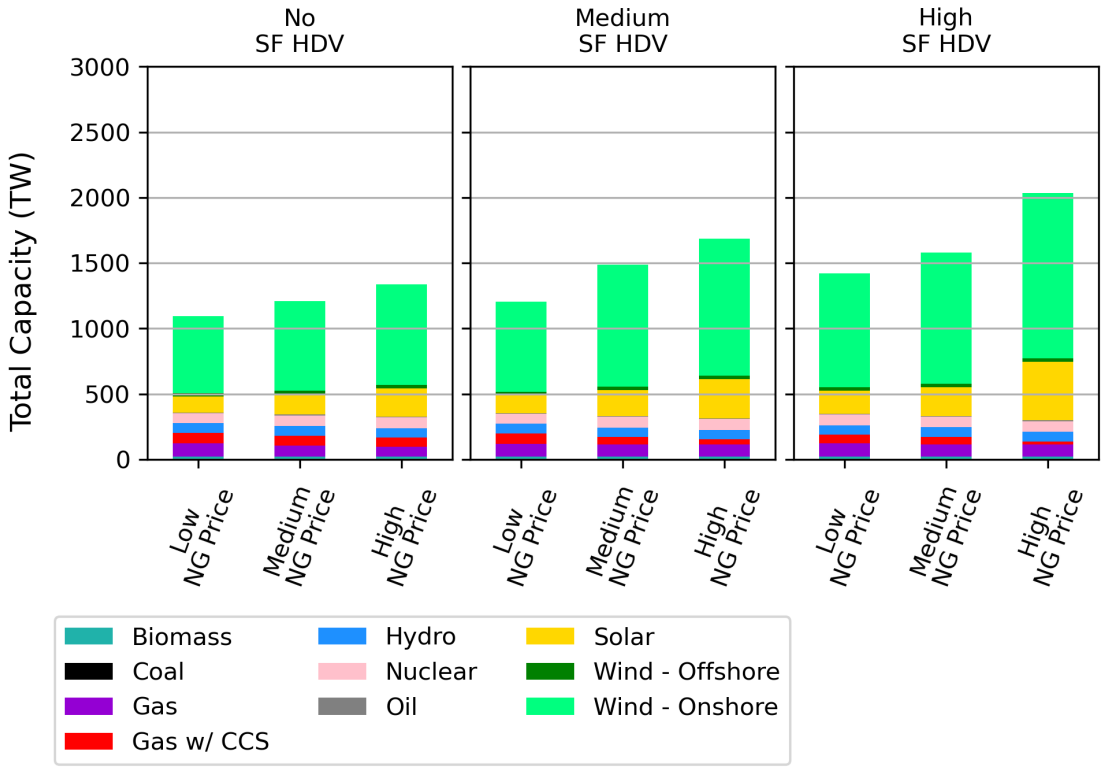

(b) Baseline CO_2 Storage

Figure C.22: Power capacity for no (sub-figure a) and baseline (sub-figure b) CO_2 sequestration scenarios under no synthetic fuel adoption. The price of natural gas increases left to right. Within each panel, the amount of synfuel adoption increases moving from left to right. The middle panels correspond to the core set of scenarios

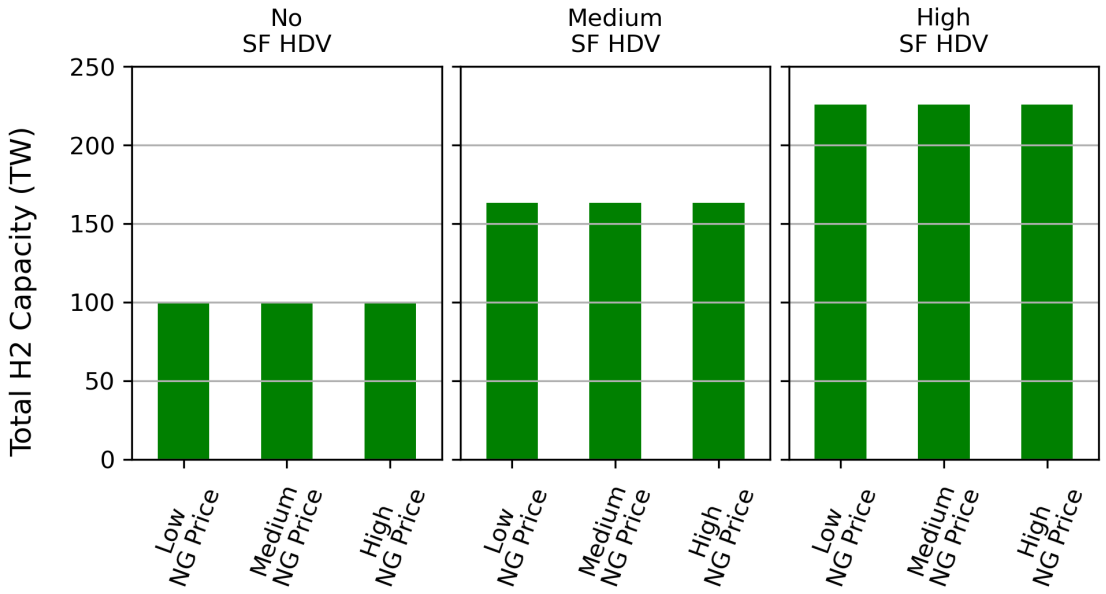

(a) No CO_2 Storage

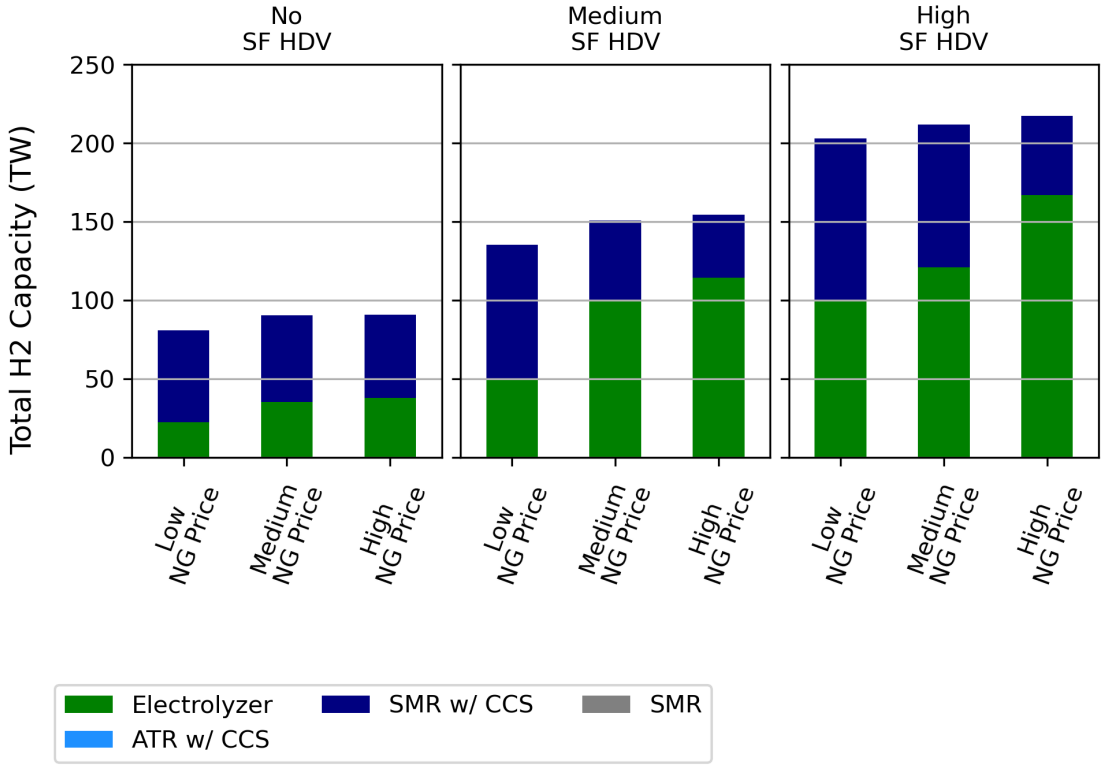

(b) Baseline CO_2 Storage

Figure C.23: H_2 capacity for no (sub-figure a) and baseline (sub-figure b) CO_2 sequestration scenarios under no synthetic fuel adoption. The price of natural gas increases left to right. Within each panel, the amount of synfuel adoption increases moving from left to right. The middle panels correspond to the core set of scenarios

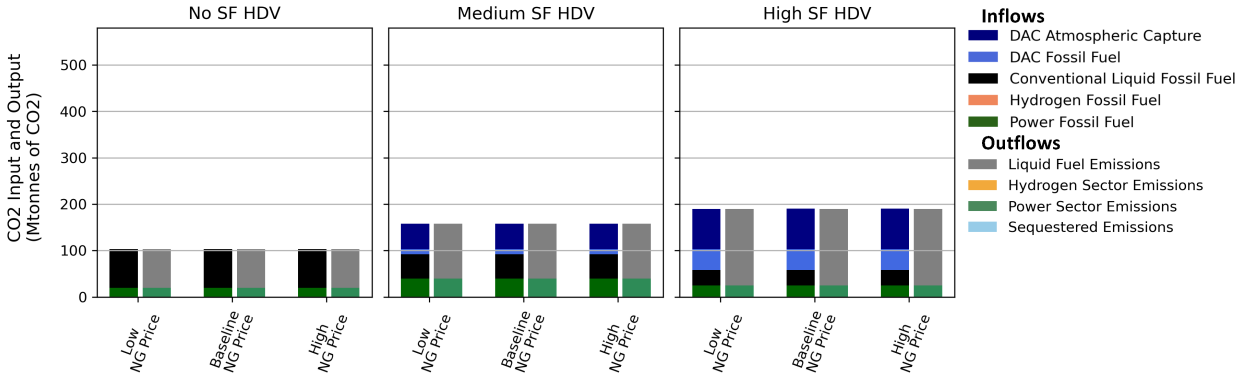

(a) No CO_2 Storage

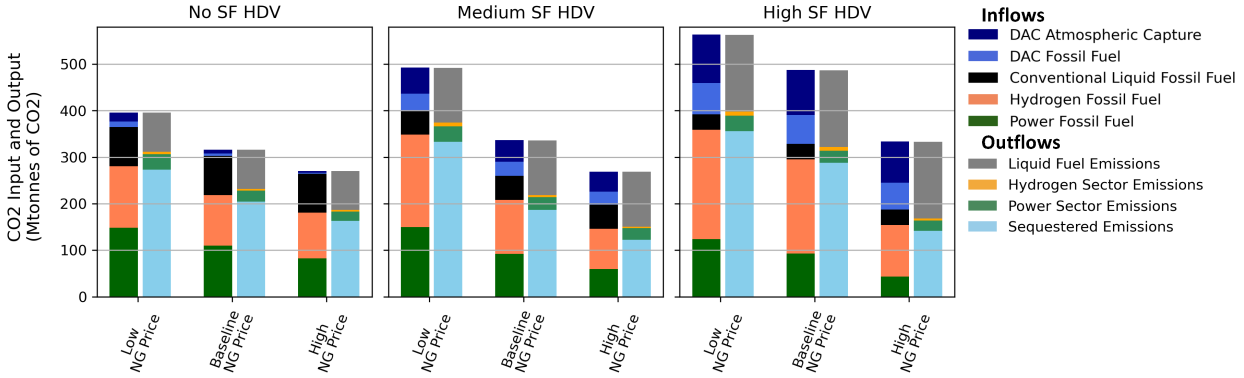

(b) Baseline CO_2 Storage

Figure C.24: System CO_2 balance under varying levels of H_2 HDV adoption and no SF adoption for no (sub-figure a) and baseline (sub-figure b) CO_2 sequestration scenarios. The price of natural gas increases left to right. Within each subplot the H_2 HDV adoption level increases left to right. The leftward column represents CO_2 input into the system, while the rightward column represents CO_2 outputted by the system. All scenarios adhere to the same emissions constraint of 103 MTonnes. The middle panels correspond to the core set of scenarios. Emissions constraint can be calculated from the chart by subtracting sequestered emissions and DAC atmospheric capture from the emission outflows. Emissions constraint can be calculated from the chart by subtracting sequestered emissions and DAC atmospheric capture from the emission outflows.

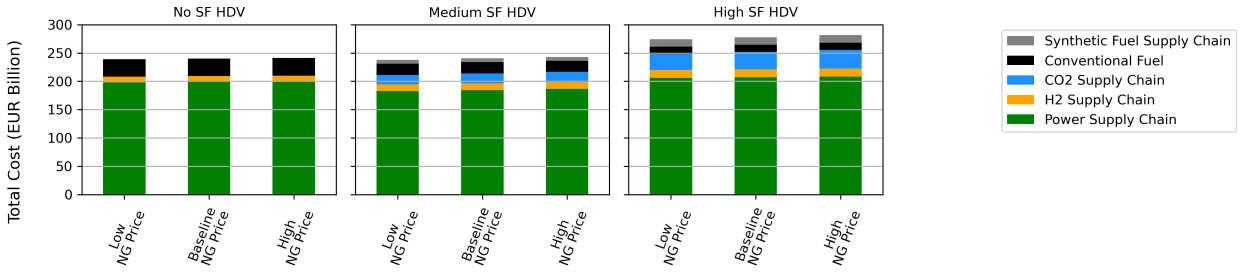

(a) No CO_2 Storage

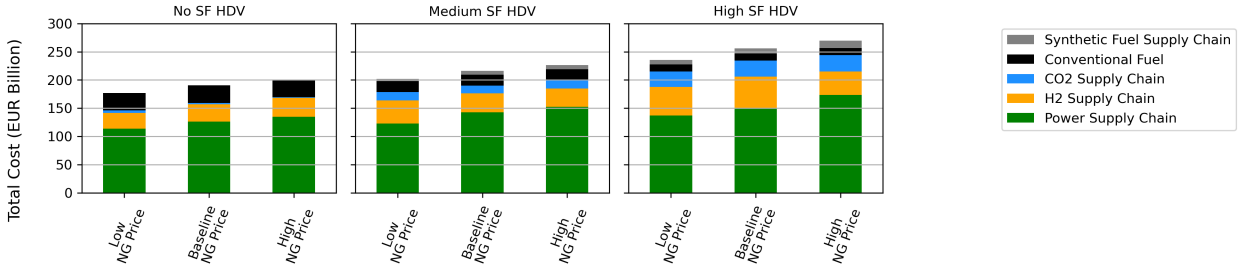

(b) Baseline CO_2 Storage

Figure C.25: Annualized bulk-system costs under varying levels of H_2 HDV adoption and no SF adoption for no (sub-figure a) and baseline (sub-figure b) CO_2 sequestration scenarios. The price of natural gas increases left to right. Within each subplot the H_2 HDV adoption level increases left to right. The middle panels correspond to the core set of scenarios. The costs do not include vehicle replacement or H_2 distribution costs.

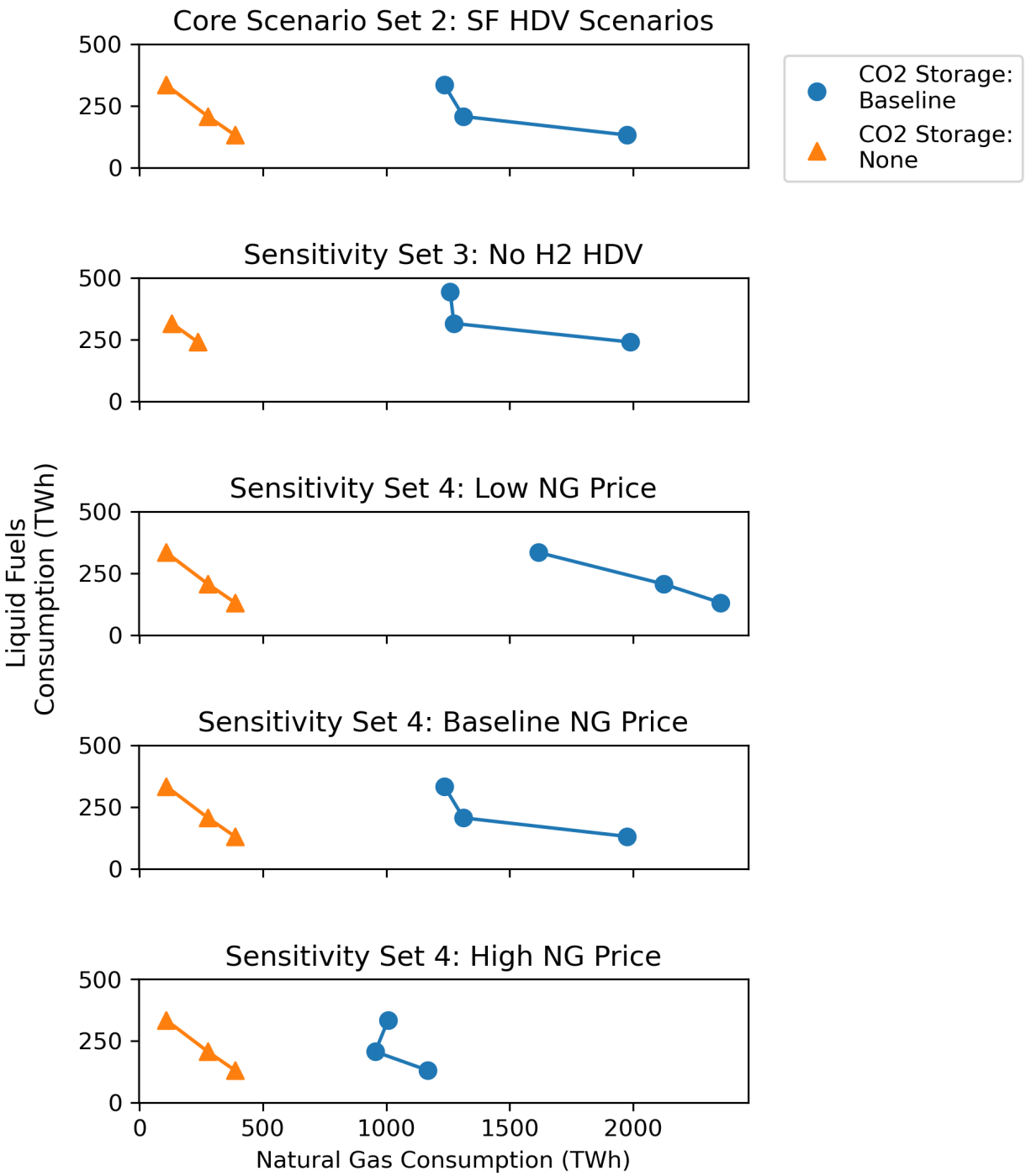

Figure C.26: Trade-off between natural gas (NG) and liquid fossil fuel utilization for scenarios where amount of SF adoption is varied. The subfigure on the top shows the relationship for the core SF HDV scenarios(i.e. scenario set 2), while the second plot shows the results for the SF scenario with no H_2 adoption (i.e. sensitivity scenario set 3). The last 3 shows the results for the natural gas price sensitivities (i.e. sensitivity scenario set 4). Within each subplot the amount of natural gas consumption can be examined on the x-axis, while the amount of liquid fossil fuel consumption can be examined on the y-axis. The amount of SF HDV adoption increases from top to bottom. The amount of liquid fossil fuel consumption includes diesel and gasoline, and excludes jet fuel as well as excess synthetic fuels.

References

[1] European Environment Agency, *EEA greenhouse gases Data Viewer*, en, Dashboard (Tableau), Apr. 2023. [Online]. Available: https://www.eea.europa.eu/data-and-maps/data/data-viewers/greenhouse-gases-viewer (visited on 08/03/2023).

[2] Energy - Eurostat, *SHARES - Energy Eurostat*, May 2023. [Online]. Available: https://ec.europa.eu/eurostat/web/energy/database/additional-data#Short%20assessment%20of%20renewable%20energy%20sources%20(SHARES) (visited on 08/03/2023).

[3] ACEA, *Fuel types of new passenger cars in the EU*, en-GB, May 2023. [Online]. Available: https://www.acea.auto/figure/fuel-types-of-new-passenger-cars-in-eu/ (visited on 08/03/2023).

[4] S. J. Davis, N. S. Lewis, M. Shaner, *et al.*, "Net-zero emissions energy systems," *Science*, vol. 360, no. 6396, eaas9793, Jun. 2018, Publisher: American Association for the Advancement of Science. DOI: 10.1126/science.aas9793. [Online]. Available: https://www.science.org/doi/10.1126/science.aas9793 (visited on 05/26/2023).

[5] O. Bethoux, "Hydrogen Fuel Cell Road Vehicles: State of the Art and Perspectives," en, *Energies*, vol. 13, no. 21, p. 5843, Jan. 2020, Number: 21 Publisher: Multidisciplinary Digital Publishing Institute, ISSN: 1996-1073. DOI: 10.3390/en13215843. [Online]. Available: https://www.mdpi.com/1996-1073/13/21/5843 (visited on 05/26/2023).

[6] M. d. l. N. Camacho, D. Jurburg, and M. Tanco, "Hydrogen fuel cell heavy-duty trucks: Review of main research topics," en, *International Journal of Hydrogen Energy*, vol. 47, no. 68, pp. 29 505–29 525, Aug. 2022, ISSN: 0360-3199. DOI: 10.1016/j.ijhydene.2022.06.271. [Online]. Available: https://www.sciencedirect.com/science/article/pii/S0360319922029068 (visited on 05/26/2023).

[7] A. M. Mowry and D. S. Mallapragada, "Grid impacts of highway electric vehicle charging and role for mitigation via energy storage," *Energy Policy*, vol. 157, p. 112 508, Oct. 2021, ISSN: 0301-4215. DOI: 10.1016/j.enpol.2021.112508. [Online]. Available: https://www.sciencedirect.com/science/article/pii/S0301421521003785 (visited on 12/27/2023).

[8] M. Eddy and E. Solomon, "Germany Pushes for Exception in Law Banning Combustion Engines," en-US, *The New York Times*, Mar. 2023, ISSN: 0362-4331. [Online]. Available: https://www.nytimes.com/2023/03/22/business/germany-eu-climate-combustion-engines.html (visited on 08/03/2023).

[9] Mallapragada, Dharik, He, Guannan, Zhang, Yuheng, Shaker, Youssef, Law, Jun Wen, Shi, Nicole, and Cybulsky, Anna, *DOLPHYN: Decision Optimization for Low Carbon Power and Hydrogen Nexus*, original-date: 2021-11-01T16:01:42Z, May 2023. [Online]. Available: https://github.com/macroenergy/DOLPHYN (visited on 05/28/2023).

[10] F. Holz, T. Scherwath, P. Crespo del Granado, C. Skar, L. Olmos, Q. Ploussard, A. Ramos, and A. Herbst, "A 2050 perspective on the role for carbon capture and storage in the European power system and industry sector," *Energy Economics*, vol. 104, p. 105 631, Dec. 2021, ISSN: 0140-9883. DOI: 10.1016/j.eneco.2021.105631. [Online]. Available: https://www.sciencedirect.com/science/article/pii/S0140988321004941 (visited on 12/26/2023).

[11] European Commission, *COMMUNICATION FROM THE COMMISSION TO THE EUROPEAN PARLIAMENT, THE EUROPEAN COUNCIL, THE COUNCIL, THE EUROPEAN ECONOMIC AND SOCIAL COMMITTEE AND THE COMMITTEE OF THE REGIONS The European Green Deal*, en, Dec. 2019. [Online]. Available: https://eur-lex.europa.eu/legal-content/EN/TXT/?uri=COM%3A2019%3A640%3AFIN (visited on 05/26/2023).

[12] European Commission, *REGULATION OF THE EUROPEAN PARLIAMENT AND OF THE COUNCIL amending Regulation (EU) 2019/1242 as regards strengthening the CO emission performance standards for new heavy-duty vehicles and integrating reporting obligations, and repealing Regulation (EU) 2018/956*, English, Feb. 2023. [Online]. Available: https://eur-lex.europa.eu/legal-content/EN/TXT/?uri=COM%3A2023%3A88%3AFIN.

[13] J. Krause, C. Thiel, D. Tsokolis, Z. Samaras, C. Rota, A. Ward, P. Prenninger, T. Coosemans, S. Neugebauer, and W. Verhoeve, "EU road vehicle energy consumption and CO2 emissions by 2050 – Expert-based scenarios," en, *Energy Policy*, vol. 138, p. 111 224, Mar. 2020, ISSN: 03014215. DOI: 10.1016/j.enpol.2019.111224. [Online]. Available: https://linkinghub.elsevier.com/retrieve/pii/S0301421519308067 (visited on 12/10/2021).

[14] N. Winton, *Volvo Sells 1,000 Battery-Electric Trucks, Makes Hydrogen Progress*, en, Section: Transportation, May 2023. [Online]. Available: https://www.forbes.com/sites/neilwinton/2023/05/22/volvo-sells-1000-battery-electric-trucks-makes-hydrogen-progress/ (visited on 05/26/2023).

[15] Tesla, *Tesla Semi*, en. [Online]. Available: https://www.tesla.com/semi (visited on 05/26/2023).

[16] European Commission, *New law agreed to deploy alternative fuels infrastructure*, en, Text, 2023. [Online]. Available: https://ec.europa.eu/commission/presscorner/detail/en/ip_23_1867 (visited on 05/26/2023).

[17] Posaner, Joshua, *Brussels to Berlin: We'll find a way to save the car engine*, en, Mar. 2023. [Online]. Available: https://www.politico.eu/article/brussels-to-berlin-well-find-a-way-to-save-the-combustion-car-engine-emissions-synthetic-fuels/ (visited on 03/29/2023).

[18] S. Brynolf, M. Taljegard, M. Grahn, and J. Hansson, "Electrofuels for the transport sector: A review of production costs," en, *Renewable and Sustainable Energy Reviews*, vol. 81, pp. 1887–1905, Jan. 2018, ISSN: 1364-0321. DOI: 10.1016/j.rser.2017.05.288. [Online]. Available: https://www.sciencedirect.com/science/article/pii/S1364032117309358 (visited on 10/20/2021).

[19] S. Hänggi, P. Elbert, T. Bütler, U. Cabalzar, S. Teske, C. Bach, and C. Onder, "A review of synthetic fuels for passenger vehicles," en, *Energy Reports*, vol. 5, pp. 555–569, Nov. 2019, ISSN: 2352-4847. DOI: 10.1016/j.egyr.2019.04.007. [Online]. Available: https://www.sciencedirect.com/science/article/pii/S235248471830266X (visited on 10/06/2021).

[20] G. Harrison and C. Thiel, "Policy insights and modelling challenges: The case of passenger car powertrain technology transition in the European Union," en, *European Transport Research Review*, vol. 9, no. 3, pp. 1–14, Sep. 2017, Number: 3 Publisher: SpringerOpen, ISSN: 1866-8887. DOI: 10.1007/s12544-017-0252-x. [Online]. Available: https://etrr.springeropen.com/articles/10.1007/s12544-017-0252-x (visited on 12/17/2023).

[21] B. Li, Z. Ma, P. Hidalgo-Gonzalez, A. Lathem, N. Fedorova, G. He, H. Zhong, M. Chen, and D. M. Kammen, "Modeling the impact of EVs in the Chinese power system: Pathways for implementing emissions reduction commitments in the power and transportation sectors," *Energy Policy*, vol. 149, p. 111 962, Feb. 2021, ISSN: 0301-4215. DOI: 10.1016/j.enpol.2020.111962. [Online]. Available: https://www.sciencedirect.com/science/article/pii/S030142152030673X (visited on 12/17/2023).

[22] B. Li, M. Chen, Z. Ma, G. He, W. Dai, D. Liu, C. Zhang, and H. Zhong, "Modelling integrated power and transportation sectors decarbonization with hydrogen energy storage," *IEEE Transactions on Industry Applications*, pp. 1–1, 2021, Conference Name: IEEE Transactions on Industry Applications, ISSN: 1939-9367. DOI: 10.1109/TIA.2021.3116916.

[23] F. Ueckerdt, C. Bauer, A. Dirnaichner, J. Everall, R. Sacchi, and G. Luderer, "Potential and risks of hydrogen-based e-fuels in climate change mitigation," en, *Nature Climate Change*, vol. 11, no. 5, pp. 384–393, May 2021, Number: 5 Publisher: Nature Publishing Group, ISSN: 1758-6798. DOI: 10.1038/s41558-021-01032-7. [Online]. Available: https://www.nature.com/articles/s41558-021-01032-7 (visited on 12/17/2023).

[24] M. Millinger, P. Tafarte, M. Jordan, A. Hahn, K. Meisel, and D. Thrän, "Electrofuels from excess renewable electricity at high variable renewable shares: Cost, greenhouse gas abatement, carbon use and competition," en, *Sustainable Energy & Fuels*, vol. 5, no. 3, pp. 828–843, Feb. 2021, Publisher: The Royal Society of Chemistry, ISSN: 2398-4902. DOI: 10.1039/D0SE01067G. [Online]. Available: https://pubs.rsc.org/en/content/articlelanding/2021/se/d0se01067g (visited on 12/17/2023).

[25] G. Zang, P. Sun, A. Elgowainy, A. Bafana, and M. Wang, "Life Cycle Analysis of Electrofuels: Fischer–Tropsch Fuel Production from Hydrogen and Corn Ethanol Byproduct CO2," *Environmental Science & Technology*, vol. 55, no. 6, pp. 3888–3897, Mar. 2021, ISSN: 0013-936X. DOI: 10.1021/acs.est.0c05893. [Online]. Available: https://doi.org/10.1021/acs.est.0c05893 (visited on 09/22/2021).

[26] C. F. Heuberger, P. K. Bains, and N. Mac Dowell, "The EV-olution of the power system: A spatio-temporal optimisation model to investigate the impact of electric vehicle deployment," *Applied Energy*, vol. 257, p. 113 715, Jan. 2020, ISSN: 0306-2619. DOI: 10.1016/j.apenergy.2019.113715. [Online]. Available: https://www.sciencedirect.com/science/article/pii/S0306261919314023 (visited on 12/17/2023).

[27] S. Powell, G. V. Cezar, L. Min, I. M. L. Azevedo, and R. Rajagopal, "Charging infrastructure access and operation to reduce the grid impacts of deep electric vehicle adoption," en, *Nature Energy*, vol. 7, no. 10, pp. 932–945, Oct. 2022, Number: 10 Publisher: Nature Publishing Group, ISSN: 2058-7546. DOI: 10.1038/s41560-022-01105-7. [Online]. Available: https://www.nature.com/articles/s41560-022-01105-7 (visited on 12/02/2022).

[28] P. Colbertaldo, G. Guandalini, and S. Campanari, "Modelling the integrated power and transport energy system: The role of power-to-gas and hydrogen in long-term scenarios for Italy," *Energy*, vol. 154, pp. 592–601, Jul. 2018, ISSN: 0360-5442. DOI: 10.1016/j.energy.2018.04.089. [Online]. Available: https://www.sciencedirect.com/science/article/pii/S0360544218306960 (visited on 12/17/2023).

[29] M. Millinger, *Are biofuel mandates cost-effective? - An analysis of transport fuels and biomass usage to achieve emissions targets in the European energy system | Elsevier Enhanced Reader*, en, 2022. DOI: 10.1016/j.apenergy.2022.120016. [Online]. Available: https://reader.elsevier.com/reader/sd/pii/S0306261922012739?token=EFCE51151607128698F8C29307A2F3912C058BE0B88695DAD67E269AE60B81550DFCDB096067C2DDE1C03E3D34443017&originRegion=us-east-1&originCreation=20221210025251 (visited on 12/10/2022).

[30] G. He, D. S. Mallapragada, A. Bose, C. F. Heuberger, and E. Gençer, "Hydrogen Supply Chain Planning With Flexible Transmission and Storage Scheduling," *IEEE Transactions on Sustainable Energy*, vol. 12, no. 3, pp. 1730–1740, Jul. 2021, ISSN: 1949-3037. DOI: 10.1109/TSTE.2021.3064015.

[31] MITEI, *GenX*. [Online]. Available: https://energy.mit.edu/genx/ (visited on 09/01/2021).

[32] J. D. Jenkins and N. A. Sepulveda, "Enhanced Decision Support for a Changing Electricity Landscape: The GenX Configurable Electricity Resource Capacity Expansion Model," en, MIT Energy Initiative, Tech. Rep., Nov. 2017. [Online]. Available: https://energy.mit.edu/wp-content/uploads/2017/10/Enhanced-Decision-Support-for-a-Changing-Electricity-Landscape.pdf.

[33] ENTSOE, *ENTSO-E Transparency Platform*. [Online]. Available: https://transparency.entsoe.eu/ (visited on 06/29/2023).

[34] ENTSOE, *TYNDP 2022 Scenario Building Guidelines*, en, Apr. 2022. [Online]. Available: https://2022.entsos-tyndp-scenarios.eu/wp-content/uploads/2022/04/TYNDP_2022_Scenario_Building_Guidelines_Version_April_2022.pdf.

[35] European Commission, *EU Reference Scenario 2020*, en, 2020. [Online]. Available: https://energy.ec.europa.eu/data-and-analysis/energy-modelling/eu-reference-scenario-2020_en (visited on 06/07/2023).

[36] EMISIA, *TRACCS*, 2014. [Online]. Available: https://traccs.emisia.com/ (visited on 06/07/2023).

[37] E. Commission, *Technology Assumptions EU Reference Scenario 2020 - European Commission*, en, 2020. [Online]. Available: https://energy.ec.europa.eu/document/download/5959845e-435c-4780-9281-b64a709b273b_en?filename=ref2020_technology_assumptions.zip (visited on 01/08/2024).

[38] J. Hörsch, F. Hofmann, D. Schlachtberger, T. Brown, and F. Neumann, *Complete Data Bundle for PyPSA-Eur: An Open Optimisation Model of the European Transmission System*, eng, Oct. 2019. DOI: 10.5281/zenodo.3517935. [Online]. Available: https://zenodo.org/record/3517935 (visited on 06/29/2023).

[39] NREL, *NREL ATB*, 2022. [Online]. Available: https://atb.nrel.gov/electricity/2022/technologies (visited on 06/29/2023).

[40] N. A. Sepulveda, J. D. Jenkins, F. J. de Sisternes, and R. K. Lester, "The Role of Firm Low-Carbon Electricity Resources in Deep Decarbonization of Power Generation," en, *Joule*, vol. 2, no. 11, pp. 2403–2420, Nov. 2018, ISSN: 2542-4351. DOI: 10.1016/j.joule.2018.08.006. [Online]. Available: https://www.sciencedirect.com/science/article/pii/S2542435118303866 (visited on 06/29/2023).

[41] I. I. I. James, D. Keairns, M. Turner, M. Woods, N. Kuehn, and A. Zoelle, "Cost and Performance Baseline for Fossil Energy Plants Volume 1: Bituminous Coal and Natural Gas to Electricity," English, National Energy Technology Laboratory (NETL), Pittsburgh, PA, Morgantown, WV, and Albany, OR (United States), Tech. Rep. NETL-PUB-22638, Sep. 2019. DOI: 10.2172/1569246. [Online]. Available: https://www.osti.gov/biblio/1569246 (visited on 06/29/2023).

[42] T. Schmitt, S. Leptinsky, M. Turner, *et al.*, "Cost and Performance Baseline for Fossil Energy Plants Volume 1: Bituminous Coal and Natural Gas to Electricity," English, National Energy Technology Laboratory (NETL), Pittsburgh, PA, Morgantown, WV, and Albany, OR (United States), Tech. Rep. DOE/NETL-2023/4320, Oct. 2022. DOI: 10.2172/1893822. [Online]. Available: https://www.osti.gov/biblio/1893822 (visited on 08/22/2023).

[43] J. Valentine, A. Zoelle, S. Homsy, H. Mantripragada, M. Woods, N. Roy, A. Kilstofte, M. Sturdivan, M. Steutermann, and T. Fout, "Direct Air Capture Case Studies: Sorbent System," English, National Energy Technology Laboratory (NETL), Pittsburgh, PA, Morgantown, WV, and Albany, OR (United States), Tech. Rep. DOE/NETL-2021/2865, Jul. 2022. DOI: 10.2172/1879535. [Online]. Available: https://www.osti.gov/biblio/1879535 (visited on 08/03/2023).

[44] M. Wacket, "Exclusive: EU drafts plan to allow e-fuel combustion engine cars," en, *Reuters*, Mar. 2023. [Online]. Available: https://www.reuters.com/business/autos-transportation/eu-proposes-exception-e-fuel-combustion-engines-2035-2023-03-21/ (visited on 05/13/2023).

[45] G. He, D. S. Mallapragada, A. Bose, C. F. Heuberger-Austin, and E. Gençer, "Sector coupling via hydrogen to lower the cost of energy system decarbonization," en, *Energy & Environmental Science*, vol. 14, no. 9, pp. 4635–4646, 2021, Publisher: Royal Society of Chemistry. DOI: 10.1039/D1EE00627D. [Online]. Available: https://pubs.rsc.org/en/content/articlelanding/2021/ee/d1ee00627d (visited on 01/10/2024).

[46] D. S. Mallapragada, C. Junge, C. Wang, H. Pfeifenberger, P. L. Joskow, and R. Schmalensee, "Electricity pricing challenges in future renewables-dominant power systems," *Energy Economics*, vol. 126, p. 106 981, Oct. 2023, ISSN: 0140-9883. DOI: 10.1016/j.eneco.2023.106981. [Online]. Available: https://www.sciencedirect.com/science/article/pii/S0140988323004796 (visited on 12/26/2023).

[47] IEA, *A 10-Point Plan to Reduce the European Union's Reliance on Russian Natural Gas*, en-GB, Mar. 2022. [Online]. Available: https://www.iea.org/topics/russias-war-on-ukraine (visited on 12/18/2023).

[48] A. B. Jaffe, R. G. Newell, and R. N. Stavins, "A tale of two market failures: Technology and environmental policy," *Ecological Economics*, Technological Change and the Environment, vol. 54, no. 2, pp. 164–174, Aug. 2005, ISSN: 0921-8009. DOI: 10.1016/j.ecolecon.2004.12.027. [Online]. Available: https://www.sciencedirect.com/science/article/pii/S0921800905000303 (visited on 12/17/2023).

[49] N. E. T. Lab, "COMPARISON OF COMMERCIAL, STATE-OF-THE-ART, FOSSIL-BASED HYDROGEN PRODUCTION TECHNOLOGIES," NETL, Tech. Rep. DOE/NETL-2022/3241, Apr. 2022. [Online]. Available: https://www.netl.doe.gov/projects/files/ComparisonofCommercialStateofArtFossilBasedHydrogenProductionTechnologies_041222.pdf.

[50] IEA, "The Future of Hydrogen," en, Jun. 2019. [Online]. Available: https://iea.blob.core.windows.net/assets/9e3a3493-b9a6-4b7d-b499-7ca48e357561/The_Future_of_Hydrogen.pdf.

[51] D. D. Papadias and R. K. Ahluwalia, "Bulk storage of hydrogen," *International Journal of Hydrogen Energy*, vol. 46, no. 70, pp. 34 527–34 541, Oct. 2021, ISSN: 0360-3199. DOI: 10.1016/j.ijhydene.2021.08.028. [Online]. Available: https://www.sciencedirect.com/science/article/pii/S0360319921030834 (visited on 12/29/2023).

[52] Vangkilde-Pedersen, Thomas, "EU GeoCapacity: Assessing European Capacity for Geological Storage of Carbon Dioxide," De Nationale Geologiske Undersøgelser for Dan- mark og Grønland, Tech. Rep., 2009. [Online]. Available: https://cordis.europa.eu/docs/results/518/518318/126625721-6_en.pdf (visited on 06/25/2023).

[53] G. M. Mortensen, "CO2 storage atlas for Sweden - a contribution to the Nordic Competence Centre for CCS, NORDICCS," Nordics CCS Competence Center, Tech. Rep., Jan. 2014. [Online]. Available: https://www.sintef.no/globalassets/sintef-energi/nordiccs/d-6.1.7.1407-1-co2-storage-atlas-for-sweden-a-contribution-to-the-nordic-competence-centre-for-ccs-nordiccs_web.pdf (visited on 12/29/2023).

[54] Barchart, *Dutch TTF Gas Prices and Dutch TTF Gas Futures Prices*, en, Dec. 2023. [Online]. Available: https://www.barchart.com/futures/quotes/TGZ33/futures-prices (visited on 12/16/2023).

[55] Lisazeyen, Euronion, M. Millinger, F. Neumann, M. Parzen, T. Brown, L. Franken, Martavp, and Lukasnacken, *PyPSA/technology-data: Technology Data v0.6.2*, Aug. 2023. DOI: 10.5281/ZENODO.3994163. [Online]. Available: https://zenodo.org/record/3994163 (visited on 12/16/2023).

[56] *Verbraucherpreise*, de-DE. [Online]. Available: https://en2x.de/service/statistiken/verbraucherpreise/ (visited on 01/24/2024).

[57] A. Hoffer, *Gas Taxes in Europe*, en-US, Jul. 2022. [Online]. Available: https://taxfoundation.org/data/all/eu/gas-taxes-in-europe-2022/ (visited on 01/24/2024).

[58] *Jet Fuel - Monthly Price (Euro per Gallon) - Commodity Prices - Price Charts, Data, and News - IndexMundi*, en. [Online]. Available: https://www.indexmundi.com/commodities/?commodity=jet-fuel&months=60&currency=eur (visited on 01/24/2024).

[59] Y. Shaker, *Transportation Characterization, Model Creation Workflow, DOLPHYN Visualization*, original-date: 2023-02-27T19:06:43Z, Feb. 2023. [Online]. Available: https://github.com/shakesy94/dolphyn_viz (visited on 01/02/2024).

[60] D. S. Mallapragada, N. A. Sepulveda, and J. D. Jenkins, "Long-run system value of battery energy storage in future grids with increasing wind and solar generation," en, *Applied Energy*, vol. 275, p. 115 390, Oct. 2020, ISSN: 0306-2619. DOI: 10.1016/j.apenergy.2020.115390. [Online]. Available: https://www.sciencedirect.com/science/article/pii/S0306261920309028 (visited on 05/28/2023).

[61] A. Reuther, J. Kepner, C. Byun, *et al.*, "Interactive Supercomputing on 40,000 Cores for Machine Learning and Data Analysis," in *2018 IEEE High Performance extreme Computing Conference (HPEC)*, ISSN: 2377-6943, Sep. 2018, pp. 1–6. DOI: 10.1109/HPEC.2018.8547629. [Online]. Available: https://ieeexplore.ieee.org/document/8547629 (visited on 01/02/2024).